CONJUGATED POLYMER ELECTROCHROMIC AND LIGHT-EMITTING DEVICES

By

AUBREY L. DYER

A DISSERTATION PRESENTED TO THE GRADUATE SCHOOL
OF THE UNIVERSITY OF FLORIDA IN PARTIAL FULFILLMENT
OF THE REQUIREMENTS FOR THE DEGREE OF
DOCTOR OF PHILOSOPHY

UNIVERSITY OF FLORIDA

2007

To Nathan

ACKNOWLEDGMENTS

I can honestly say that this process has been one of the most difficult that I have yet to go through. It's not that the Ph.D. process is inherently hard, just the emotional toll that conducting research while trying to obtain a degree, and remain a sane person, takes on you. There's the good days, the bad days, the times of self-doubt, the considerable amount of stress you put on yourself, and the challenges of working so closely with other people who, while going through the same process, are so different from yourself. I feel that to successfully get through this with your spirit still intact, you need strong support from others in your life. I am happy to say that there have been many people along the way who have fulfilled that role and I would like to say thanks.

The one person who has been there through it all and never once let me give in and give up has been Nathan Dyer, my husband. He understood how important this degree is and, while not able to relate to what I was going through, stood by me and did everything he could to show support, understanding, and most of all, patience. Another person who has been there and who I could not have done this without is my advisor, John Reynolds. His ability to relate with every single person in the group on a personal level is one of the things that sets him apart from most advisors. He not only keeps the group running by securing funding and keeping the research we do relevant, but also ensures we, as individuals, are making progress in our research, our professional lives and our personal lives. He is the group cheerleader, and his level of enthusiasm for what he does and we do is infectious and it's what makes this group great to work in.

I would like to thank the many people who I've worked with on various projects over the years: Christophe Grenier, Ben Reeves, and Bob Brookins. Thanks for handing over your "babies" to me to tinker with in the lab. I'd also like to thank Dr. Tanner for the optics

discussions, Evan Donoghue and Ken Graham for putting the time into designing and fabricating the “black box”. Special thanks to Nate Heston for the hard work and effort in keeping the glovebox in such good shape and the evaporator running for me. A final thanks to Evan, and Eric Shen for volunteering their expertise at the 11th hour in order to help me make sure I get this done. Thanks Evan for the AFM measurements, and Eric for the distillation. You guys were there when I really needed help. Also, thanks to my friend Jack for the early morning coffee breaks.

Over the past five years, there have been a large number of people come and go from the group and each individual has leant their personality to the dynamics of the Reynolds group and the Polymer Floor in general. I would like to thank those who have been there for me, as either a shoulder to cry on, an ear to listen, or just to make me laugh. These people include the MCCL orphans (Nate Heston, and Ece Unur), Emilie Galand, Sophie Bernard, Maria Nikolou, Cheryl Googins, Genay Jones, and Gena Borrero. In addition, I’d like to thank my friends Heshan “Grasshopper” Illangkoon, Dr. Mike Bowen, and Susan Bongiolatti. Looking back, I still can’t believe some of the things we’ve been a part of on this campus. It was fun and I could honestly say, a valuable eye-opening experience. I’d also like to thank the many people who I’ve encountered over the past five years (in the research lab and across campus) who have, in some way or another, taught me valuable lessons. Some have taught me how to be a good person and a great friend, others have taught me patience and understanding, probably some of the most valuable things I’ve received from this education and of which I’m still learning. Finally, I’d like to thank my family: my mother, Sheila Dedrickson, my sister, Stevie, and my brother, Shaun.

TABLE OF CONTENTS

LIST OF FIGURES

LIST OF ABBREVIATIONS

ACN:	Acetonitrile.
E_g:	Bandgap energy.
Cbz:	Carbazole.
CB:	Conduction band.
EC:	Electrochromic.
ECD:	Electrochromic display.
EL:	Electroluminescent.
Fl:	Fluorene.
ITO:	Indium-doped tin oxide.
LiOTf:	Lithium trifluoromethanesulfonate.
MEM:	Microelectromechanical.
OLED:	Organic light-emitting display.
Ph:	Phenylene.
PAc:	Polyacetylene.
PEDOT:	Poly(3,4-ethylenedioxythiophene).
PEO:	Poly(ethylene oxide).
PLED:	Polymer light-emitting diode.
PLEC:	Polymer light-emitting electrochemical cell.
PMMA:	Poly(methylmethacrylate).
PPV:	Poly(para-phenylenevinylene).
PProDOP:	Poly(3,4-propylenedioxypyrrole).
PProDOT:	Poly(3,4-propylenedioxythiophene).
PSS:	Poly(styrenesulfonate).

PC:	Propylene carbonate.
SWNT:	Single-walled carbon nanotubes.
VB:	Valence band.
VOA:	Variable optical attenuator.

Abstract of Dissertation Presented to the Graduate School
of the University of Florida in Partial Fulfillment of the
Requirements for the Degree of Doctor of Philosophy

CONJUGATED POLYMER ELECTROCHROMIC AND LIGHT-EMITTING DEVICES

By

Aubrey L. Dyer

December 2007

Chair: John R. Reynolds
Major: Chemistry

Conjugated conducting polymers are among some of the most versatile materials to emerge in the past 20 years. They have been researched for applications that range from photovoltaics, to light-emitting diodes, electrochromic windows, actuators, and field effect transistors. This work details the analytical characterization of π-conjugated polymers to understand their redox and optical properties, along with the development of several new types of devices that employ these polymers as the active materials for both variable optical attenuators and as dual electrochromic/electroluminescent displays. Within this work, a phenomenon that we term unsymmetrical switching has been uncovered for the first time in reflective electrochromic cells. The unsymmetrical switching in these displays is explored and a model devised to illustrate that the presence of a conductive front propagating through the polymer film on electrochemical oxidation is the contributing cause for this observation. For these experiments, a variety of analytical techniques have been utilized to characterize the devices and materials contained therein and include electrochemistry, spectroelectrochemistry, and photometry.

The first application utilizes the large near infrared electrochromic contrasts of some dioxythiophene-based polymers when incorporated in reflective electrochromic displays. For the

first time, it is demonstrated that these devices can be utilized as electrochromic variable optical attenuators, important components for the optical telecommunications industry, exhibiting optical attenuation values of 12 decibels while maintaining optical loss values, in the off state, as low as 0.1 decibels. These devices offer the benefit of yielding mechanically flexible, miniaturized electrochromic variable optical attenuators that operate with a low drive voltage (± 1.2 volts).

A new concept is also introduced for conjugated conducting polymers as the active material in dual electrochromic/electroluminescent displays that are unique in that a single active polymer film is employed as both the emitter and electrochrome. In using a soluble para-phenylene-vinylene-based polymer, a device is developed that shows orange to blue electrochromism and orange-red electroluminescence from the same pixel. This type of device potentially fulfills a need in the display industry for a device that exhibits light emission in low ambient lighting while maintaining a high optical contrast, without sacrificing image quality, in directly lit situations. This device also offers the possibility of a flexible, patterned display as desired in the consumer electronics industry.

CHAPTER 1
DOPED CONJUGATED POLYMERS IN DISPLAY DEVICES

Introduction

The field of conducting polymers can be dated to as far back as 1862 when Letheby described the production of a dark green film on an electrode when oxidizing aniline under acidic conditions.[1] The most studied conducting polymer, polyactetylene (PAc), can even be dated to 1955 when Natta produced the polymer using the coordination catalyst system commonly used to polymerize ethylene and propylene.[2] PAc was even found to behave as a semiconductor by various researchers in the 1960s on treatment with reagents such as boron trifluoride and ammonia, producing dramatic changes in conductivity.[3-6] It was not until the 1970s when Shirakawa and coworkers improved the procedure for the synthesis of PAc,[7, 8] combined with further work by Heeger and MacDiarmid,[9-11] that the field of conducting polymers really emerged with PAc established as the first conducting organic polymer.

In their work, Heeger, MacDiarmid, and Shirakawa demonstrated that the conductivity of PAc films increased many orders of magnitude on exposure to halogen vapors.[10] Other researchers have also demonstrated that reacting PAc with oxidants (e.g., I_2, $Fe(ClO_4)_3$) or reductants (e.g., $NaC_{10}H_8$), forms highly conducting derivatives of PAc. [12, 13] These reactions are called “doping”, analogous to terminology used in semiconductor physics with p-doping an oxidative reaction, with insertion of charge-balancing anions, and n-doping a reduction with insertion of charge-balancing cations. The two most commonly used methods for chemical doping are exposing the polymer to a gas-phase dopant, such as iodine vapors, or a solution of the dopant, such as $SbCl_5$, diluted in an appropriate solvent.[14] The rate of doping and maximum doping level can be controlled by dopant concentration and exposure time.

While chemical doping has been instrumental in initial demonstrations of the theoretical and technological promise of PAc by allowing tunable conductivity of the polymer film from the semiconducting to the metallic regime, the applicability of this method is lacking. In many cases, the chemical dopants are highly reactive and difficult to handle, not allowing for the utilization of these polymers outside the research laboratory. In 1979, Nigrey and coworkers demonstrated that PAc could be reversible p- or n-doped electrochemically, but the material's instability remained as an obstacle to commercial applications.[15] The neutral polymer is not air stable and decomposes quite rapidly and therefore must be handled in an inert atmosphere and is additionally difficult to process with melt processing resulting in degradation.

It was not until that same year when Diaz et al., electrochemically polymerized pyrrole to produce free-standing, air-stable polymer films that had conductivities of 100 $\Omega^{-1}cm^{-1}$.[16, 17] The method they used was a modification of that originally reported by Dall'Olio in 1968 with the main difference being that Diaz et al, obtained continuous films that could be peeled off the platinum electrodes as opposed to a powdery, insoluble precipitate.[18] Not only did this demonstrate the ability to electrochemically polymerize directly onto an electrode and reversibly switch the polymer between a neutral and oxidized state, but it introduced the field to polyheterocycles, which would become the most important class of conducting polymer to date. The impact of pyrrole systems stems from several factors that include chemical and thermal stability of the polymers, the ease of preparation of polymer films, and the ability to synthesize derivatives that allow for modification of the electrical and physical properties of the final polymer.

This opened the door for other electrochemically active polymer systems to enter the field and demonstrate their applicability as the active materials in areas ranging from batteries,

capacitors,[19] light-emitting displays,[20] field-effect transistors,[21] electrochromic displays,[22] solar cells,[23] and actuators.[24] Conducting polymers hold much promise for these, and many other, applications as they allow tuning of physical and electronic properties through structural modification of the polymer backbone; a feature not available in any other material. This introduction will cover two applications of doped conjugated polymers (electrochromism and light-emission), the methods by which these physical processes occur and the types of devices in which they are employed.

Electrochromism

Electrochromics are materials that can induce a reversible change in the absorption, reflection, or transmission of optical radiation when the material is involved in an electrochemical reductive or oxidative process.[25] Electrochromism not only includes changes in the visible region, but also in the ultraviolet (UV), infrared (IR), and even the microwave regions of the spectrum.[26-28] Some of the most commonly researched electrochromes are those based on transition metal oxides (e.g., tungsten oxide, WO_3), 4,4'-bipyridinium salts (e.g., methyl viologen), and polynuclear transition metal hexacyanometallates (e.g., Prussian Blue, $[Fe^{III}Fe^{II}(CN)_6]^-$).[29-35]

Over the past two decades, conjugated polymers have emerged as one of the most promising electrochromic materials available.[22] This is due to the fact that they offer color tunability, faster switching, and improved processability over the inorganic and molecular electrochromes mentioned. Electrochromism in conjugated conducting polymers arises from the polymer's bandgap and any midgap states created on doping. The optical bandgap is determined by the onset of the π-π^* transition of the polymer in the neutral, undoped state and is the electronic transition, as shown in Figure 1-1A, that occurs with the minimum energy difference from the valence band to the conduction band.

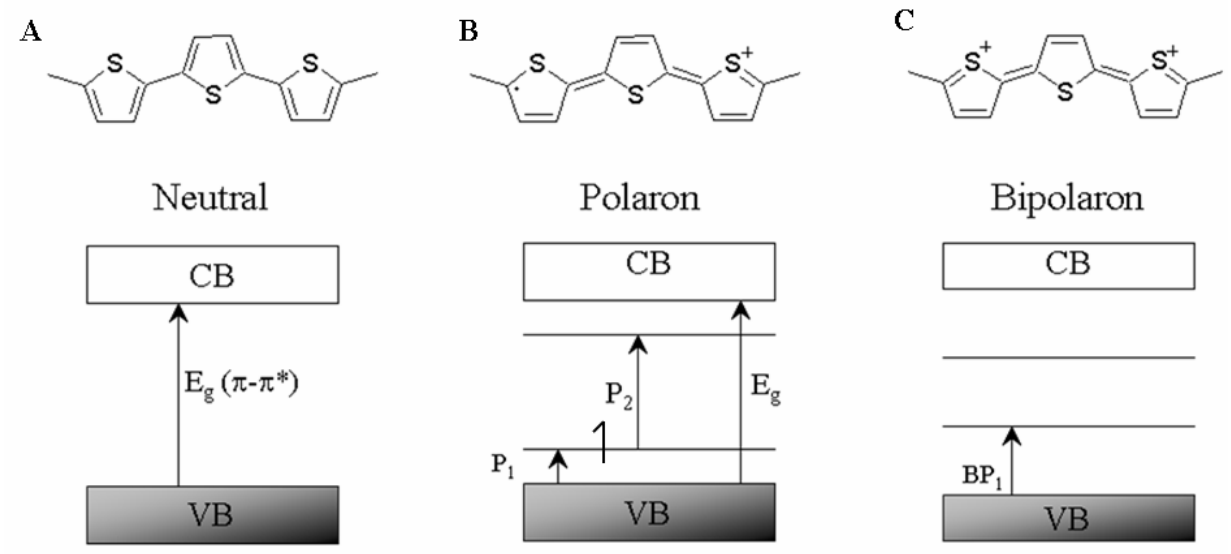

Figure 1-1. Geometric structure of a thiophene trimer showing the allowed electronic transitions. A) Neutral; B) Polaron; C) Bipolaron states. Note: The forbidden transitions are not shown for clarity.

As the polymer is oxidized, electrons are removed from the valence band and lower energy absorptions begin to emerge in the electronic spectra at the expense of the π-π* transition. This is due to the removal of the π-electrons from the valence band, creating half-filled polaron levels that are symmetric about the bandgap center. Figure 1-1B shows the allowed electronic transitions for these new lower energy states. This newly formed radical cation is delocalized over a polymer segment and behaves as a polaronic charge carrier. This oxidation induces a relaxation of the aromatic geometry to a quinoid-like structure in the polymer chain and is accompanied by a charge balance by the electrolyte anions.

On further oxidation, a dication is formed (with the cations coupled to one another) and is a bipolaronic charge carrier delocalized over the same polymer segment. As is shown in Figure 1-1C, only electronic transitions from the top of the valence band occur as the bipolaron levels are unoccupied. At this point, only lower energy absorptions are seen in the electronic spectra, and the π-π* is depleted. This can be seen in Figure 1-2 for the spectroelectrochemical series of poly(3,4-ethylenedioxythiophene) or PEDOT. The neutral polymer is dark blue as the bandgap

is in the visible region at 1.65 electron volts (eV). As the polymer is p-doped, an absorption emerges in the NIR and the color of the polymer begins to bleach, finally becoming a highly transmissive sky blue.

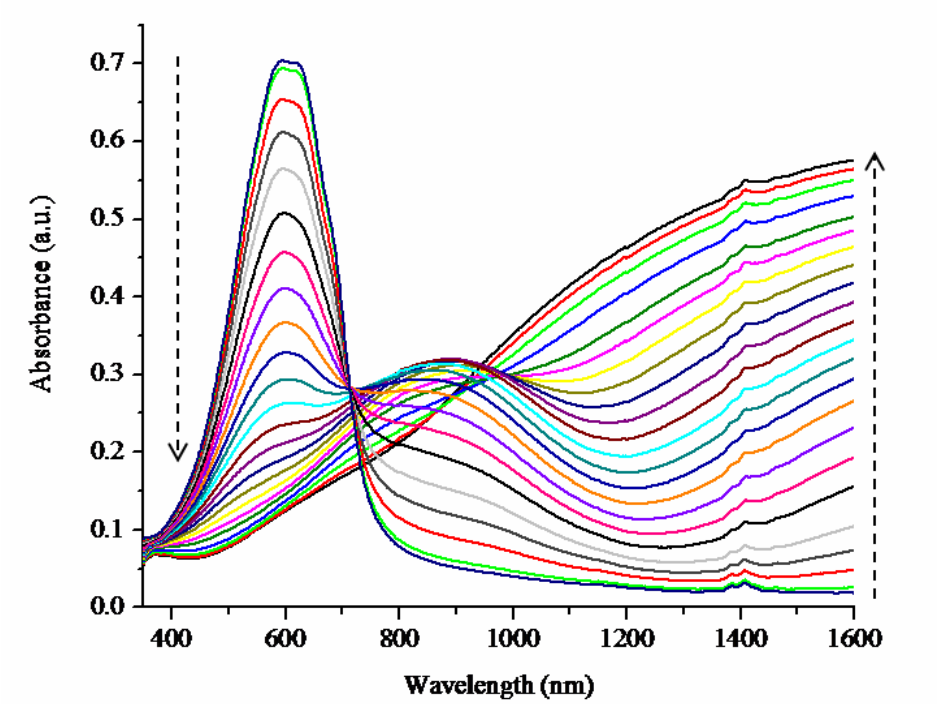

Figure 1-2. Spectroelectrochemical series for a film of poly(3,4-ethylenedioxythiophene) (PEDOT). Dashed arrows show direction of spectral growth or recession.

As mentioned previously, conducting polymers offer the advantage of color tailorability in the neutral and doped states through synthetic methods. This can be seen when comparing polythiophene to PEDOT. Unsubstituted polythiophene has a bandgap of 2.0-2.2 eV, switching from red in the neutral state to blue upon oxidation. However, it is difficult to obtain uniform polymer films because the polymer overoxidizes at the potentials required for electropolymerization and side reactions can occur at the β-position causing undesirable structural defects.[36-39] To overcome these issues, research became focused towards substitution at the 3-position or the 3- and 4-positions of the thiophene ring yielding polymers with bandgaps that ranged from less than 1 eV to higher than the parent thiophene.

One of the most commercially successful polymers to date, PEDOT was produced with the goal of not only lowering the polymer bandgap, but also exhibit a lower oxidation potential and higher stability. PEDOT not only has a lower bandgap than the unsubstituted thiophene, it is also easily oxidized and highly stable in the doped state. This is due to the presence of the electron-donating oxygens adjacent to the thiophene ring. On oxidation, PEDOT becomes highly conducting and transmissive in the visible region. However, this polymer has the drawback of insolubility. To overcome this limitation, the aqueous dispersion of the doped form of PEDOT with the polyelectrolyte, poly(styrenesulfonate) (PSS), was produced. Cast films of PEDOT:PSS have greater than 75% transmissivity in the visible region and greater than 120 S/cm film conductivity.[40] Applications for this polymer have been mostly for its use as a conductor for antistatic coatings, solid state capacitors, organic electronic devices, and even as a transparent electrode material.[19, 41-44]

Recent synthetic effort has been towards producing polymers, especially those based on the alkylenedioxythiophenes, that are processable. Through the introduction of alkyl and alkoxy chains on the propylene bridge, a family of poly(3,4-propylenedioxythiophenes) (PProDOTs) has been synthesized that is soluble in common organic solvents such as toluene and chloroform.[45-48] This allows uniform, thick films to be cast from solution using methods such as drop-casting, spincoating, spraycoating, and inkjet or screen printing. In addition to the improved processability, the PProDOTs have faster switching speeds and larger optical contrasts. The tetrahedral substitution pattern on the propylene bridge causes the alkyl and alkoxy groups to be positioned above and below the plane of the polymer chain. This allows the polymer chains to separate, opening up the film for more facile counter ion movement and leading to higher doping levels. This also hinders π-stacking, causing a decrease in the polymer conductivity.

The dioxythiophene family of conjugated polymers are colored in their neutral state and switch to a highly transmissive state on oxidation and are therefore cathodically coloring. Another class of polymers are those that are anodically coloring, and highly transmissive when neutral, switching to colored on oxidation.[49-53] The *N*-substituted alkylenedioxypyrroles are such a family of polymers with the polymer bandgap shifted into the ultraviolet region of the spectrum allowing for near-transparency in the neutral state. Substitution at the N-position introduces steric interactions that vary the degree of π-overlap along the polymer backbone. This induces a twist in the polymer backbone that causes a decrease in the effective conjugation length leading to an increase in the bandgap.[22, 54, 55] As previous calculations have shown,[22] substitution with the bulky ethoxyethoxyethanol at the N-position in poly(3,4-propylenedioxypyrrole) (PProDOP-*N*-Gly) causes a twist angle between the pyrrole rings of 71.6º whereas the unsubstituted PProDOP is fully planar.

The unsubstituted PProDOP has a bandgap of 2.2 eV and is orange in the neutral state switching to light gray-blue on oxidation, while PProDOP-*N*-Gly has a bandgap of 3.4 eV and is colorless in the neutral state and blue-gray when oxidized. The electron-rich character of the pyrrole along with the presence of the alkylenedioxy bridge reduces both the monomer and polymer oxidation potentials. This allows for polymerization to occur under relatively mild conditions and the polymer to have an increased stability under ambient conditions in the doped conducting state with the family of PProDOPs having the lowest reported polymer oxidation potentials to date.[50] The anodically coloring properties of the *N*-substituted PProDOPs along with the low polymer oxidation potential makes them complementary to the PProDOTs when both are incorporated into absorptive/transmissive electrochromic windows.[53] Additionally, the

fast switching speeds, large optical contrasts (in the visible and NIR), and high redox stability of the PProDOTs makes them ideal for absorptive/reflective electrochromic displays.[56, 57]

Electrochromic Devices

Electrochromic devices are electrochemical cells in which a redox reaction occurs at a working electrode and counter electrode by application of an electric field across the device. Typically, one or more electrochromic materials are deposited on both the working electrode and counter electrode and the electromagnetic radiation absorbed, transmitted, or reflected from the device is modulated.[29, 58-60] Most commonly, electrochromic materials are deposited as films on both the working and counter electrodes with the material on the counter electrode acting as a charge-balancing source for the redox reaction and, in some cases, as a complementary electrochrome to that at the working electrode. In dual polymer ECDs, both materials are electrochromic polymers, while in hybrid devices, the material at the counter electrode can be any other class of electrochromic material and has included Prussian Blue, viologens, and WO_3.[61-66]

An electrolyte layer is deposited between the two electrodes with the requirement that the material used have a high conductivity, transparency in the wavelength range measured, wide window of electrochemical stability, and low volatility. Materials used include gel electrolytes, solid electrolytes, and ionic liquids.[53, 67-71] The electrodes utilized in these devices are dependent on how the light is to be modulated with reflective metallic electrodes in the absorptive/reflective devices and transparent electrodes utilized in the absorptive/transmissive devices. The reflective electrodes can be metallized, porous membranes that allow for ion transport through the membrane while exhibiting a high specular reflectance.[56, 72-74] Metals used include gold, platinum, and aluminum. Transparent electrodes include indium-doped tin oxide (ITO) on glass,

fluorine-doped tin oxide (SnO_2:F) on glass, PEDOT:PSS on glass or plastic, and single-walled carbon nanotubes (SWNT) on glass or plastic.[75, 76]

Absorptive/transmissive, or window-type, displays operate by reversibly switching the device between a highly absorptive, colored state and a highly transparent, bleached state. Both the working electrode and counter are transparent for light to pass with the conductive materials (ITO, SnO_2:F, PEDOT:PSS, or SWNT) deposited on glass or plastic substrates. As is shown in Figure 1-3, films of two complementary electrochromic materials, one anodically coloring, the other cathodically coloring, are deposited on the electrodes with a layer of electrolyte sandwiched in between.

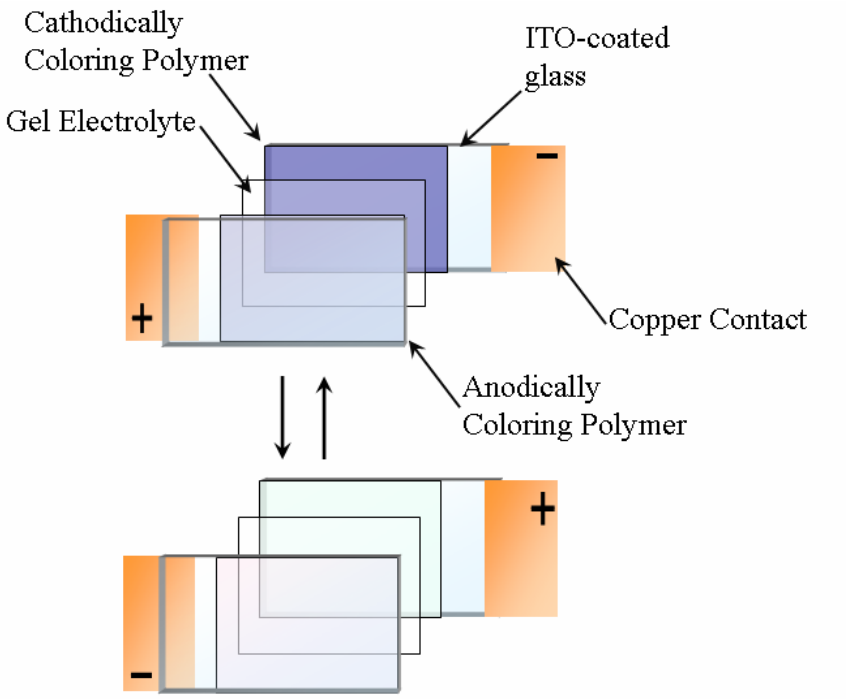

Figure 1-3. Schematic of a typical absorptive/transmissive electrochromic polymer window.

The device becomes highly absorptive when biased with a negative potential applied to the cathodically coloring electrode and becomes bleached when the bias is reversed. The colors of the device are additive in that they are a combination of those exhibited by both materials. The absorptive/transmissive window devices typically operate in the visible region, but recent

research towards the production of IR-transparent electrodes (e.g., SWNT) has allowed for the fabrication of dual polymer devices that operate in the NIR through far-IR regions of the spectrum.[76]

The absorptive/reflective electrochromic displays can also operate not only in the visible region, but also at the longer wavelengths of the NIR and far-IR as most metals utilized as the working electrode are highly reflective through those regions of the spectrum.[47, 56, 57, 72-74] One type of electrode demonstrated is a gold-coated ion permeable porous membrane. As is shown in Figure 1-4, this electrode is outward facing, with the active electrochromic material deposited on top. Behind the electrode is the electrolyte layer and counter electrode. The counter electrode in this case only acts as a redox-balancing layer, not contributing any optical properties to the electrochromism of the device. This allows for probing of the electrochromic properties of the active layer alone. The entire device is encapsulated with a cover window that is transparent to the wavelengths measured with ZnSe utilized in the NIR to mid-IR, glass for visible to NIR, and polyethylene for visible to mid-IR.[56, 57] As an example, when the active polymer layer is a cathodically coloring polymer, the device is highly absorptive in the visible region and highly reflective in the NIR when a negative bias is applied. When the bias is switched, the polymer becomes oxidized and the device is highly reflective in the visible region, with the metal electrode visible underneath, and absorptive in the NIR.

Both types of device platforms allow for patterning of not only the electrodes but also the active electrochromic layer. In window-type devices with PEDOT:PSS as the transparent conductor, the electrode can be patterned by screen printing, inkjet printing, and micro-contact printing, not only on glass, but also on a flexible substrate such as plastic.

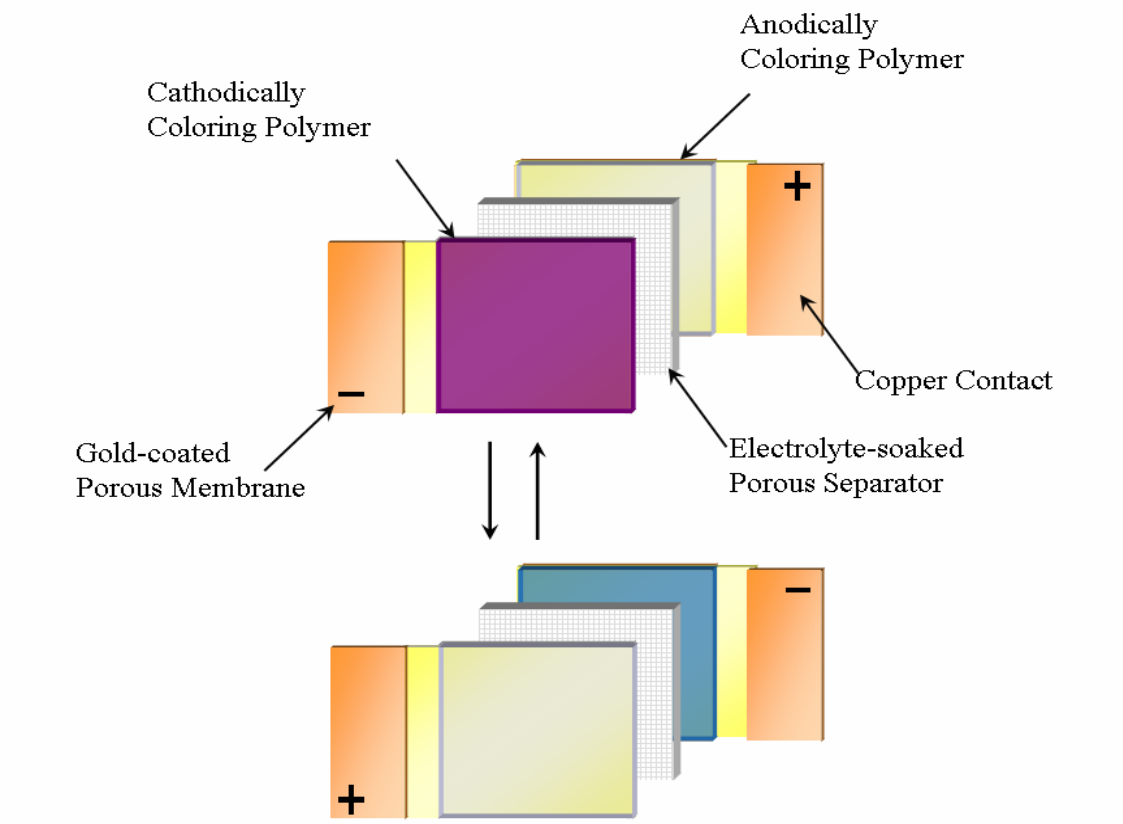

Figure 1-4. Schematic of a typical absorptive/reflective electrochromic polymer display.

Similarly, the metallic conductor in the reflective devices can also be patterned by metal vapor deposition, or line patterning and micro-contact printing followed by electroless plating. The polymer layers can then be selectively deposited by electrochemical polymerization onto the patterned electrode or, with the increasing number of soluble polymers becoming available, printing by inkjet or screen printing.[77-80]

The combination of the various device platforms available, along with the versatility of the electrochromic polymers and the large variety of colors available makes them ideal for most display applications. While these devices and materials offer enhanced performance over other electrochromic materials in color tailorability, subsecond switching speeds, optical memory, and low power consumption, some challenges still exist. These include increasing device lifetime to that needed in commercial applications by improving environmental stability and decreasing

switching speeds to below millisecond rates. Meanwhile, there exist applications where these issues are not imperative, one of which is applications where the display or device is disposable, being discarded after only a few uses, for example, and the other is the variable optical attenuator that will be discussed in detail in this dissertation.

Light-Emitting Devices of Doped Polymers

One of the most highly researched and publicized uses of conjugated conducting polymers is as the active material in polymer light-emitting displays. In 1987, it was demonstrated that display-brightness could be achieved for organic light-emitting diodes (OLEDs). These devices consisted of vacuum-deposited layers of an aromatic diamine and the fluorescent metal chelate complex 8-hydroxyquinoline aluminum (Alq_3).[81] A drawback to these materials is that the requirement of vacuum sublimination of films is difficult to translate to practical commercial devices.

It was not until three years later when the first conjugated polymer LED (PLED) was introduced with high quality films being prepared by thermal treatment of a solution-processable precursor polymer.[20, 82] These PLEDs utilize the undoped, pristine form of the polymer with the mobile charge carriers (electrons and holes) supported by the delocalized π-bonding along the polymer chain. The electrons are injected from the cathode into the π^* band of the semiconducting polymer and holes are injected into the π band from the anode. The oppositely charged carriers in the two bands capture one another (recombination) within the polymer film, form neutral bound excited states (excitons), and radiatively decay as is shown in Figure 1-5.

Ideally, the work functions of the metal contacts are perfectly matched to the π and π^* bands; however, in real devices the match is imperfect, requiring hole and electron injection by tunneling through or thermal activation over the energy barriers formed at the polymer/metal interface.[83] The energy levels of a conjugated luminescent polymer (poly(2-methoxy, 5-(2'-

ethyl-hexyloxy)paraphenylene vinylene) (MEH-PPV), and the electrodes used in a typical PLED are shown in Figure 1-6.

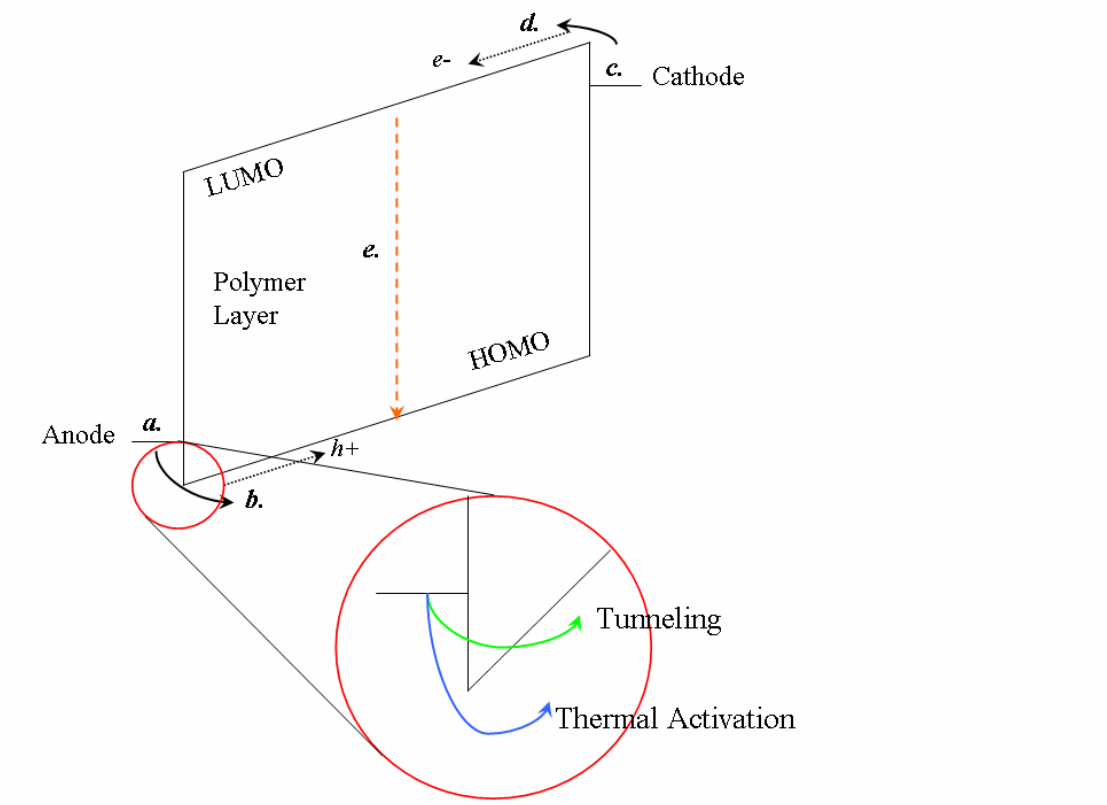

Figure 1-5. Schematic diagram of a PLED in forward bias showing charge injection (a. and c.), carrier transport (b. and d.), and recombination (e.), with a focus on the two possible methods for charge injection, tunneling and thermal activation.

In order to have efficient and balanced dual-charge injection, a low work-function cathode (e.g., calcium) and high work-function anode (e.g., ITO) are required to match the energy levels of the luminescent polymer. The most commonly utilized materials are calcium, magnesium, or lithium as the cathode and ITO coated with a thin layer of PEDOT:PSS as the transparent anode. The PEDOT:PSS acts to not only lower the hole-injection barrier by ~0.5 eV to better match with the polymer highest occupied molecular orbital (HOMO), but has also been suggested to smooth the relatively rough ITO surface, providing a better surface for the active polymer layer to be deposited.[43, 84-86]

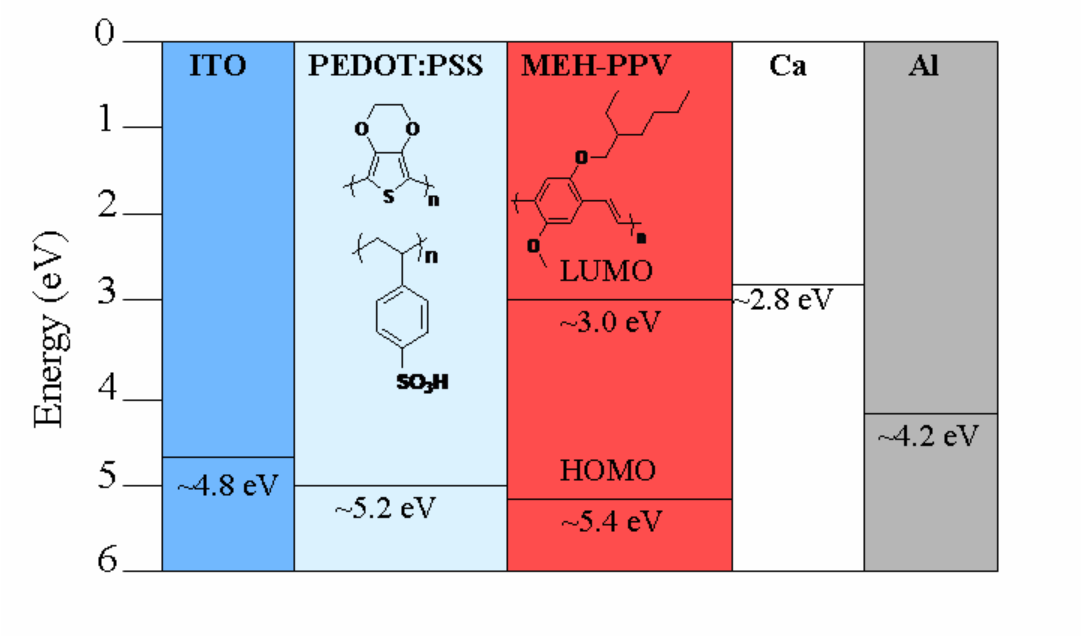

Figure 1-6. Energy-level diagram, relative to vacuum, for the materials used in a typical PLED. The HOMO and LUMO levels of MEH-PPV[87] and the Fermi level positions of the electrodes are shown.

The high-lying lowest unoccupied molecular orbital (LUMO) levels of luminescent conjugated polymers requires the use of low work-function, and therefore highly reactive, metals such as calcium, magnesium, or cesium. These metals have been shown to interact with the organic polymer layer and quench luminescence in addition to interacting with the environment leading to quick degredation.[88, 89] In most cases, the reactive cathode layer is capped with another metal layer, such as aluminum, to protect the cathode from exposure to oxygen and moisture. In addition, the operating voltage and efficiency of the device is determined by the active polymer layer thickness with ideal thicknesses under 100 nm. The typical device layout for a PLED is shown in Figure 1-7. The device consists of the transparent anode, onto which the luminescent polymer layer is cast. The metal cathode contacts are then thermally evaporated onto the polymer layer and the entire device encapsulated to exclude moisture and oxygen.

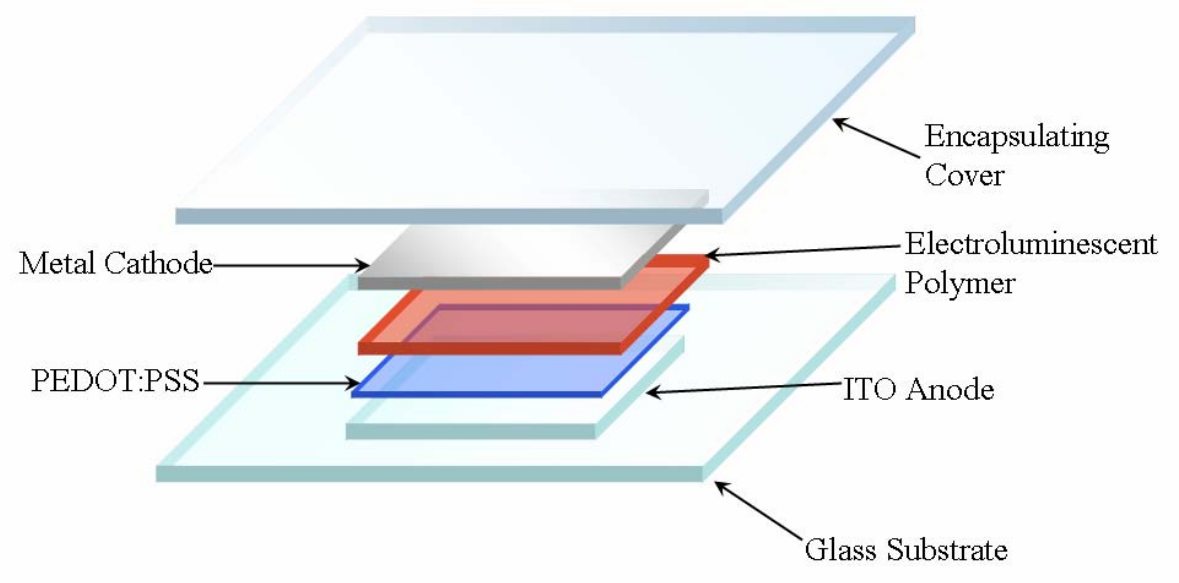

Figure 1-7. Schematic of a typical PLED.

The intense interest in PLEDs for use in display applications results from the processing advantages, opportunities for the use of flexible substrates, and with a significant number of today's conducting polymers being highly luminescent, there is an availability of emission colors that span the entire visible spectrum and beyond.[28, 90-96] Results have been reported for devices with brightness values comparable to color televisions (100 cd/m^2), fluorescent lamps (4,000 cd/m^2), and even in excess of 10,000 cd/m^2.[91]

In the PLEDs described above, the semiconducting polymer layer is oxidized at the anode (holes are injected) and reduced at the cathode (electrons are injected); however, doping does not take place as there are no ionic species in the polymer layer to compensate the charges on the polymer chains. An interesting alternative to the PLED is the polymer light-emitting electrochemical cell (PLEC) introduced by Pei et al.[97] The PLEC is a solid state electrochemical cell that is a blend of a conjugated luminescent polymer and a solid electrolyte that acts as the active layer for light-emission. Since that seminal publication demonstrating these devices, there has been much disagreement on the fundamentals of the device operation.[98-100] The argument centers around whether the formation of an electrochemical junction is the operating principle of

the device. While not entirely resolved, much recent research has been focused towards this effort with experimental observations agreeing with this initial model.[101, 102]

In general, as is shown in Figure 1-8, when a sufficiently high voltage is applied between the cathode and anode, charges are injected from the electrodes into the luminescent polymer. Counter ions from the solid electrolyte redistribute to compensate the charges on the oxidized and reduced polymer chains, and simultaneous electrochemical p- and n-doping occur at the anode and cathode, respectively. Since the electrical conductivity of doped conjugated polymers increases significantly on doping, the polymer/electrode interfaces become low-resistance contacts. Once electrochemical equilibrium is reached in the cell, a p-n junction is formed and the ionic contribution to the current goes to zero. The electronic contribution to the current, on the other hand, continues under the influence of the applied voltage with the holes in the π-band (p-type carriers) and electrons in the π^*-band (n-type carriers) migrating through the high-conductivity doped regions. After a turn-on time, a thin insulating region is formed separating the doped regions, creating a p-i-n junction, where the charge carriers recombine to form neutral charge carrier pairs that radiatively decay to the ground state.[97, 100, 103-110]

Unlike conventional inorganic LEDs, the p-n junction is dynamic in that the device will discharge after the external bias is removed and the junction will need to be reestablished when the device is to be once again turned on. Additionally, given the electrical conductivity of conducting polymers on doping, most of the external bias is applied across the p-i-n junction. The minimum bias required to maintain the junction is equal to the built-in potential difference of the p-n junction and is ideally equal to the HOMO-LUMO gap of the polymer.

It can be seen that the turn-on time of a LEC is dictated by the speed of electrochemical doping of the conjugated polymer and the rate of formation of the p-i-n junction, which are

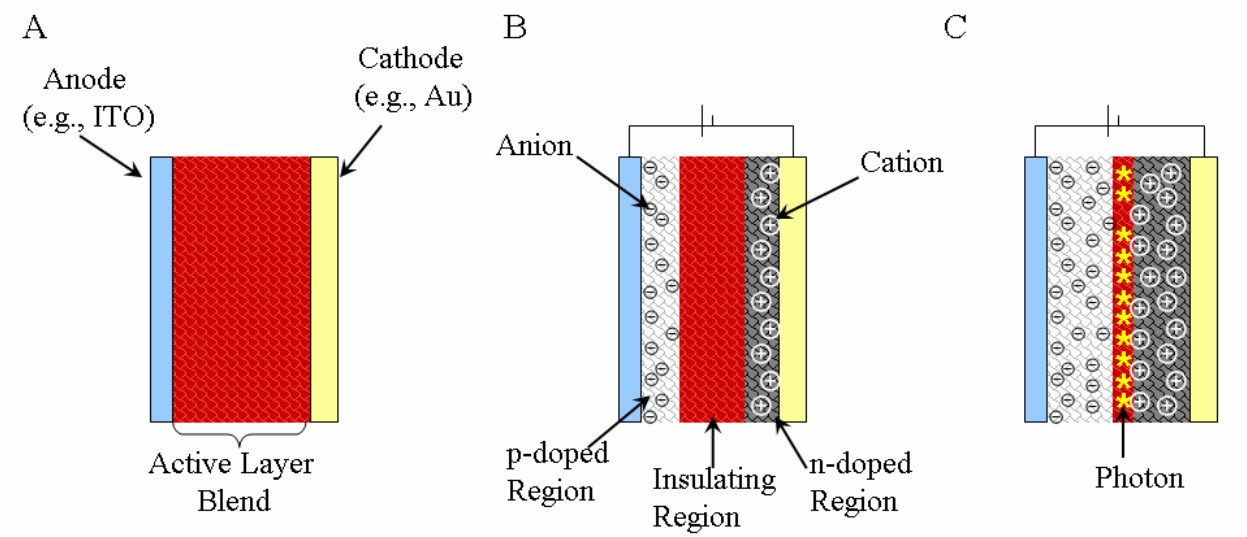

Figure 1-8. Schematic of PLEC device operation. A) Unbiased device, B) Low voltage applied with p-doping of the polymer at the anode, n-doping at the cathode, and an undoped insulating region, C) Charge migration with emission of a photon on carrier recombination.

directly related to the redistribution of ions and initial injection and transport of electronic charge carriers. Given that ion mobilities are significantly lower than mobilities of electronic charge carriers, it is the ion mobility that then limits the device turn-on time. The solid electrolyte component of the active layer blend typically consists of an ionically conductive polymer or liquid additive that can effectively complex with ions and separate them from the counter ions allowing them to move within the polymer matrix. Among various ionically conductive polymers, poly(ethylene oxide) (PEO) has been the most widely studied in combination with a variety of lithium salts, such as lithium trifluoromethanesulfonate (LiOTf). However, conjugated polymer and PEO/lithium salt mixtures have been observed to phase separate into a conjugated polymer phase and a PEO/LiX phase, due to the entropy of mixing polymer/polymer blends being quite low and the mismatch in polarity between the typically non-polar conjugated polymer, such as MEH-PPV, and the polar PEO/LiX complex.[111-114] Given that this can limit device performance, much effort has been directed towards other materials that show an

improved morphology on blending with luminescent polymers.[115-119] Such materials include crown ethers complexed with various salts. These devices have been demonstrated to show a higher luminance and longer lifetimes than devices containing the PEO/LiOTf solid electrolyte. In addition, binary systems of conjugated luminescent polymers containing ion solvating side groups complexed with a salt and luminescent/ionic liquid blends have gained increasing attention as there would be no need for an additional ion solvating material and complications arising from phase separation are decreased.[120-126]

An important characteristic of the PLEC is that, due to the low resistivity of the doped polymer and the tendency to form ohmic contacts with the metal electrodes, the performance of the device is insensitive to the electrode materials. Not only can the use of highly reactive, low work function cathodes be avoided, but the same metal can be utilized for both anode and cathode.[127-129] Another unique property of LECs includes the fact that light emission can occur for both forward bias as well as for reverse bias with onset voltages equal in both directions. Onset voltages have also been demonstrated to be nearly independent of the active layer thickness. This has been effectively demonstrated by the use of a planar electrode configuration with two parallel gold electrodes of 1 mm spacing.[129] In this case, the light is emitted from within the zone between the metal contacts.[128, 130] Even though these devices have turn-on voltages at or near the polymer bandgap, while being independent of film thickness and without the need for highly reactive metal contacts, quantum efficiencies can be achieved that rival those of PLEDs. As the switching speeds and lifetimes are improved, their impact in the field of light-emitting displays will be distinct.

Dual-Purpose Devices

Electroactive conjugated polymers can exhibit electrochromism and light-emission, as has been discussed, but they also have been demonstrated as the active component in many devices

such as photovoltaics, actuators, field-effect transistors, and supercapacitors with more than one of these devices utilizing the same family of polymers. Many of these properties operate on similar principles or by similar mechanisms. This opens the door for dual purpose devices or displays that perform multiple functions with the same active material or same device by the fabrication of creative device architectures.

For example, both electrochromic devices and actuators operate by electrochemical oxidation or reduction of the polymer film with simultaneous ingress/egress of charge balancing counterions. With the electrochromic devices, the property desired from this action is the resulting color change on oxidation/reduction. For the actuator devices, the action is contraction or expansion of the polymer film due to a volume change from the counter ion movement. A device demonstrated in the literature that takes advantage of this dual property exhibited within the same material was an electrochromic moveable pixel.[24] This device utilized polypyrrole as the active layer in which the polymer acted as an actuator joining two electrodes. The volume change induced on oxidation of the polypyrrole layer causes a rotation between the electrodes, creating a hinge-type device. Additionally, polypyrrole layers are deposited on the electrodes where their electrochromic response can be altered along with the position of the electrode giving a color-changing movable pixel.[24] Similarly, Andersson et al. have demonstrated a "smart pixel" that operates in a similar fashion in that the electrochemical reaction of a polymer film is used for multiple purposes. In their device, a film of PEDOT is used as the active electrochromic layer and also as an electrochromic transistor for matrix addressing switches. The result is an electrochemical active matrix addressed electrochromic display[131]

Another type of dual-purpose device is one that operates as both a light-emitting display and a photovoltaic device. These types of devices offer the possibility of an electroemissive

display that can be powered by reversing the operation of the device from light-emission to light-harvesting within the same active layer.[132-135] Yet another dual-purpose device is an electrochromic/electroluminescent (EC/EL) display. This device can operate as a color changing display in ambient lighting conditions where the electrochromic contrast is sufficient while operating as an electroemissive display when lighting conditions are low. A dual EC/EL display would offer advantages over currently utilized emissive devices that operate with the use of a liquid crystal display or light-emitting diodes. Both liquid crystal and LED devices have a low display contrast in direct or bright light situations sacrificing image quality. A device that operates in this manner has been demonstrated in the literature.[136] However, the electrochromism and electroluminescence occur from different layers within the device and not from the same material. It is our goal to demonstrate a dual EC/EL display utilizing the same active layer for both electrochromic and electroluminescent operation of the device, simplifying device fabrication and operation.

Before the concept of a dual EC/EL device is discussed, we investigate unique properties of reflective electrochromic displays utilizing soluble propylenedioxythiophene polymers as the active electrochromic layer. The phenomenon of unsymmetrical switching is introduced and the factors contributing to this property are explored with a model proposed. In addition, we study the possibility of an application of these ECDs as electrochromic variable optical attenuators due to the high optical contrasts seen in the NIR region.

The next two chapters will focus towards the goal of creating a dual EC/EL device with Chapter 3 directed towards the examination of both MEH-PPV/solid electrolyte blends and carbazole-based copolymers with ion solvating groups as the active layers in reflective ECDs. In this chapter, two types of electrochromic device configurations will be analyzed with the

carbazole-based copolymers and MEH-PPV as the active electrochromic layers. One device contains an ITO/glass working electrode and an aluminized porous membrane as the reflector while the other has an ITO-glass working electrode with reflection occurring off a porous white reflector. In Chapter 4, the fabrication of model MEH-PPV PLEDs devices is described which allow for the optimization of device fabrication and characterization protocols. This then leads to the fabrication of MEH-PPV/PEO/LiOTf blend PLECs followed by the combination of both ECD and LEC concepts into a dual EC/EL device with MEH-PPV as the active layer. We will show that, depending how the electrodes are biased, the device can exhibit electrochromism and light emission from the MEH-PPV layer. The dissertation will be concluded with a chapter detailing the instrumentation and materials used throughout this work in Chapter 5. The unifying theme throughout this dissertation is the utilization of soluble electrochemically doped polymers in both electrochromic and light-emitting devices for both NIR applications (as with the EC/VOAs) and visible light displays

CHAPTER 2
REFLECTIVE ELECTROCHROMIC DEVICES OF DISUBSTITUTED POLY(ProDOTS) AS VARIABLE OPTICAL ATTENUATORS

Reflective electrochromic devices act to modulate incident electromagnetic radiation by varying the amount of light reflected from the device. This is accomplished through employing an electrochromic material at the active working electrode. Traditionally, the focus has been on visible light electrochromism with the device acting as a display or electrochromic mirror, switching between highly colored and highly reflective states. Recent attention has been paid to the possibility of modulating light at longer wavelengths extending from the NIR into the far IR regions of the spectrum.[26-28, 57]

Of the available electrochromic materials, conjugated conducting and electroactive polymers hold the most promise due to their processability, fast switching speeds, and high optical contrasts. Many conjugated polymers synthesized in recent years are soluble in common organic solvents, allowing for processing through spray-casting or roll-to-roll fabrication of devices. Switching speeds considerably improved over other electrochromic materials, such as WO_3, have been demonstrated for several conjugated polymers in the reflective device platform with full optical contrast achieved in a tenth of a second. Optical contrasts in the visible region in excess of 50%, 80% in the NIR and 50% in the mid-IR have been demonstrated.[56, 57]

Reflective Device Construction

The reflective electrochromic devices were constructed as shown in the schematic and photographs in Figure 2-1. The polymer-coated counter electrode was fabricated by electrochemically depositing PEDOT onto a square of gold-coated Kapton® contacted with copper tape. The next layer of the device consists of three pieces of porous separator soaked with gel electrolyte. The top layer is a gold-coated porous membrane onto which the active electrochromic polymer layer has been either electrochemically deposited or spray-cast. The

entire device is then encapsulated by sandwiching between a back support layer and a transparent window and sealed on all four edges with transparent tape. A more detailed description of the materials utilized in fabricating the devices can be obtained in Chapter 5.

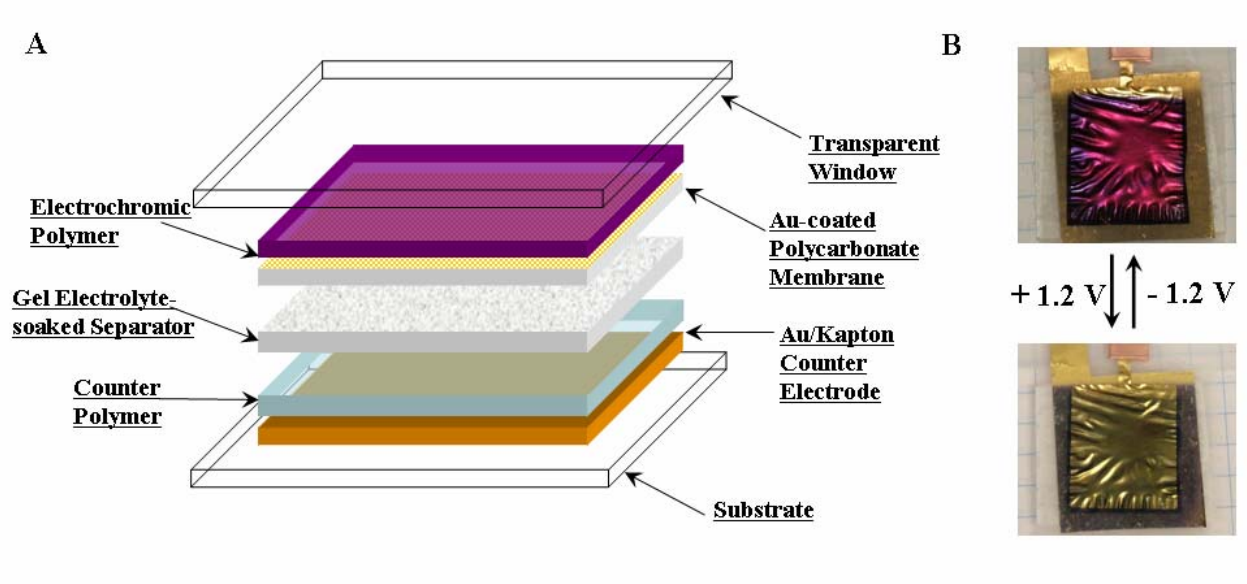

Figure 2-1. Schematic of a reflective electrochromic display (A). Photographs (B) of a PProDOT-$(CH_2OEtHx)_2$ reflective electrochromic device when fully reduced (top) and fully oxidized (bottom).

The PEDOT layer is polymerized to a thickness such that the charge to switch is greater for the counter electrode than for the working active electrode. This ensures that the electrochromic switching at the working electrode is the most efficient, yielding a full optical contrast. As the counter polymer layer does not lend any of its optical properties to the device, only acting as a charge-balancing layer in the electrochemical cell, practically any electrochromic polymer can be used. The properties of interest for this polymer layer are electrochemical stability and relative switching speed over the potential range the device is switched.

The porous separator acts to physically separate the working electrode and the counter electrode, preventing electrical shorts in the device. This layer also prevents any optical changes that occur at the counter electrode from being seen and, as a result, spectral changes from being

measured at that electrode. The gel electrolyte utilized consists of an appropriate salt (typically $TBAPF_6$) dissolved in a propylene carbonate (PC) swollen PMMA matrix. The addition of PMMA to the electrolyte increases the viscosity of the solution, preventing leaks, allowing for long-term storage and testing of the device, while not affecting electrochemical stability.

The working active layer consists of a porous polycarbonate membrane that has been metallized by thermal evaporation of gold to a thickness of 60 nm. This thickness provides for a sufficiently conducting electrode that is highly reflective. The active polymer layer is deposited by electrochemical polymerization from a monomer solution at a constant potential, or spray-casting from solution using a commercial airbrush. The device is placed on a plastic transparency film support and a transmissive window is placed on top, also composed of plastic transparency film for this study. The device is sealed by either using epoxy or wrapping transparent tape around the edges. With the materials utilized in this particular device construction, the entire device is flexible and, in addition, can be patterned to a variety of sizes and shapes.

The reflectance spectroelectrochemistry for a device containing bis(ethylhexyloxy)-substituted poly(3,4-propylenedioxythiophene) (PProDOT-$(CH_2OEtHx)_2$) as the active electrochromic layer is shown in Figure 2-2. The spectroelectrochemistry of the device is measured by applying a potential between the two electrodes (counter and working) and measuring the reflectance spectra at each applied potential. The reflectance measured is both specular and diffuse by utilizing an integrating sphere attachment to the spectrophotometer. As each potential is applied and held (typically in increments of 50 to 200 mV), the reflectance of the device is measured in the wavelength range of 2.0 μm to 350 nm. For all spectroelectrochemical measurements, the reflectance is taken as a difference from that of a

reference device that contains all of the same components as the device measured except for the active polymer layer. For the disubstituted PProDOT devices, the active layer is fully neutralized at -0.8 V and fully oxidized at +1.2V.

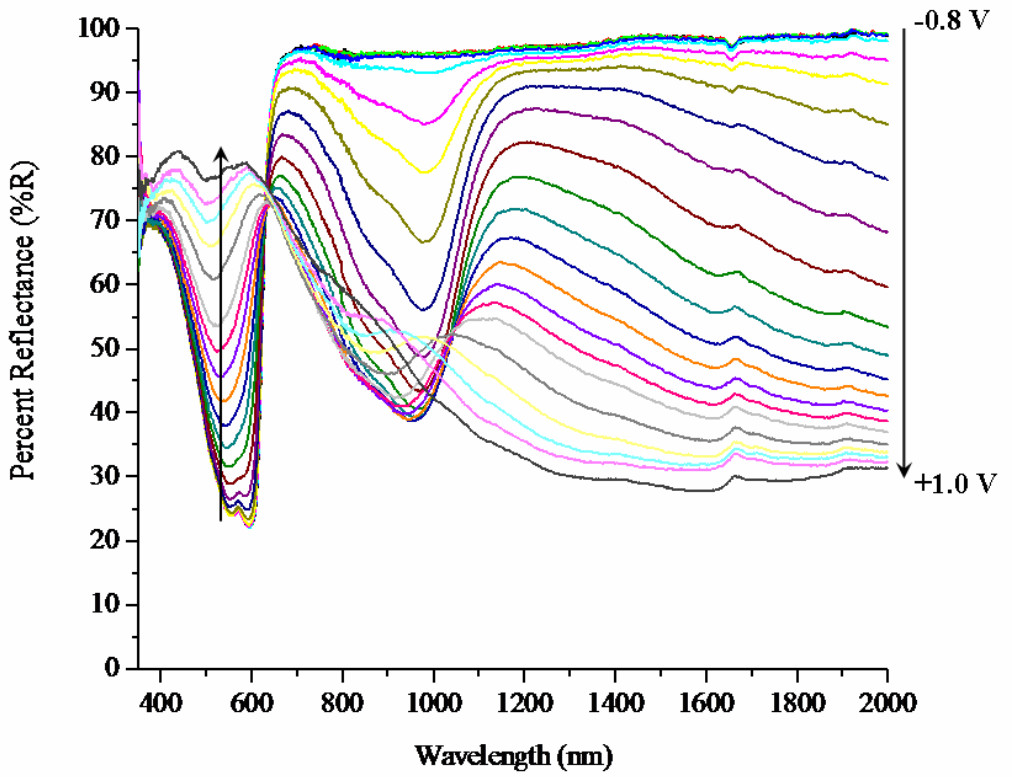

Figure 2-2. Reflectance spectroelectrochemistry of a 236 nm thick PProDOT-$(CH_2OEtHx)_2$ film in a reflective ECD.

Unsymmetrical Switching

On switching reflective electrochromic devices with PProDOT-$(CH_2OEtHx)_2$ as the active electrochrome, it was realized that at low applied potentials, there were large reflectance contrasts in the NIR with little to no change in the visible region. This is illustrated in Figure 2-3A, where the spectroelectrochemical series is shown for the potential range of -0.8 V and +0.4 V for a device having a 750 nm thick film. In the visible region, there is a 2.5% reflectance change, whereas a large 70-90% change occurs in the NIR extending from 0.8 to 2.0 μm. When higher potentials are applied to the device, +0.5 V to +1.2 V, the visible region reflectance

begins to increase with a contrast of 30-40% occurring between 500 and 550 nm as is shown in Figure 2-3B. This phenomenon is unexpected given that the introduction of the mid-gap states, and hence increase in absorbance at longer wavelengths, occurs at the expense of the π-π^* transition as is shown in Figure 1-1 and as seen in the transmittance spectroelectrochemistry of a similar polymer (PEDOT) in Figure 1-2.

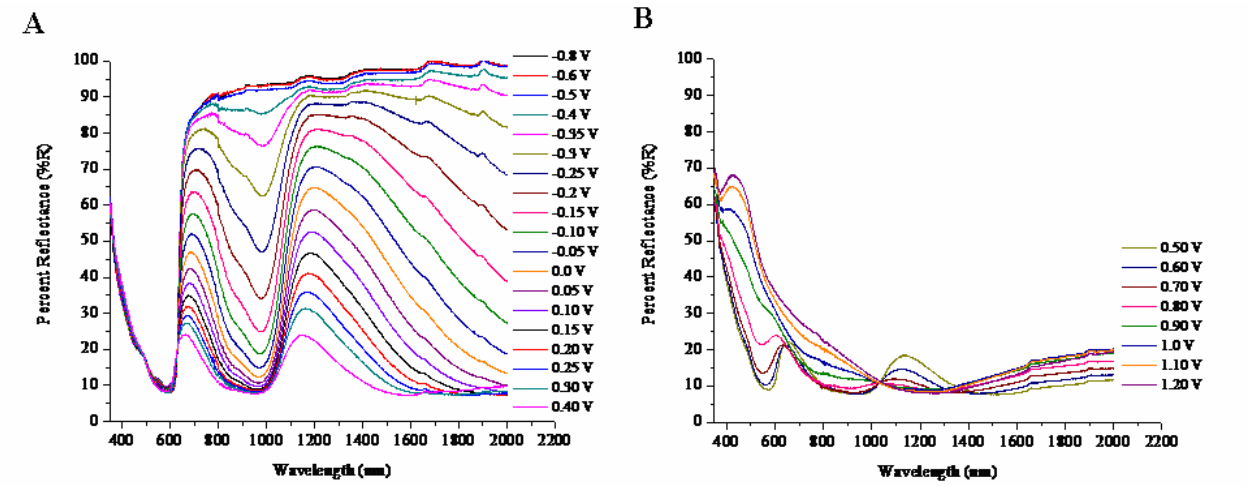

Figure 2-3. Reflectance spectroelectrochemistry of a 750 nm thick PProDOT-$(CH_2OEtHx)_2$ film in a reflective ECD between the applied potentials of A) -0.8 V and +0.4 V and B) +0.5 V and +1.2 V.

To determine the factors contributing to this phenomenon, a comparison of devices of two different disubstituted PProDOTs were made of various film thicknesses, and by different film deposition methods. The reflectance of these devices were then compared to the transmittance spectra of films on ITO of the same polymers, film deposition methods, and film thicknesses.

Films of several different thicknesses (181, 236, and 450 nm) were spray-cast on the gold-coated membranes for the reflective ECDs and onto ITO-glass for transmittance measurements. As can be seen in Figure 2-4, on comparison of the percent reflectance versus applied cell potential (A) for the reflective device and percent transmittance versus applied potential (B) for the film on ITO-glass, both with a polymer film thickness of 450 nm, the change in NIR

reflectance occurs 400 mV before any change in the visible region reflectance occurs in the device, exhibiting unsymmetrical switching.

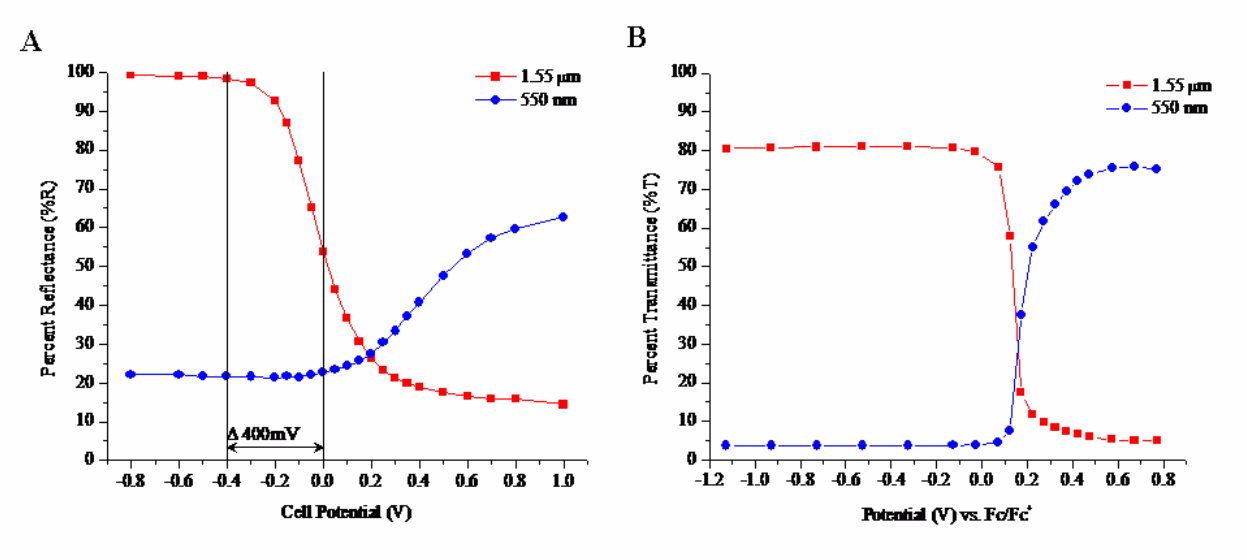

Figure 2-4. Percent reflectance versus cell potential (A) for a 450 nm thick PProDOT-$(CH_2OEtHx)_2$ film reflective ECD. Transmittance versus potential (B) for a film of the same polymer and thickness on ITO-glass in 0.2 M $TBAPF_6$/PC electrolyte.

On the other hand, for that same polymer thickness, the NIR and visible region transmittance change occurs at the same potential, as is seen in Figure 2-4B, not exhibiting any unsymmetrical switching. As the film thickness is decreased in the reflective ECDs, the extent of unsymmetrical switching decreases, shown in Figure 2-5, for a 181 nm thick film with the device exhibiting no unsymmetrical switching, indicating a polymer film thickness dependence of this phenomenon

In order to determine whether this phenomenon is isolated to only the chemically polymerized spray-cast polymer, films of PProDOT-$(CH_2OEtHx)_2$ were electrochemically polymerized potentiostatically directly onto ITO-glass. The final film thickness was controlled by setting the polymerization to terminate when a predetermined charge had passed at the working electrode. The resulting film thickness at the ITO electrode was then measured by profilometry. The polymer films on the gold-coated porous membrane working electrodes were

obtained by the same method. Given that the thickness of the polymer films on the gold-coated porous membranes could not be measured by profilometry, it was assumed that the thickness produced on the membrane was similar to that on ITO with the charge passed for polymerization corrected for the electrode area differences.

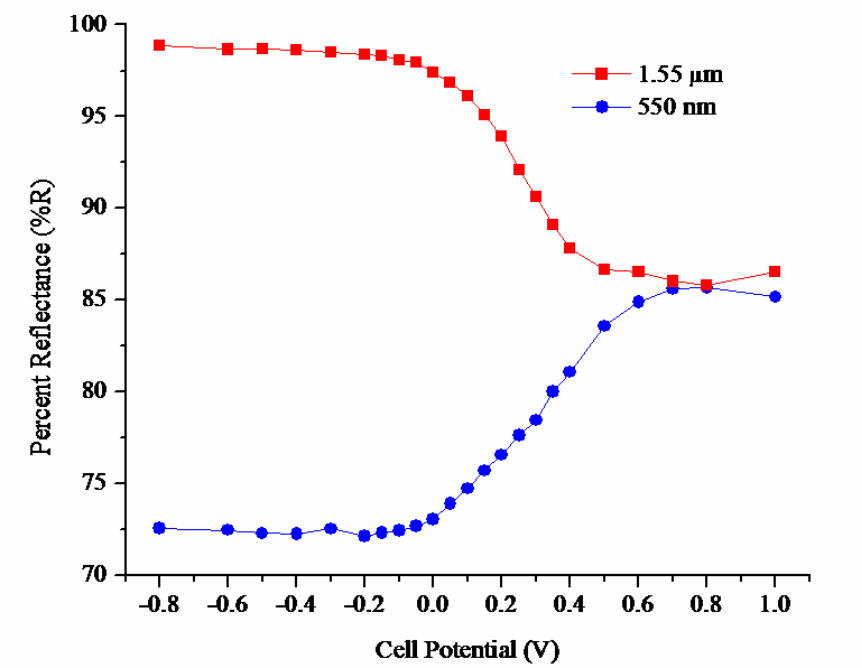

Figure 2-5. Percent reflectance versus cell potential for a 181 nm thick PProDOT-$(CH_2OEtHx)_2$ film reflective ECD demonstrating the lack of unsymmetrical switching in the thinner films.

The reflectance spectroelectrochemical series for a polymer film 998 nm thick in an ECD is shown in Figure 2-6A and that of the same film thickness measured by transmittance on ITO-glass is shown in Figure 2-6B. The NIR reflectance begins to decrease at -0.4 V while the visible region reflectance begins to increase at +0.1 V, 500 mV later for the polymer film in the reflectance device. On the other hand, the NIR transmittance decreases at the same applied potential for the polymer film on ITO-glass. This can be more clearly see in Figure 2-7 where the percent reflectance versus cell potential for the three different film thicknesses (111, 538, and 998 nm) of electropolymerized polymer are shown. Similarly, with the spray-cast films, this

extent of unsymmetrical switching in the reflective ECDs shows a film thickness dependence on the electrochemically polymerized films.

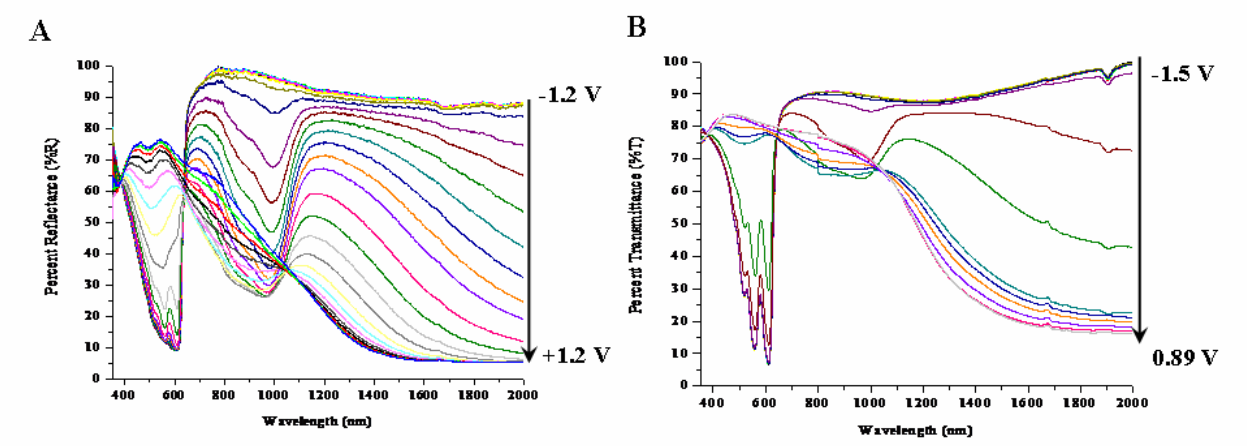

Figure 2-6. Reflectance spectroelectrochemistry (A) for a 998 nm thick electropolymerized PProDOT-$(CH_2OEtHx)_2$ film in an ECD. Transmittance spectroelectrochemistry (B) for a film of the same thickness on ITO-glass in 0.2 M $TBAPF_6$/PC with potentials referenced versus Fc/Fc^+

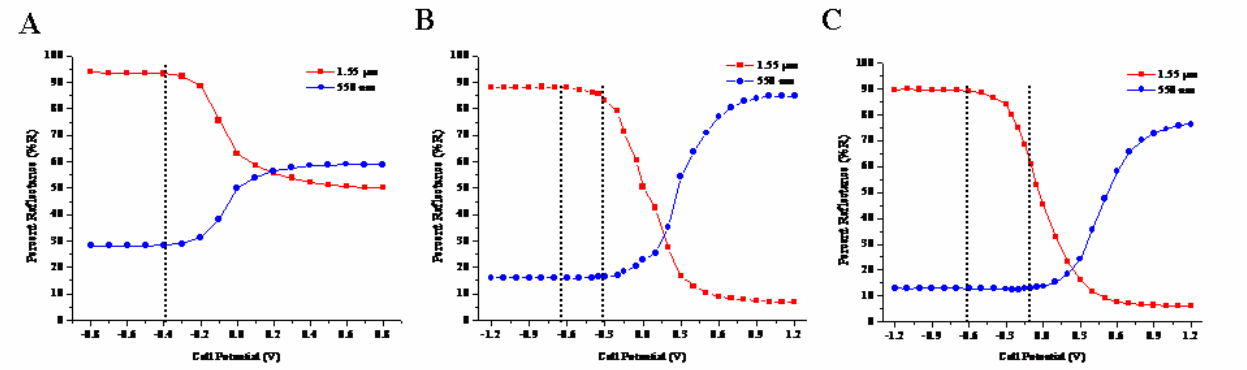

Figure 2-7. Percent reflectance versus cell potential for reflective ECDs of electrochemically polymerized PProDOT-$(CH_2OEtHx)_2$ of thickness A) 111 nm, B) 538 nm, and C) 998 nm.

A comparison was made between films on ITO-glass and in reflective ECDs of two different spray-cast polymers, PProDOT-$(CH_2OEtHx)_2$ and PProDOT-Hx_2. Initial experiments where the unsymmetrical switching was evident were performed on devices containing the alkoxy branched polymer, PProDOT-$(CH_2OEtHx)_2$. The linear alkyl derivative was then investigated for the presence of unsymmetrical switching when incorporated in reflective devices

to determine whether this phenomenon is isolated to one specific polymer or is present in the family of disubstituted PProDOTs.

As Figure 2-8 shows, unsymmetrical switching is found to occur in the linear alkyl derivative as well when incorporated into reflective ECDs, but not when measured by transmittance on ITO-glass. This indicates that the phenomenon is not due to the branched alkoxy groups on the polymers, but rather to the large optical contrasts in the NIR and the relative ease with which to prepare thick films, both spray-cast and electrochemically polymerized, for this family of polymers.

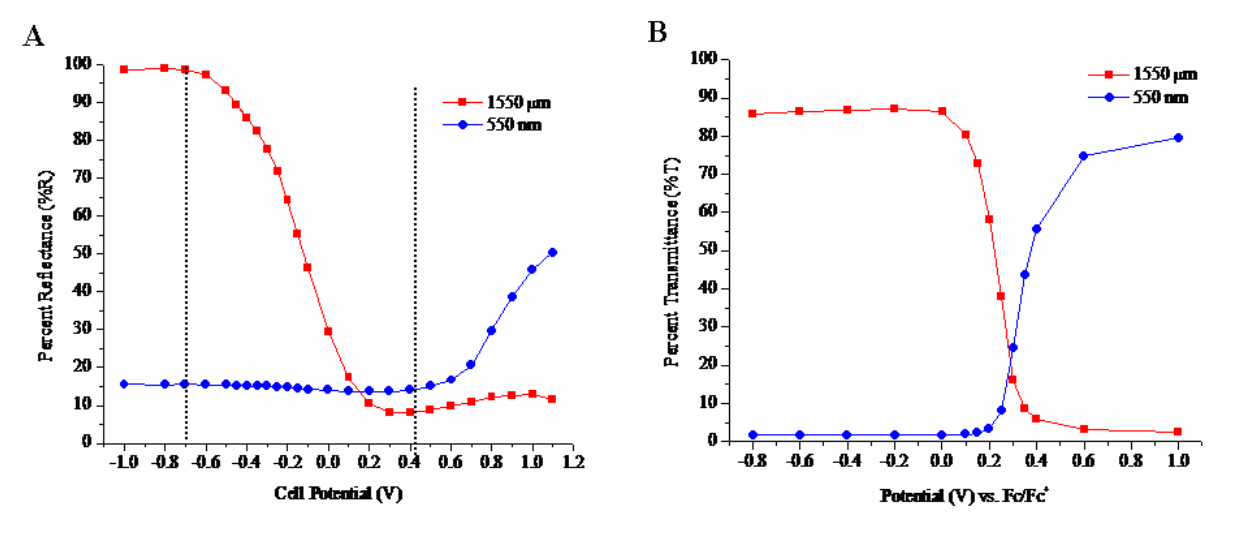

Figure 2-8. Percent reflectance versus cell potential(A) for a 351 nm spray-cast film of PProDOT-Hx_2 in a reflective ECD. Percent transmittance (B) versus potential for a film of the same thickness on ITO-glass in 0.2 M $TBAPF_6$/PC. Potentials are referenced vs. Fc/Fc^+.

Conductive Front

Here, a model is proposed for the effect of unsymmetrical switching in reflective ECDs of conjugated conducting polymers. As was discussed previously in Chapter 1, a conjugated conducting polymer is insulating in its neutral, undoped state. Other researchers have shown that there is a process whereby the neutral polymer film is oxidized electrochemically in a localized

area beginning at the electrode/polymer interface.[137-143] This oxidized area is now conductive and acts as an extension of the metallic electrode to further oxidize to conductive domains farther from the electrode surface. This process continues until the conductive zone, or front, reaches the polymer film surface and is shown schematically in Figure 2-9.

When the film is neutral and insulating, the polymer is highly absorptive in the visible region and highly transmissive in the NIR. As can be seen in the spectra in Figure 2-9A, a large amount of light in the visible region is absorbed (~90% at λ_{max}) and therefore only a small amount is able to traverse the entire film and be reflected back by the gold electrode. On the other hand, ~90% of the light in the wavelength range of 800 to 2000 nm is measured, indicating that nearly all the light is able to penetrate through the entire film, be reflected by the electrode and travel through the film a second time to be measured.

At low applied potentials, the film becomes oxidized to a small distance from the polymer/electrode interface. The concentration of conductive sites is low and the redox-doped front does not penetrate far into the insulating film as shown in Figure 2-9B. Given that the NIR light is able to penetrate the entire polymer film, this small increase in the concentration of oxidized species at the polymer/electrode interface is able to be probed at those wavelengths and a change in the spectra is observed. However, nearly all of the visible region light is absorbed by the polymer film before reaching the conductive front and no change in the redox state of the polymer is measured by this wavelength range. This can be seen in the reflectance spectra where an absorbance change is seen in the wavelength range of 700 to 2000 nm with no change in the visible region below 700 nm. As the doping level increases at higher applied potentials, the concentration of oxidized sites increases and the conductive front propagates farther into the polymer film, as shown in Figure 2-9C.

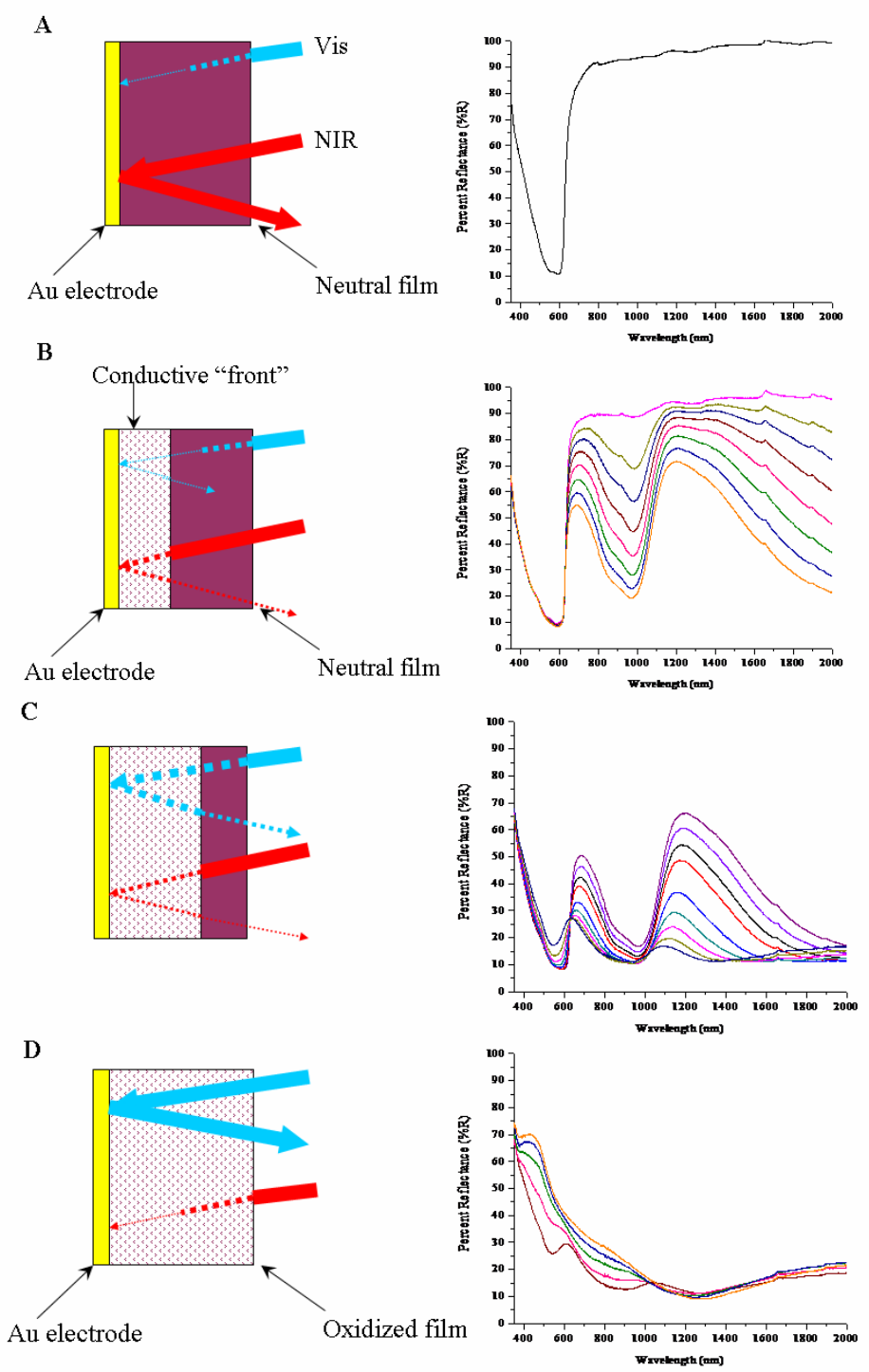

Figure 2-9. Conductive front model. A) Schematic of fully neutralized film showing penetration of visible (blue line) and NIR (red line) and respective spectra. Width and dashing of lines indicate intensity of light. B) Conductive front propagating through film at low applied potentials. C) Conductive front propagating further into film at higher applied potentials, past the penetration depth of visible light. D) Fully oxidized film.

An even higher concentration of oxidized species is probed by the NIR light and, since the conductive front has now extended past the penetration depth of the visible light, there is now a measure of the oxidized portion of the film by this wavelength range as shown with a change in the visible region absorbance. The NIR absorbance is constantly increasing as the concentration of doped polymer is increasing, but the measurement of optical change in the visible region cannot occur until the conductive front extends past the penetration limit of visible light. Once the entire film becomes fully oxidized, as is shown in Figure 2-9D, the polymer is highly absorbing in the NIR and highly transmissive in the visible region, with the visible light now able to penetrate through the entire film to the exposed gold electrode underneath.

The distance to which light can penetrate a material can be determined from the penetration depth, δ, also known as the skin depth. This depth is dependent on the absorption coefficient of the sample and is defined as the depth at which the intensity of radiation inside the material falls to 1/*e* of the original value at the material surface and is calculated by:

$$\delta = 2/\alpha \tag{2-1}$$

where α is the absorption coefficient and can be determined from the transmission through the sample of known thickness as shown schematically in Figure 2-10. To determine this value for the entire wavelength range, polymer films of several different thicknesses were deposited on glass and the transmittance through the polymer film from the wavelength range of 350 nm to 2000 nm were measured. These films can be treated as planar layered structures from which the optical transmission can be determined while taking internal reflections into considerations. For the case of an absorbing layer (polymer film) on a nonabsorbing substrate (glass), the relation between optical transmission and absorption coefficient has previously been determined[144] and is as follows:

$$T = \frac{(1 - R_{01})(1 - R_{12})(1 - R_{23})A}{1 - R_{12}R_{23} - A^2 R_{01}(R_{12} + R_{23} - 2R_{12}R_{23})} \tag{2-2}$$

and the value of A is defined as $A = e^{-\alpha t}$ (where t is the thickness of the absorbing polymer layer), and R_{jk} is the layer-layer power reflection coefficient for each layer noted in Figure 2-10.

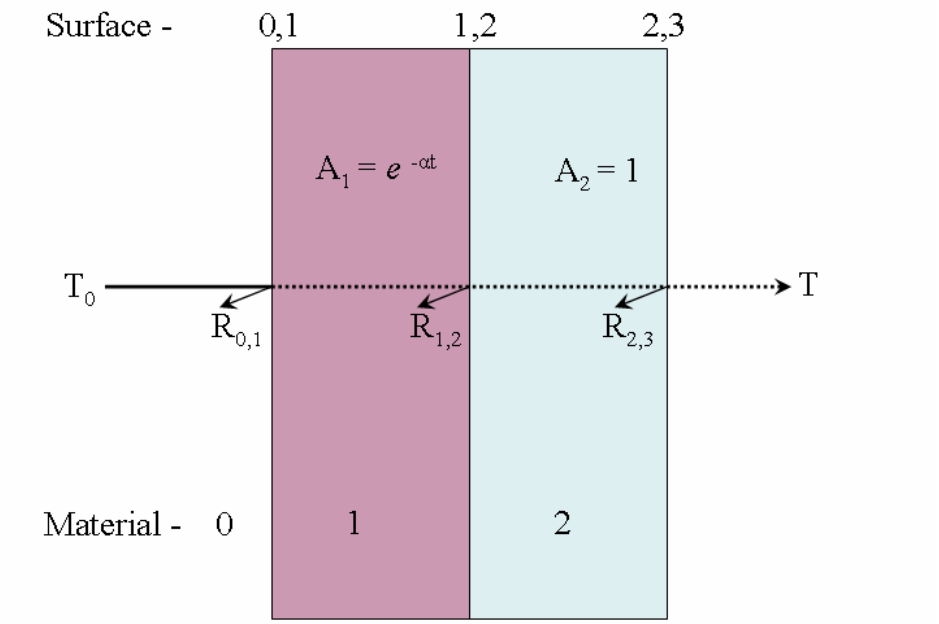

Figure 2-10. Schematic of multilayer geometry used in analysis of penetration depth of optical radiation through the polymer sample. Material 1 is the absorbing polymer film, material 2 is the nonabsorbing glass substrate. The reflections at each surface are indicated by R_{jk}.

Given that the reflections at each surface are much less than 1, the denominator in equation 2-2 reduces to 1 and the transmission then becomes:

$$T = (1 - R_{01})(1 - R_{12})(1 - R_{23})e^{-\alpha t} \tag{2-3}$$

If the ratio of the transmission,T, for samples of two different thicknesses (A and B) are taken, the equation reduces further to:

$$\frac{T_B}{T_A} = \frac{e^{-\alpha t_B}}{e^{-\alpha t_A}} = e^{-\alpha(t_B - t_A)} \tag{2-4}$$

The penetration depth, δ, is now calculated by:

$$\delta = \frac{2}{\alpha} = \frac{-2\,(t_B - t_A)}{\ln T_B - \ln T_A} \tag{2-5}$$

The penetration depth for spray-cast films of PProDOT-$(CH_2OEtHx)_2$ were determined by measuring the transmittance of samples of various thicknesses (specifically 93, 133, and 189 nm) over the wavelength range of 350 nm to 2000 nm and calculating the penetration depth from equation 2-5. The average penetration depth at 1.55 μm was calculated to be 15 μm and that at 550 nm (the λ_{max} for this polymer) was calculated to be 0.35 μm. Therefore, film thicknesses of this polymer of 0.15 μm or less should exhibit no unsymmetrical switching when incorporated into reflective ECDs as the light in the visible region is able to travel through the entire polymer film, be reflected off the gold electrode and travel back to be measured. In films thicker than 0.35 μm, the penetration depth is not far enough for the light to reach the polymer/electrode interface to measure any optical changes that occur close to the electrode at low oxidation potentials, which is the case as was shown in Figure 2-7 for three different film thicknesses of PProDOT-$(CH_2OEtHx)_2$ in reflective ECDs.

This phenomenon of unsymmetrical switching exhibited by these devices has possible applications with one being variable thermal control. It can be imagined a reflective device that, when in the fully reduced state, allows for all NIR light to be fully reflected while the device is colored. By adjusting the device bias, it remains in that colored state in the visible region, but the NIR light is absorbed and can be collected and transferred using a heat conducting element. Another possible application for this feature is the utilization of this device in combination with a solar cell placed such that light is reflected off the ECD before being directed to the solar cell. The amount of light in the near to mid IR impinging on a photovoltaic device can be tuned while excluding light from the visible region. In effect, the device would act as a tunable filter for the

solar cell. Yet another possible application is in the area of optical telecommunications and will be discussed in the next section.

Reflective ECDs as Variable Optical Attenuators

A device that can take advantage of the large, tunable NIR contrasts exhibited with conjugated polymer ECDs is the variable optical attenuator (VOA). VOAs are key components in fiber-optic telecommunications networks and are utilized to reduce signal power by inducing a fixed or variable loss.[145, 146] VOAs are also often required in applications where photosensitive components require dissimilar incident optical signals, and hence variable sensitivities and saturation points. The attenuator regulates the light intensity to be within the dynamic range of the component, preventing any damage or overloading.

In recent years, the use of wavelength division multiplexing (WDM) has become important to handle the increased demand placed on optical telecommunications by fiber-optic transmission.[147, 148] With WDM, a number of signals of differing wavelengths are combined onto a single fiber allowing for increased signal density without increasing the amount of optical fiber used. These systems require that the optical power between all channels be equalized before combination. Direct control of the source for each signal is not practical as changes in the laser drive current can lead to an undesirable wavelength shift. VOAs allow for adjustment of the channel power while maintaining wavelength stability.

Another application of VOAs is for channel balancing to optimize the optical power of signals at key points in the networks. Optical power levels are determined by the optical loss along the transmission line and can vary with the length of the line, the number of connection points, and the efficiency of optical components (e.g., couplers, amplifiers, and source) and deterioration of the signal-to-noise ratio may reduce the optical transmission quality. A VOA is

capable of maintaining the light level acting as a noise discriminator, reducing the intensity of spurious signals to below a threshold value.

Additionally, VOAs serve to control feedback in optical amplifier control loops to maintain a constant output (e.g., as an automatic gain control element (AGC)). In WDM systems, transmission loss is compensated by utilizing erbium-doped amplifiers (EDFAs), which amplify the signal made up of numerous wavelengths. However, EDFA gain is wavelength-dependent and a gain equalizer is needed that has a wavelength dependence profile that is the inverse of the EDFA in order to maintain a flat transmission bandwidth. However, when there is a change in the optical power to the EDFA, the wavelength dependence of the EDFA gain profile changes. Since the profile of the gain equalizer is fixed, there is a shift in the flattening effect that it provides. The VOA allows for tuning of the signal to compensate for this gain tilt and flattens the transmission profile.

When considering the optical performance of a VOA, the most important specifications are insertion loss and range of optical attenuation. These values are typically reported for the most commonly used wavelengths, 1.55 and 1.31 μm as these are the wavelengths where absorption and dispersion are the lowest for silica fibers. The range of optical attenuation is the minimum and maximum attenuation values achievable by the device with optical attenuation measured by:

$$\text{Optical Attenuation (dB)} = 10 \log_{10} (I_{off}/I_{on}) \tag{2.6}$$

where I_{off} and I_{on} are the intensity of the signal when the attenuator is in the "off" state and "on" state, respectively. Many VOAs either transmit or reflect light so intensity is the percent reflected or transmitted by the attenuator. For a variable optical attenuator, the on state can be tuned as a function of voltage applied to the device yielding a dynamic attenuation range. Typical VOA attenuation values range from 10 to 25 dB with many VOAs able to achieve up to

50 dB attenuation. To illustrate the significance of such values, a 3 dB loss leaves 50% of the original light signal, a 10 dB loss leaves 10%, and a 20 dB loss leaves 1%.

Ideally, when the attenuator is in the off state, the amount of light transmitted or reflected would be 100%, very often this is not the case. The insertion loss (or optical loss) is the amount of light lost when the attenuator is off and is calculated by:

$$\text{Optical Loss (dB)} = 10 \log_{10}(100\%/I_{off}) \tag{2.7}$$

where again, I_{off} is the intensity of the optical signal when the attenuator is off and is commonly expressed as percent transmittance or percent reflectance. Optical loss in a fiber-optic system is additive, therefore the loss due to the introduction of a VOA into the network is needed to be kept to a minimum. Given that the loss due to fiber attenuation alone can be as low as 1 dB/km, for many applications, the maximum insertion loss tolerated is less than 1 dB.

Optical attenuation and insertion loss values vary with the type of attenuator device utilized with there being a large number of devices that are either commercially available or currently researched. Many of these devices differ in their operating mechanism, which also determines other performance characteristics such as drive voltage, switching speed, and size. The most common VOAs being developed are those that include liquid crystal devices, mechanical actuators, microelectromechanical (MEMs) devices, and electrochromic devices.

The liquid crystal devices operate by passing the light through a liquid crystal element.[149, 150] When a voltage is applied to the device the liquid crystal molecules are oriented in such a way that light is attenuated. These devices allow for efficient tunable attenuation; however, liquid crystals are temperature sensitive and as the temperature of the surrounding environment varies, the optical properties of the liquid crystal change, resulting in higher insertion loss and inaccurate attenuation.

The mechanical attenuators operate by a variety of methods to affect attenuation.[147, 151] One method uses a rotatable filter placed between an input fiber and an output fiber and varies the attenuation by rotating the filter. Another mechanical attenuator involves changing the alignment between the axis of input and output fibers, varying the quantity of light coupled between the fiber ends. Yet another mechanical attenuator utilizes a moveable mirror, varying the angle at which an incident ray is reflected, thereby tuning the amount of light directed to the input optical fiber, and causing attenuation. These devices offer effective attenuation and low optical loss. Unfortunately, mechanical optical attenuators have the drawbacks of high operating voltages (10-20 V) and moving parts that can be relatively slow to engage and can wear and eventually fail. In addition, these devices do not lend well to miniaturization, a feature increasingly sought after for the realization of higher density networks and the ability to attenuate individual fibers independently.

On the other hand, research of MEMs devices as VOAs has become increasingly popular as these devices offer high attenuation, low optical loss, fast switching speeds and lend themselves easily to miniaturization.[152-155] These devices are microstructures that act as actuators with the most common utilizing a mirror or rigid shutter to reflect or block a light beam when a variable voltage or current is applied. Their very elegant design, however, adds a level of complexity that makes manufacturing of these devices on a scale outside the research laboratory impractical and cost prohibitive.

Recent interest has grown in utilizing electrochromic materials and displays for VOA devices.[156-166] Many of the materials reported in the literature are based on traditional electrochromic materials such as WO_3, ruthenium complexes, and polynuclear molybdenum complexes. The molybdenum complexes, such as tris(pyrazolyl)boratomolybdenum (V), have

been reported to have the highest attenuation out of these with a value of 50 dB at a low applied voltage.[156, 159, 165] However, the prototype devices are based on a solution of the electrochrome sandwiched between two transparent electrodes. This limits the device architecture , and switching speed, as the species is required to diffuse to the electrode to be redox switched. The transition metal oxide film devices based on WO_3 have also shown impressive attenuation of 40 dB, reaching 20 dB in 2 seconds, but require an hour for the device to return to the transmissive state.[158, 164] Dendritic mixed-valence ruthenium complexes have also been researched as VOA materials with films showing attenuation values of 2-7 dB, switching within 2 seconds.[160-162]

The first reported use of a conjugated polymer as a possible electrochromic VOA material were for films of PEDOT.[163, 167] These devices were shown to have an optical attenuation of 11 dB, switching within 5-7 seconds and a low optical loss of 0.86 dB. Conjugated electrochromic polymers and their devices offer many advantages not available with the other devices and materials discussed. These include a low operating voltage (under ± 1.5 V), mechanical flexibility, improved film processability, and a variety of options in device design and patterning. It is demonstrated in this chapter the applicability of the previously introduced reflective electrochromic displays, with PProDOT-$(CH_2OEtHx)_2$ as the active layer, as an electrochromic variable optical attenuator (EC-VOA).

The reflective ECD was constructed as previously described in this chapter. Briefly, the counter electrode consisted of PEDOT electrochemically deposited onto a gold-coated Kapton® electrode. The next layer was comprised of porous filter papers soaked with a $TBAPF_6$/PMMA/PC gel electrolyte. This was followed by the outward-facing working electrode that was a gold-coated porous polycarbonate membrane onto which the active polymer layer (PProDOT-$(CH_2OEtHx)_2$) was spray-cast. The entire device was encapsulated with a plastic

transparency film back support and cover, and sealed on all four sides with transparent tape. Initial measurements were performed with a UV/Vis-NIR spectrophotometer fitted with an integrating sphere as described in Chapter 5. The percent reflectance of the device was measured for each potential applied and optical attenuation and insertion loss values were calculated using equations 2-6 and 2-7.

As is shown in Figure 2-11, for a 750 nm thick film, the maximum attenuation achieved was 11.2 dB at an applied voltage of 400 mV for the wavelength of 1.55 µm and 10.6 dB at 700 mV for 1.31 µm. The optical loss when this device was fully reduced was low with a value of 0.1 dB at 1.55 µm and 0.2 dB at 1.31 µm.

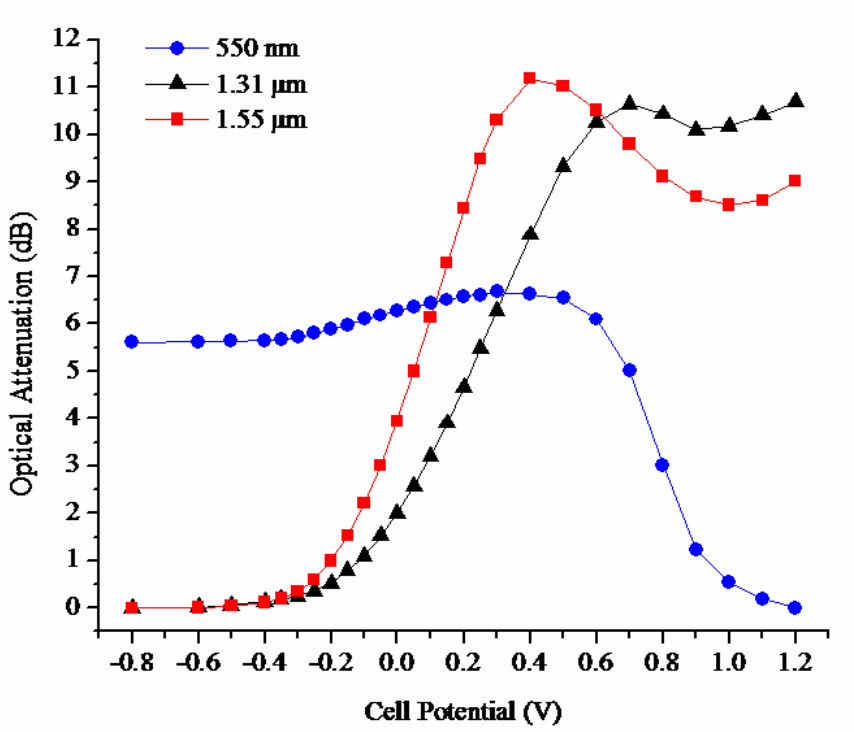

Figure 2-11. Optical attenuation at various applied potentials for a 750 nm thick film of PProDOT-$(CH_2OEtHx)_2$ in a reflective ECD as an EC-VOA at the wavelengths of 550, 1310, and 1550 nm.

To further demonstrate the possibility of this device as an EC-VOA, a model fiber-optic setup was fabricated as shown schematically in Figure 2-12A and in the photograph in Figure 2-

12B. This setup allows the device to be demonstrated in practical-use conditions by coupling the light to the device using a fiber-optic spectrophotometer (described in Chapter 5) and not subtracting the absorbance of a reference device, which would have optimized the final reflectance by taking into account the absorbances from device components. The light from a halogen light source was brought to the device surface with a silica fiber-optic cable and the light reflected at a 45º angle was coupled into another fiber-optic cable and measured using an InGaAs detector in the wavelength range of 1.3-1.55µm.

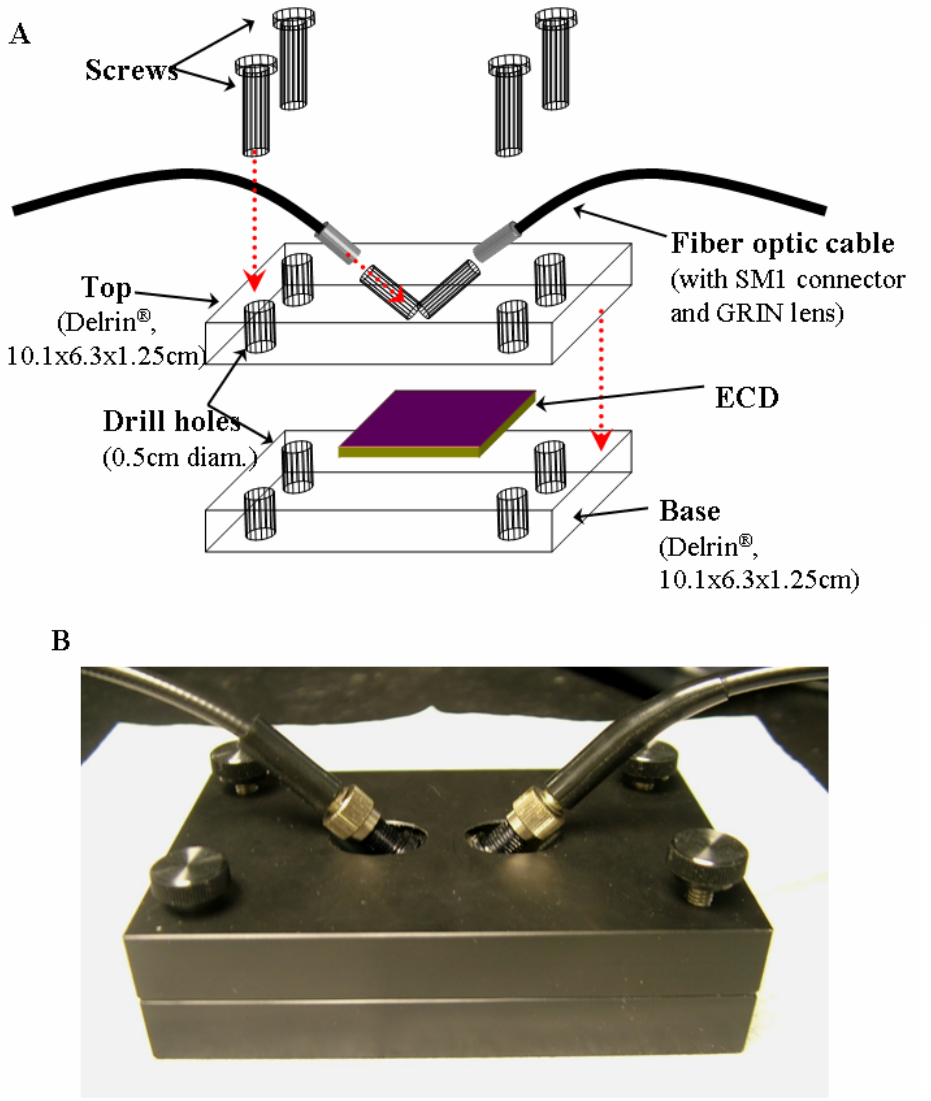

Figure 2-12. Schematic (A) and photograph (B) of setup to measure reflective EC-VOA using fiber-optic spectrophotometer.

The potential across the device was varied and the reflected spectra recorded from which the optical attenuation was calculated as is shown in Figure 2-13. With this device, containing a 430 nm thick film, the maximum attenuation value achieved was 5.4 dB at 1.55 µm and 5.0 dB at 1.31 µm. The maximum optical loss values when the device was neutralized were 0.15 dB and 0.14 dB at the wavelengths of 1.55 and 1.31 µm, respectively. These values could potentially be optimized by utilizing an antireflective coating at the NIR transparent window, to minimize scattering at that surface, and by varying the angle of the fiber-optics with respect to each other and the device to maximize light output.

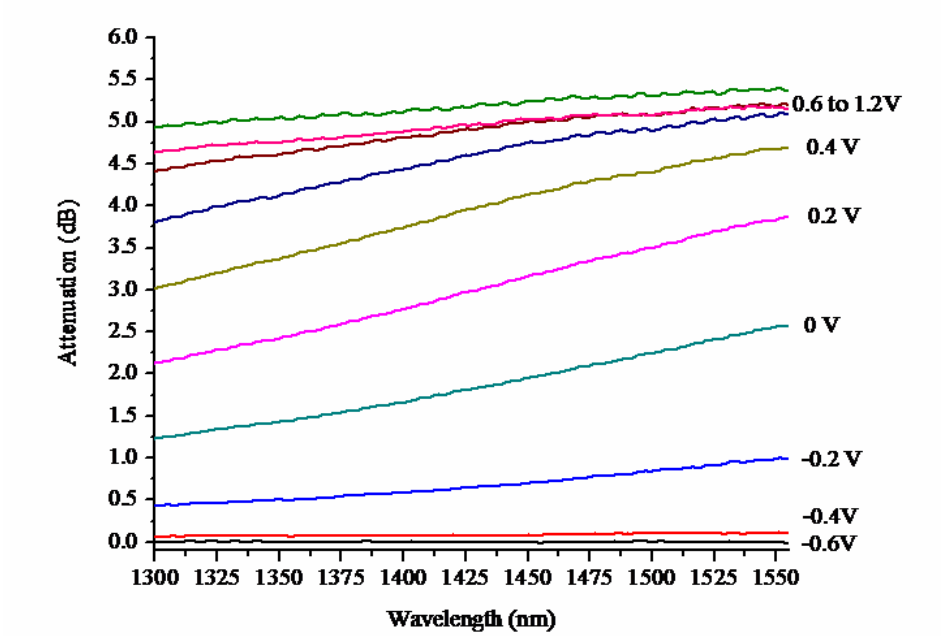

Figure 2-13. Optical attenuation across the wavelength range of 1.3 µm and 1.55 µm for a 450 nm thick film of PProDOT-$(CH_2OEtHx)_2$ in a reflective ECD as an EC-VOA measured using the fiber-optic setup shown in Figure 2-12.

To establish a possible application for the unsymmetrical switching shown previously, the device was switched within a limited voltage range while the reflectance was measured with the integrating sphere setup. When the device is switched between -0.8 V and 0.0 V, the attenuation at 1.55 µm is modulated from 1.9 dB to 0.05 dB. Within the same voltage range, the attenuation at 550 nm varies only between 3.8-4.1 dB as shown in Figure 2-14A. When the voltage is

switched between 0.6 V and 1.2 V, the attenuation in the visible, at 550 nm, varies between 0-0.81 dB, while that in the NIR is between 6.4 and 6.6 dB, as shown in Figure 2-14B. This demonstrates the possibility of modulating the NIR and visible independent of each other by maintaining the switching voltage within a specific window.

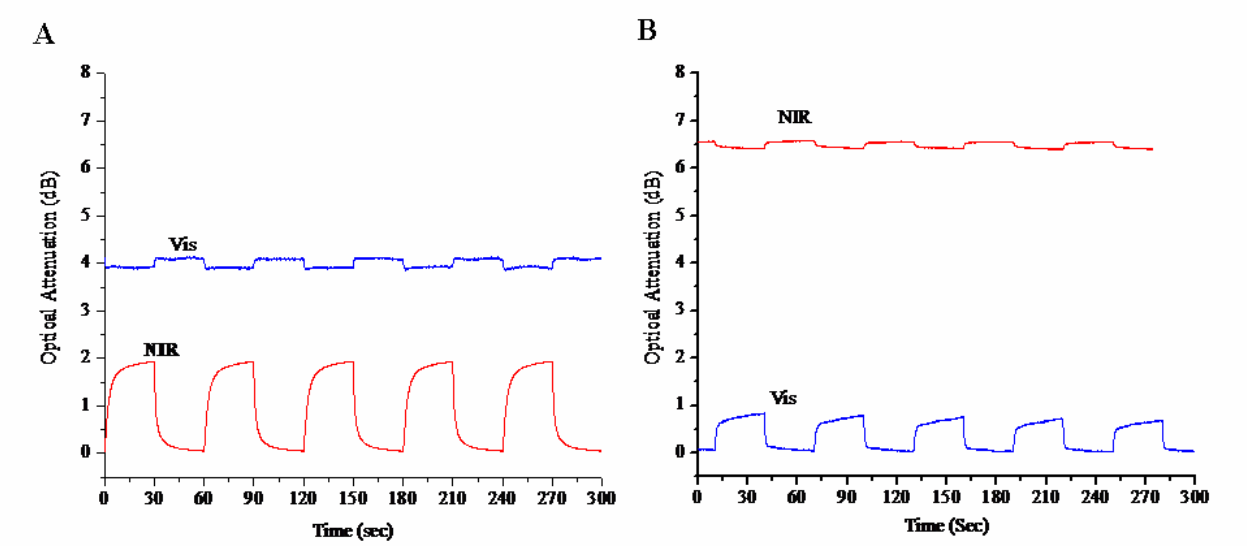

Figure 2-14. Optical attenuation at 1.55 µm (red line) and 550 nm (blue line) of a 450 nm thick film of PProDOT-$(CH_2OEtHx)_2$ in a reflective ECD as an EC-VOA when switched between the potentials of A) -0.8 V and 0.0 V, and B) 0.6 V and 1.2 V.

Conclusions

In summary, it has been demonstrated that at low applied potentials, the NIR reflectance can be modulated in a disubstituted-PProDOT reflective electrochromic device with little to no optical change in the visible region of the spectrum. This can be attributed to the presence of a conductive front that propagates through the polymer film and grows as the potential applied to the device is increased. Given that the visible light cannot penetrate as far into the entire polymer film as the NIR in devices above a specific film thickness, the NIR optical changes are observed to occur before that in the visible. This allows for modulating of the NIR independent of the visible region.

In addition, reflective ECDs containing sprayable PProDOTs have been demonstrated as electrochromic variable optical attenuators. Not only do these devices offer effective optical attenuation and low insertion loss, but also the advantage of mechanical flexibility, low drive voltage and the possibility of patterning for the fabrication of multiple, individually addressable devices in a variety of architectures. Future directions for these devices as VOAs would include optimization of the device performance. This would entail determining the optimum polymer film thickness for the highest attenuation while maintaining a low insertion loss. Additionally, coupling the fiber-optics to the device in such a way as to achieve the maximum reflectance of incident light measured. The possibilities for achieving this would include a fiber-optic holder with adjustable incident and outcoupling angles. The current fiber-optic holder is constructed such that the light measured is at a 45 degree angle to the incident light, however, this may not be the optimum angle for the measurement of reflectance from the devices. Further work could also include patterning of the devices to form individually addressable pixels each containing a separate, miniature, EC-VOA.

CHAPTER 3
ELECTROCHROMIC DISPLAYS OF MEH-PPV AND CARBAZOLE-CONTAINING COPOLYMERS

All conjugated electroactive polymers are potentially electrochromic with many polymers exhibiting multiple colored states.[22] As was introduced in Chapter 1, the color of the polymer neutral state is determined by the polymer bandgap. Some of the most highly researched electrochromic polymers are those based on the alkylenedioxy-bridged thiophenes and pyrroles. The alkylenedioxythiophenes are low bandgap polymers with a π-π^* transition in the visible region making them cathodically coloring, switching from a highly absorptive to a highly transmissive state on oxidation. The presence of electron-donating oxygens adjacent to the thiophene ring acts to raise the HOMO level, lowering the polymer oxidation potential relative to the unsubstituted thiophene polymer. For example, the onset of oxidation for the dioxythiophene polymers, PEDOT and PProDOT-$(CH_2OEtHx)_2$ are -0.2 V and 0.2 V vs. SCE, respectively.[48, 168, 169] This allows these polymers to be more stable in the oxidized form under ambient conditions as their HOMO levels are above the threshold for air stability, which is defined by the O_2 to H_2O redox couple at 0.5 V vs. SCE, shown in Figure 3-1, as they are easily oxidized by molecular oxygen.[170] On the other hand, polymers with HOMO levels lower than 0.5 V vs. SCE, such as MEH-PPV and PFO, are stable in their neutral form under ambient conditions yet become more difficult to electrochemically switch as the oxidation potential increases.[169, 171]

Similarly, the addition of an alkylenedioxy bridge to pyrrole introduces electron density to the already electron-rich pyrrole unit, acting to further lower the polymer oxidation potential to the lowest values reported for conjugated polymers.[22, 50, 54] By substitution at the nitrogen of the pyrrole ring, a reduction in the effective conjugation length can be induced by the steric interactions brought about by torsional twisting and the polymer bandgap can be increased to values greater than 3.0 eV, shifting the neutral polymer absorbance into the UV region.[52] By

increasing the polymer bandgap, the HOMO level is lowered. However, the N-substituted PProDOPs still maintain a low oxidation potential allowing these polymers to have the lowest values for anodically coloring polymers to date. As with the dioxythiophenes, the family of PProDOPs are highly stable in the oxidized state.

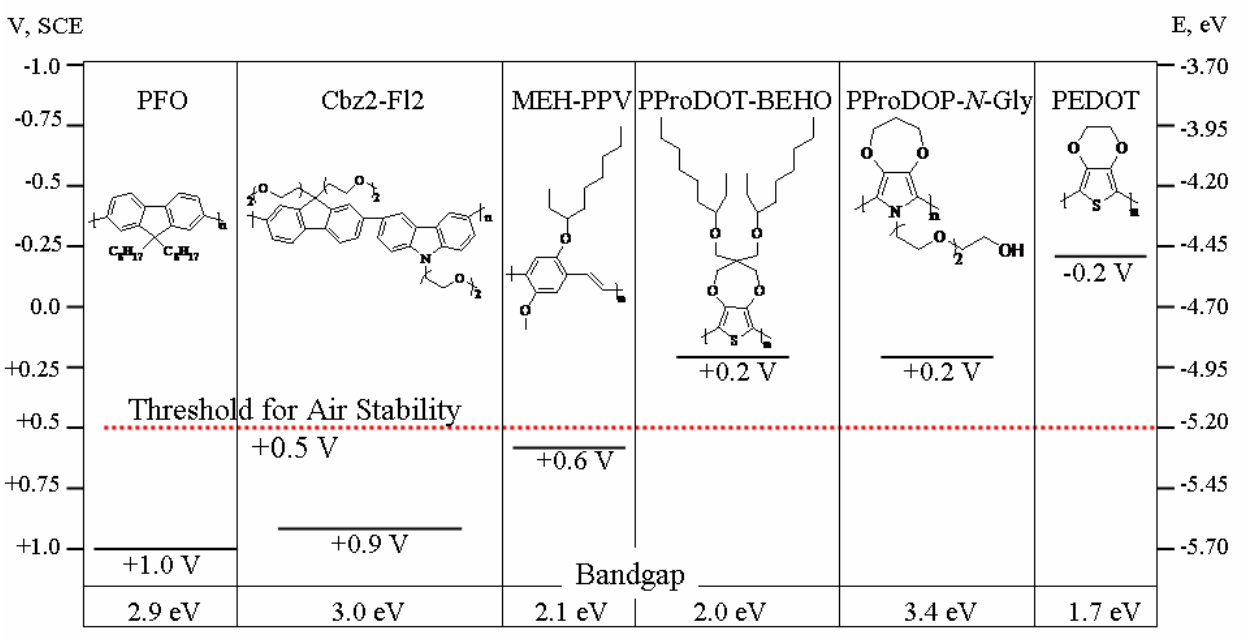

Figure 3-1. Diagram of oxidation potentials (vs. SCE) for several electrochromic and electroluminescent polymers relative to the level required for air stability along with optical bandgap values.[48, 52, 168, 169, 171]

While high HOMO values allow for a low oxidation potential and a stable p-doped state, characteristics desirable in electrochromic applications, this is not the case for light-emitting display applications. For effective hole injection to occur, the polymer HOMO level must be located at levels close to the work function of the anode. The most commonly utilized anode material is ITO with a work function of 4.8 eV or PEDOT:PSS-modified ITO with a work function of 5.2 eV.[85, 172, 173] In addition, as the polymer active layer utilized in PLEDs is in the pristine, neutral form and the presence of any doped sites quenches luminescence, it is necessary

for the polymer HOMO to be placed at values lower than 5.2 eV to preclude any possibility of oxidation by oxygen.

Several classes of polymers fulfill these requirements and include poly(phenylenevinylenes)s (PPVs), polycarbazoles (PCbzs), poly(p-phenylene)s (PPPs), and polyfluorenes (PFls), among others. There is an ever-growing number of polymers available with HOMO levels below 5.3 eV, along with bandgap values spanning 4 to 1 eV. As such, these polymers have relatively high oxidation potentials and their electrochromic properties have not been extensively studied. However, some of these polymers offer interesting electrochromism in addition to electroluminescence and may be utilized in dual purpose electrochromic/electroluminescent displays. To this end, we investigate the electrochromic properties of three conjugated electroactive polymers, the commercially available MEH-PPV, poly[(9,9-bis(methoxyethoxyethyl)-2,7-fluorene)-*alt*-(*N*-(methoxyethoxyethyl)-3,6-carbazole)] (Cbz2-Fl2), and poly[(1,4-bis(methoxyethoxyethoxyethoxy)-2,5-phenylene)-alt-(*N*-(methoxyethoxyethyl)-3,6-carbazole)] (Cbz2-Ph3) whose structures are shown in Figure 3-2.

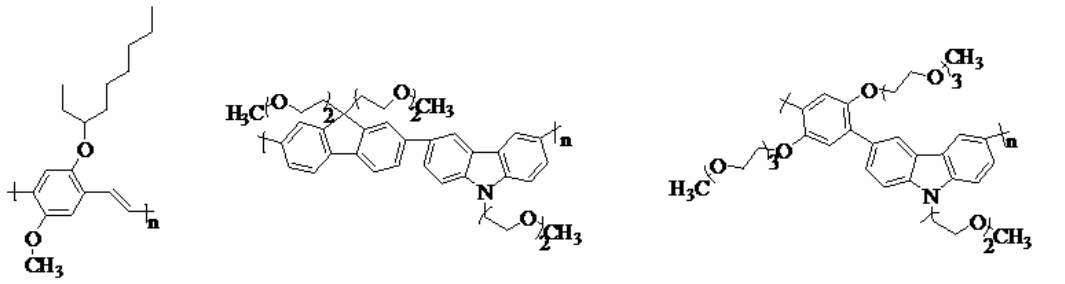

Figure 3-2. Structures of polymers studied in this chapter.

Electrochromism of MEH-PPV

Solutions of MEH-PPV were prepared by dissolving the polymer in dry and deoxygenated chloroform in a glovebox to a concentration of 5 mg/mL. The solution was allowed to stir

overnight and heated to 40ºC for the last 30 minutes. Films were prepared by drop-casting the polymer solution onto a pre-cleaned ITO/glass slide and the solvent allowed to evaporate. The slides were then placed on a hotplate at 50 ºC for 1 hour to further remove residual solvent. Electrochemical switching of the film was performed in a three-electrode cell with the polymer-coated ITO as the working electrode, Pt-flag as the counter, and a Ag wire pseudo reference (calibrated with the Fc/Fc^+ redox couple) in an electrolyte solution of 0.2 M LiOTf in ACN. Electrochemical switching was performed on the ITO/glass electrodes in order to allow the observation of spectral and color changes during redox switching. To determine the potential range for spectroelectrochemical switching, cyclic voltammetry was performed as is shown in Figure 3-3. The polymer was switched over the range of -0.9 V and 0.66 V vs. Fc/Fc^+ at a scan rate of 30 mV/s and was shown to be stable for over 50 switches.

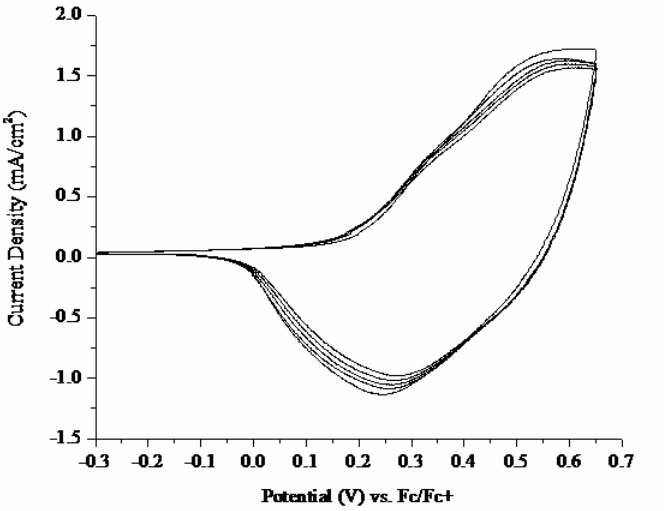

Figure 3-3. Cyclic voltammograms of a drop-cast film of MEH-PPV on ITO/glass at a scan rate of 30 mV/s switched in 0.2 M LiOTf/ACN for 50 cycles. Every tenth scan is shown for clarity.

In-situ spectroelectrochemistry of the drop-cast film on ITO was performed in an Ar-filled glovebox with a fiber-optic spectrophotometer (StellarNet). The wavelength range measured was across the visible region from 350 to 850 nm. Each potential was held for approximately 1

minute before the spectra was acquired as this was the length of time required for optical changes to equilibrate. Figure 3-4A shows the spectra of the as-cast, dry film and the spectroelectrochemistry of the film at low (-0.94 to 0.36 V) applied potentials. The spectroelectrochemistry for higher potentials is shown in Figure 3-4B for clarity. As seen in Figure 3-4A, the neutral, as-cast, film shows a λ_{max} of 483 nm with an absorption onset of 562 nm, giving an optical bandgap value of 2.2 eV. The λ_{max} is blue-shifted by 36 nm from the neutralized film (-0.94 V) as the as-cast spectra was taken on a dry film. This is because the electrochemically switched film is electronically different from the as-cast film due to electrochemical annealing of the film inducing both a shift in the absorbance to longer wavelengths and broadens the spectra.

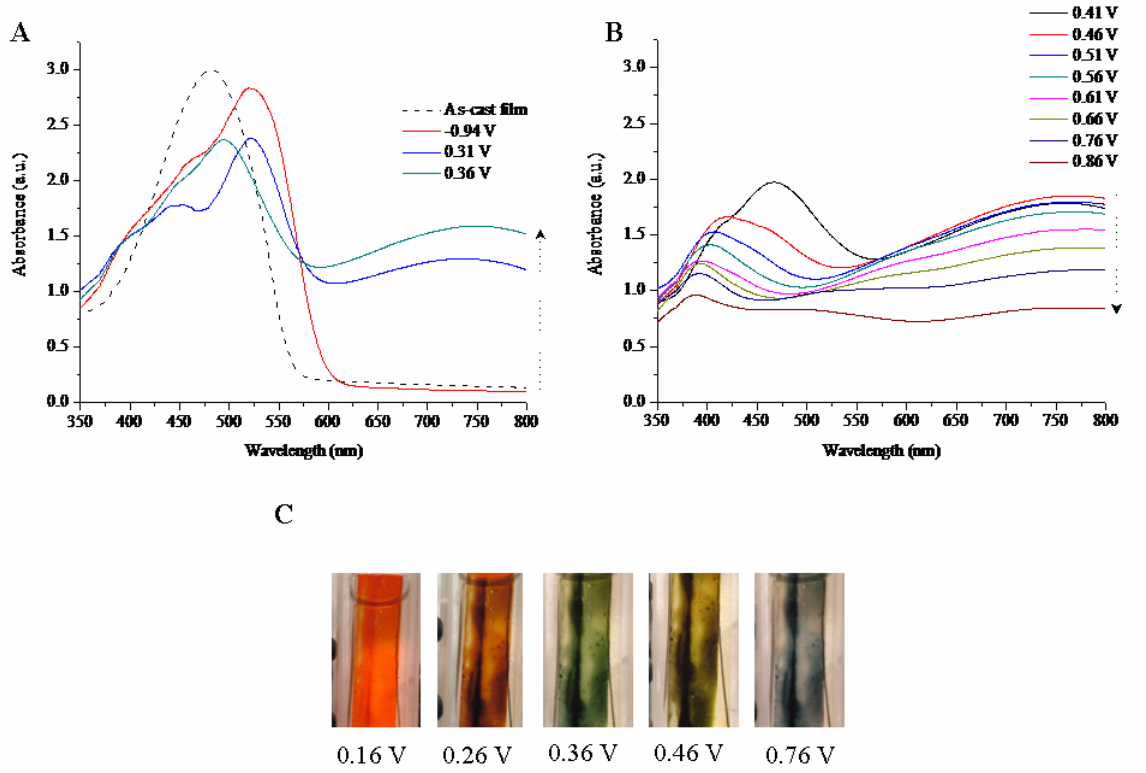

Figure 3-4. Spectroelectrochemistry (A) of a drop-cast film of MEH-PPV on ITO/glass switched in 0.2 M LiOTf/ACN. The arrow shows direction of spectral growth. Photographs (B) of the same film held at potentials indicated. All potentials given are referenced vs. Fc/Fc^{+}.

When a potential sufficiently positive enough (+0.31 V) to cause oxidation of the polymer is applied to the film the absorbance at the λ_{max} decreases while a broad absorbance beginning at 600 nm begins to increase. This is due to the introduction of lower energy midgap state and depletion of the valence band as discussed in Chapter 1. A further increase in the potential applied to the film (+0.36 V) causes a shift in the λ_{max} to shorter wavelengths and a further increase in the long wavelength absorbance. The shift in the λ_{max} is due to the widening of the bandgap. This is because as the polymer is oxidized, electrons are removed from the top of the valence band and the now the minimum energy required for the electronic transition from the HOMO to the LUMO is higher. On further oxidation, the absorbance at λ_{max} continues to decrease and shift to shorter wavelengths while the longer wavelength absorbances from 600 to 800 nm also decrease as shown in Figure 3-4B. The polymer goes through several colored states on oxidation as is seen in the photographs in Figure 3-4C. It should be noted that the unevenness in the films, as seen in the photographs, is due to the uneven evaporation of the solvent from the electrode edges during drop-casting. The fully reduced polymer is an orange-red color at -0.9 V and blue at +0.66 V vs. Fc/Fc^+ with colored states of brown and greenish-blue at intermediate potentials.

Electrochromism of Cbz2-Fl2

Solutions of the carbazole-fluorene copolymer were made by dissolving the polymer in dry and deoxygenated chloroform to a concentration of 5 mg/mL. Films were cast onto ITO/glass electrodes by spray-casting from a commercial airbrush (Testor Corp., Rockford, IL) operated at a pressure of 20 psi. The films were then dried at 50ºC in a vacuum oven for 1 hour. As this polymer is soluble in many electrochemical solvents (i.e., chloroform, ACN, propylene carbonate, methylene chloride) except water, electrochemical switching was performed in an electrolyte of 0.2 M LiOTf in water. This, however, precluded electrochemical and

spectroelectrochemical characterization in the glovebox and all experiments were performed on the bench after purging the electrolyte with Argon for at least 20 minutes. As with the MEH-PPV films, the accessible electrochemical window for in-situ spectroelectrochemistry was determined by switching the polymer film on ITO by CV. While distinct color changes could be seen and an increase in current attributed to the polymer oxidation occurred, there was no discernable redox peak found on cycling to allow for determination of a polymer $E_{1/2}$ as can be seen in Figure 3-5. The peak oxidation of the polymer occurs roughly at the same potential as the electrolyte oxidation, which is shown by the dashed line. This oxidation of the supporting electrolyte interfered with the polymer oxidation, not allowing for switching at higher potentials to observe a peak current. Therefore, polymer oxidation was determined as the onset of anodic current increase.

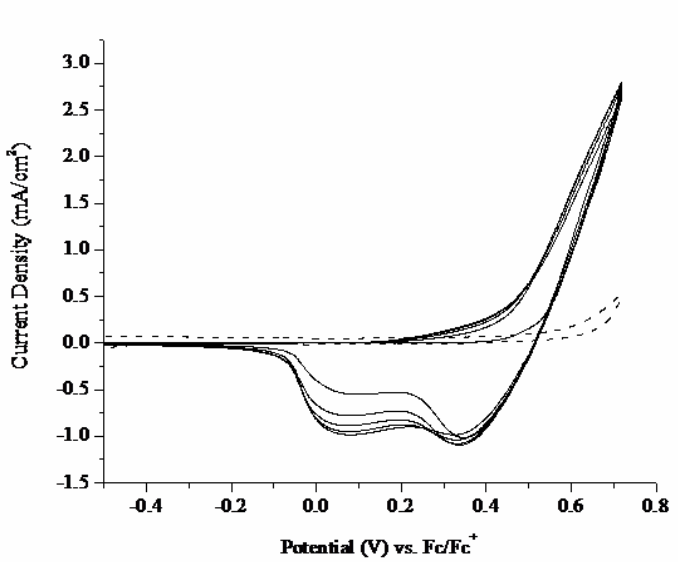

Figure 3-5. Cyclic voltammograms of a spray-cast film of Cbz2-Fl3 on ITO/glass switched at 30 mV/s in 0.2 M LiOTf/water for 50 scans. Every tenth scan is shown for clarity. The background scan (0.2 M LiOTf/water) is shown by the dashed line.

Film in situ spectroelectrochemistry was performed with a Cary 500 UV/Vis-NIR spectrophotometer by holding the potential applied to the film for one minute and recording the spectra from 350 to 800 nm. The one minute hold time was determined as with MEH-PPV by

monitoring the spectra until it no longer fluctuated. The λ_{max} of the neutral film was determined by casting the polymer onto a quartz slide as the absorbance extends into the UV and could not accurately be determined on ITO/glass. The absorbance of the neutral, dry film is shown in Figure 3-6A by the dashed line. The λ_{max} is 349 nm with an absorption onset of 310 nm giving an optical bandgap of 3.0 eV.

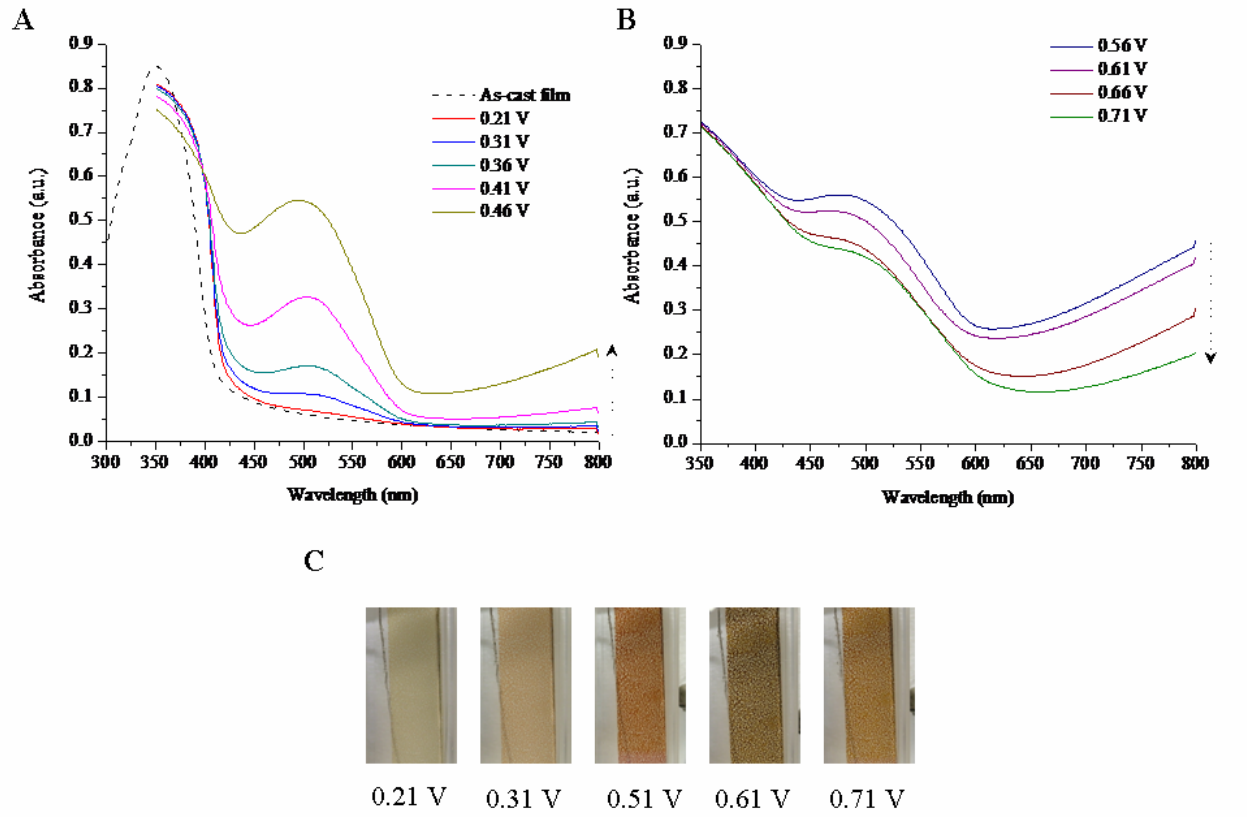

Figure 3-6. Spectroelectrochemistry (A and B) of a spray-cast film of Cbz2-Fl2 on ITO/glass in 0.2 M LiOTf/water. The arrow shows direction of spectral growth and recession. Photographs (C) of the same film held at various potentials. All potentials given are referenced versus Fc/Fc^{+}.

As with MEH-PPV, the absorbance spectra of the electrolyte-soaked film is red-shifted (by 13 nm) due to swelling of the film. The spectroelectrochemical series shows a slight decrease in absorbance at 350 nm on oxidation while an increase in absorbance at 500 nm and a broad absorbance extending from the NIR as can be seen in Figure 3-6A. The absorbances began to decrease beginning at the applied potential of 0.56 V as shown in Figure 3-6B. The polymer was

colorless in the neutral state at -0.8 V and brown when fully oxidized at +0.7 V vs. Fc/Fc^+, with the colors of orange and reddish-brown at intermediate potentials as can be seen in the photographs of the film at several potentials in Figure 3-6C.

Electrochromism of Cbz2-Ph3

As with the Cbz2-Fl2 polymer, solutions were spray-cast onto ITO/glass from a 5 mg/mL solution of the polymer in chloroform and dried in a vacuum oven at 50ºC for 1 hour. The films were electrochemically switched in 0.2 M LiOTf/water electrolyte by cyclic voltammetry. On the first scan, there was a slight oxidation peak at 0.4 V and a reduction peak at 0.1 V vs. Fc/Fc^+ as seen in Figure 3-7. However, on subsequent scans, the current decreased and both oxidation and reduction peaks disappeared due to possible overoxidation of the polymer film. In addition, the film was initially colorless in the neutral state and became a salmon pink color on oxidation, but on reneutralization, the film did not return to the colorless state and remained salmon pink during switching.

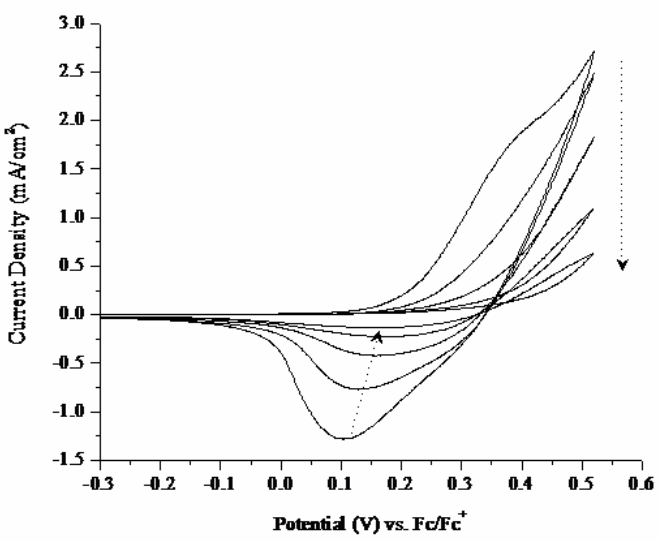

Figure 3-7. Cyclic voltammograms of a spray-cast film of Cbz2-Ph3 on ITO/glass at a scan rate of 30 mV/s in 0.2 M LiOTf/water for 5 scans. Arrows show direction of current decrease.

As this polymer is not stable to repeated switching, a fresh film was cast for spectroelectrochemical measurements without breaking-in the film by switching before measuring the spectra. Similarly with the Cbz2-Fl2 polymer, the λ_{max} of the neutral film occurred in the UV, as can be seen in Figure 3-8A for the spectra (dashed line) of the as-cast film on quartz. The λ_{max} was 334 nm with an absorption onset at 385 nm giving an optical bandgap of 3.2 eV. On oxidation, a peak began to emerge at 450 nm that broadened and shifted to 500 nm on further oxidation. On oxidation at low applied potentials, the absorption at 350 nm began to decrease while that at 450 nm increased. At potentials above 0.41 V, the absorbance centered at 500 nm decreased until 0.71 V after which no further optical changes occurred.

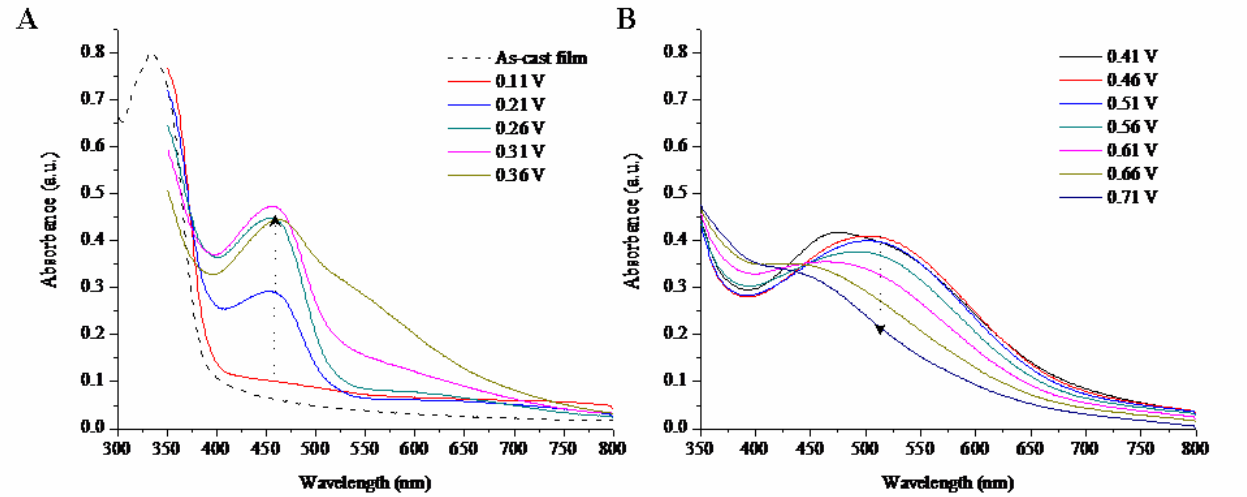

Figure 3-8. Spectroelectrochemistry of a spray-cast film of Cbz2-Ph3 on ITO/glass in 0.2 M LiOTf/water. A) The as-cast neutral and dry film (dashed line) and between the potentials of 0.11 V and 0.36 V. B) Between the potentials of 0.41 and 0.71 V. Arrow shows direction of spectral growth. Potentials are referenced vs. Fc/Fc^{+}.

All three polymers had relatively high oxidation potentials with only MEH-PPV and Cbz2-Fl2 exhibiting reversible electrochromism. Even though, Cbz2-Fl2 did change color on oxidation, the inability for the polymer to be switched as a film in solvents besides water and the lack of distinct, large contrast color changes is a limitation. As Cbz2-Ph3 is not stable on

oxidation and does not exhibit reversible electrochromism, its electrochromism will not be studied further in this chapter.

Reflective Electrochromic Displays

One goal of this dissertation is to provide a new method for using combined electrochromism and electroluminescence for a display that would exhibit both properties from the same active material and from the same pixel. To optimize the electrochromic response of a dual electrochromic/electroluminescent device, it is necessary to separately model the electrochromic display-half of the device. This design of the device would need to be modified from the ECD discussed previously in Chapter 2. While the device is a reflective type and would contain a back-hidden counter electrode and a front-positioned working electrode, there exists added requirements. One such requirement is the use of a transparent electrode, such as ITO that, during electroluminescent (EL) mode, would function as the anode. Another requirement is for a third electrode in the device that would function as the cathode and be positioned in the device so that light emission would occur between the transparent anode and the cathode. To this end, two reflective ECDs were designed that model the electrochromic half of the dual device with the intention of combining this design with a light-emitting device (as will be described in Chapter 4) to create the dual EC/EL.

As was discussed in Chapter 1, the most common types of electrochromic devices are of the absorptive/transmissive type or the absorptive/reflective type. While the absorptive/reflective device discussed thus far utilizes a reflective porous electrode, there exists the possibility for alternative designs. Two electrochromic polymer devices that are based on a new reflective design are shown for the first time in Figures 3-9A and B. Both designs are composed of a polymer-coated transparent working electrode, a porous reflector that does not

function as an electrode, and a polymer-coated counter electrode sandwiched together with the main difference being the type of reflector utilized (diffuse or mirror-like).

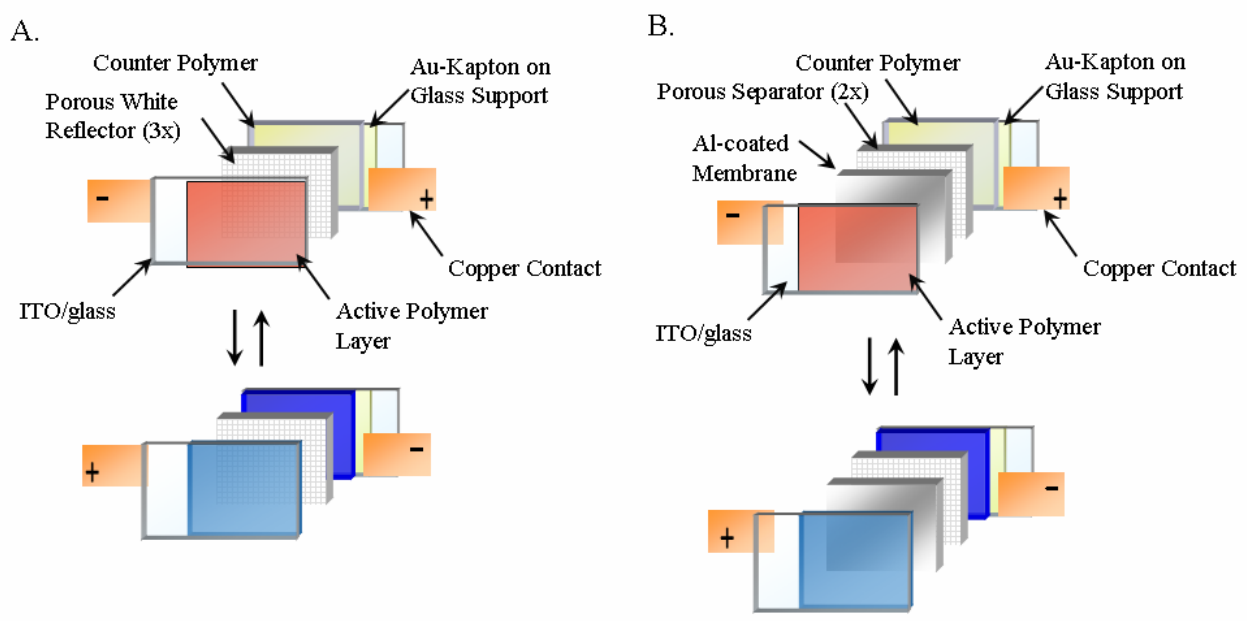

Figure 3-9. Schematic of reflective electrochromic displays with A) porous white diffuse reflector and B) aluminum-coated porous membrane.

The first device (Figure 3-9A) contains a gold-coated Kapton® counter electrode, on a glass support, onto which a layer of PEDOT is electrochemically deposited from a monomer solution containing 10 mM EDOT, and 0.2 M LiOTf in propylene carbonate. The electropolymerization was performed potentiostatically at 1.6 V until 83 mC/cm^2 of charge had passed. This is topped with three pieces of white filter paper each coated with a layer of gel electrolyte. The electrolyte was prepared by dissolving 1 g of LiOTf and 2.3 g of PMMA in 5.6 mL of propylene carbonate to form a viscous clear gel. The active working layer was prepared by casting the electrochromic polymer onto ITO/glass. The entire device was sandwiched together, electrodes contacted with copper tape and the device sealed with epoxy on all four sides to hold the device together.

The second device, Figure 3-8B, is fabricated similar to the first device, except with an aluminum-coated porous membrane and two pieces of filter paper sandwiched between the working and counter electrodes. The metallized membrane was prepared by thermally evaporating aluminum to 60 nm thickness onto porous polycarbonate membranes. With the first device, device A, the white porous membrane acts as a paper-like diffuse reflector while in the second device, device B, the aluminum membrane is the metallic mirror-like reflector. For both devices, the active polymer layer is coated onto the ITO/glass that is inward facing. This is different from the reflective ECD described in Chapter 2 in which the polymer was coated onto the outward facing metallized porous membrane that functioned as the working electrode. As the active polymer layer is cast onto a rigid substrate (ITO/glass), this allows for application of the polymer by spray-casting or spin-coating, as is required for the active layer in the dual EC/EL device. The reflective porous electrode detailed in Chapter 2 does not allow for spin-coating of the polymer films given that the membranes are very thin (10 μm) and deformable and highly porous. This is because the method by which substrates (the membranes in this case) are secured to the spin-coater chuck is through vacuum suction. For that reason, electrodes coated onto rigid substrates (glass or ~0.2 mm thick plastic film) are required.

To test the device designs, a model electrochromic polymer, with known reproducible electrochromic behavior was utilized as the active layer. The polymer chosen for this study was the previously mentioned PProDOT-$(CH_2OEtHx)_2$ for its ease of processability, high ambient stability, and known electrochromic response in a device configuration.[47] The active polymer layer was prepared by spray-casting a solution of 5 mg/mL of PProDOT-$(CH_2OEtHx)_2$ in toluene onto 1.5x1.5 cm ITO/glass slides. The spectroelectrochemical series of both devices were measured using a Cary 500 UV/Vis-NIR spectrophotometer fitted with an integrating

sphere with the spectra of a reference device taken as the baseline. The reference device was constructed with the same materials and same configuration as device A and device B, but with no active polymer layer deposited on the working electrode. A potential sufficient to fully neutralize the active polymer layer was applied across the device (-1.2 V) and the potential was then stepped in 200 mV increments and held for 1 minute before each spectrum was taken. This was continued until the fully oxidized state of the polymer was achieved. The spectroelectrochemical series for both devices, A and B, containing a spray-cast film of PProDOT-$(CH_2OEtHx)_2$ as the active layer are shown in Figures 3-10A and B.

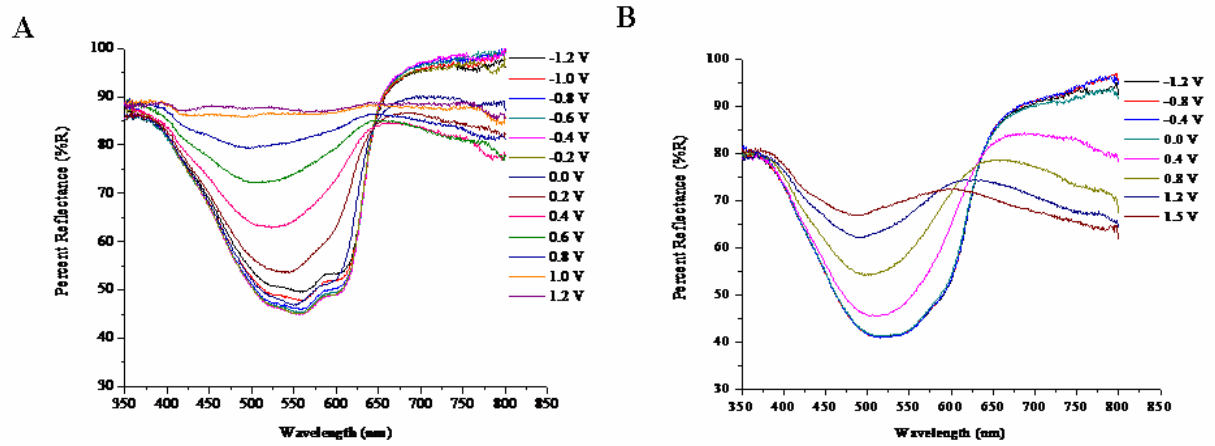

Figure 3-10. Reflectance spectroelectrochemistry of spray-cast PProDOT-$(CH_2OEtHx)_2$ in an electrochromic display with a A) porous white reflector and B) aluminum-coated porous membrane.

The absorbance of the polymer film was broad across the visible region with the maximum absorbance centered around 550 nm. As oxidizing potentials are applied across the device, the reflectance in the visible region begins to increase as was also seen for the same polymer film in the reflective ECDs in Chapter 2. Similarly to the spectroelectrochemistry for MEH-PPV earlier in this chapter, the λ_{max} shifts to shorter wavelengths on oxidation of the polymer while a decrease in the reflectance in the red region occurs. While this spectroelectrochemical series is

only taken of the visible region out to 800 nm, it is expected that the reflectance at longer wavelengths would decrease on oxidation.

It can be seen that the active polymer layer is fully oxidized at +1.2 V for device A, with a maximum contrast of 42% in the visible region. However, even beyond an applied voltage of +1.5 V in device B, there remains a residual absorbance in the visible region with a maximum contrast of 26%. This can be attributed to the aluminum porous reflector in this device. As the device is switched over time it can be seen that the aluminum metal takes on a grey haze that decreases the reflectance of this device, possibly due to oxidation. This also causes the background correction taken with the reference device to no longer be adequate in correctly subtracting contributions to the spectra from the device components not involved in the electrochromic switching, such as the aluminum reflector. This could possibly be due to a side reaction occurring in the electrochemical cell between the lithium triflate electrolyte in contact with the aluminum electrode, causing corrosion of the aluminum while at the same time reneutralizing the oxidized polymer layer, not allowing for full electrochromic switching.

To effectively model the electrochromic response of the luminescent conjugated polymers in the dual EC/EL display, devices based on the designs of device A and device B were constructed with the blends of the electroluminescent polymers with solid electrolytes as the active layer. The blends were comprised of either MEH-PPV or Cbz2-Fl2 as the active electrochromic material, LiOTf as the salt, and PEO as the ion solvator (for the MEH-PPV blend only). The Cbz2-Fl2 blend does not contain PEO as this polymer contains ion-solvating oligoethoxy side chains.

The MEH-PPV blend solution was made by preparing master solutions of the three components separately. The master solutions were comprised of MEH-PPV, PEO, and LiOTf in

concentrations of 10 mg/mL, 13 mg/mL, and 13 mg/mL each in cyclohexanone, respectively. The blend solution was then prepared by adding each component in a weight ratio of 10:3:1 (MEH-PPV:PEO:LiOTf) and diluting with cyclohexanone such that the final MEH-PPV concentration was 5 mg/mL. The films were prepared by spin-casting the blend solution onto ITO/glass slides at 1000 rpm to obtain a final thickness of 170 nm. Devices were constructed with designs of device A and B with the MEH-PPV blend as the active electrochromic layer. Figure 3-11A shows the spectroelectrochemical series for the electrochromic device A, with the white paper reflector along with photographs of the device in the neutral (orange) and fully oxidized (blue) states in Figure 3-11B Figures 3-11C and D show the spectroelectrochemical series and photographs of the MEH-PPV device with the porous aluminum reflector (device design B).

The maximum spectral contrast for the device based on design A was ~15% at 480 nm and 35% at 600 nm while that based on design B was ~60% at 480 nm and near 30% at 600 nm. This difference in maximum contrast between the two devices at the shorter wavelength can be explained by the incomplete oxidation of the polymer film in device A as seen in the photograph in Figure 3-11B. As the encircled area of the photograph shows, there are portions of the film that do not become oxidized to the blue color, but rather remain orange. This can be attributed to the already high oxidation potential of this polymer along with the unevenness of application of the gel electrolyte layer. In the areas where the polymer is not fully switched, the concentration of gel electrolyte could be very thin, and switching of these areas are not as efficient, leading to incomplete oxidation.

In the device based on design B, porous aluminum reflector, there are residual absorbances at the high energy end of the spectrum (below 400 nm) and the low energy end of the spectrum

(above 650 nm). This can be attributed to the aforementioned ineffective background correction due to the variations between the reference device (without active polymer layer) and the actual measured device. On initially preparing the metallized membranes, the aluminum metal layer is highly reflective with a silvery finish. However, after being repeatedly switched, the finish of the aluminum layer loses the luster and becomes a dull grey. This can cause a difference between the reference device (that retains its high reflectance) and the working device in which the aluminum layer is oxidized and the reflectance is decreased. It should be noted that on resting for several days (~3 days) the aluminum layer in the reference device also loses luster.

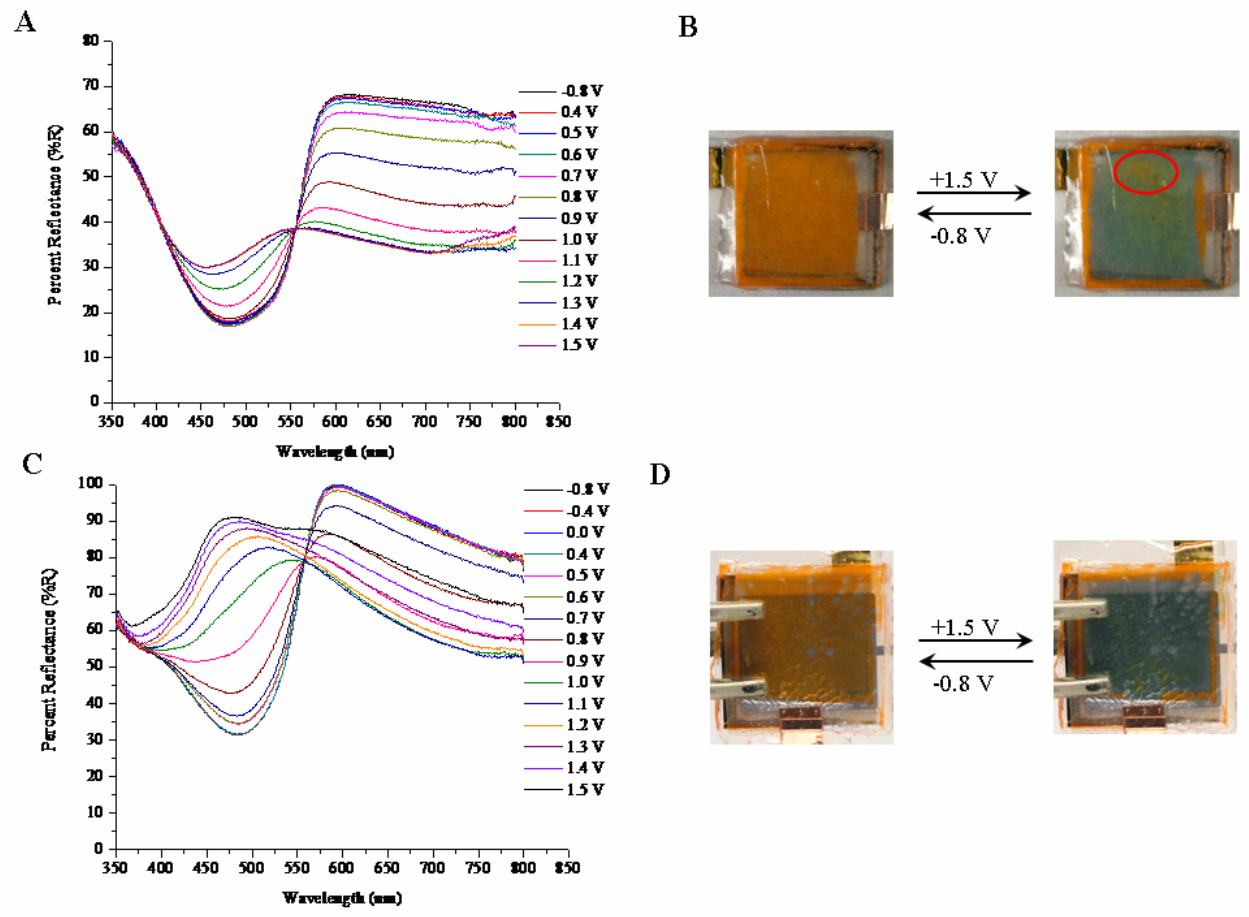

Figure 3-11. Spectroelectrochemistry (A) and photographs (B) of MEH-PPV/PEO/LiOTf blend reflective ECD with porous white reflector. Spectroelectrochemistry (C) and photographs (D) of MEH-PPV/PEO/LiOTf blend reflective ECD with aluminum-coated membrane.

To further demonstrate an electroluminescent polymer as the electrochromic layer in a reflective electrochromic device, Cbz2-Fl2 blended with LiOTf was utilized as the active layer in both device designs A and B. A solution of Cbz2-Fl2 (5 mg/mL) blended with LiOTf in a weight ratio of 20:4 in cyclohexanone was spin-cast onto ITO/glass at a rate of 500 rpm yielding a film thickness of 47 nm. As mentioned previously, an ion solvating material, such as PEO, is not needed as the polymer contains ion solvating oligoethoxy pendant groups. This leads to a decreased solution viscosity compared to the MEH-PPV/PEO blend and makes producing thick films by spin-coating difficult. Any future work involving this polymer would involve investigating blending of the Cbz2-Fl2 with PEO. While the presence of oligoethoxy side-chains is intended to solvate the LiOTf without the need for PEO, the side-chains could allow for improvement of film quality and morphology on blending with PEO and other ion conducting polymers

Spectroelectrochemistry of the Cbz2-Fl2/LiOTf blend as the active layer in device A and device B are shown in Figure 3-12A and B, respectively. Both devices switched from a colorless state to a pale orange color on oxidation, however the optical contrast was not high as the film was rather thin and the polymer does not exhibit highly colored states as was also seen in the photographs in Figure 3-6C. The device based on the porous white reflector (device A) had an optical contrast of 20-25% at 500 nm, requiring a potential of at least 1.4 V to reach the oxidized state. The device based on design B, porous aluminum reflector, exhibited a maximum contrast of 30% at 500 nm. This device had little change in color or spectra until an applied potential of 2.0 V. As with the MEH-PPV device with the aluminum reflector, there is a residual absorbance at longer wavelengths, possibly due to the difference in the reflectance of the reference device compared to the active device.

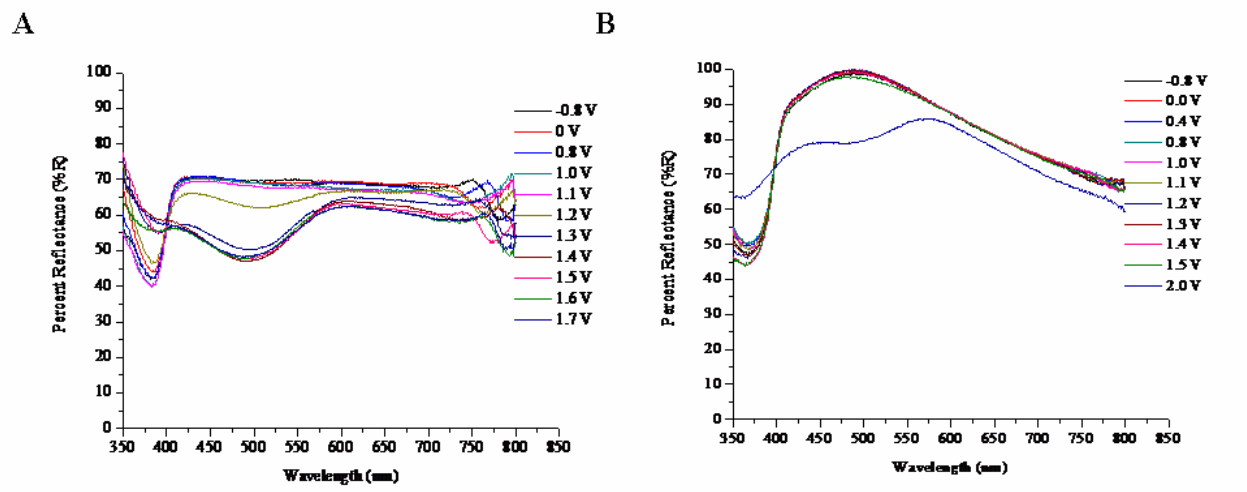

Figure 3-12. Spectroelectrochemistry of Cbz2-Fl2/LiOTf blend reflective ECD with A) porous white reflector and B) aluminum-coated membrane.

On comparison of the reflectance spectra of the device containing Cbz2-Fl2 as the active layer and the absorbance spectra of that same polymer switched in a LiOTf/water electrolyte, a peak for λ_{max} is clearly seen for the film in the devices while none could be determined for the films switched in water, while the onset for absorbance is at the same wavelength in all spectra. This shift in the absorbance peak into the visible region can be attributed to solvent effects as the film in the device is switched in a propylene carbonate-based gel electrolyte. It should be noted that after switching both devices to the oxidized state, the polymer film would not completely change color back to the neutral, colorless state. This is due to the high solubility of the polymer in propylene carbonate, although as a gel, in which the polymer dissolves, not allowing it to be further switched effectively. Due to this complication as well as the low optical contrast, this polymer will not be further studied as a possible material in the dual EC/EL device and attention will be focused on MEH-PPV as the active material for this specific study.

Conclusions

A newly designed reflective electrochromic display based on two different porous reflective layers, white paper and aluminized membrane, has been demonstrated for the soluble

electrochromic polymer PProDOT-($CH_2OEtHx)_2$ and two electroluminescent polymers MEH-PPV and Cbz2-Fl2. These devices model the electrochromic half of the dual EC/EL display that will be the focus of Chapter 4. While the devices introduced in this chapter effectively demonstrated the possible utilization of two different electroluminescent polymers as the active electrochromic layer, several modifications to the device would need to be made in further studies to optimize display performance. Various salts, such as $LiClO_4$, $TBABF_4$, and even ionic liquids, could be utilized as well as other ion-solvating materials such as crown ethers, and other ionically conducting polymers. In addition, other reflective metals could be utilized in the place of aluminum, such as gold, that are resistant to oxidation. The contrast of the white reflective layer in device A could be optimized by using a white porous paper that does not darken when wetted or applying a coating to the paper to increase the brightness of the white. This can be achieved by utilizing a porous Teflon® membrane or coating the white filter paper with a white laminate that is impervious to the solvents being used. Other electroluminescent materials can also be investigated as the active layer such as ruthenium complexes, or other conjugated electroactive polymers and copolymers. As the study to be detailed in Chapter 4 will be the first demonstration of a dual EC/EL device, the focus of the work in this chapter has been placed on demonstration of the device components to achieve the desired result of electrochromism and electroluminescence from a single active layer at the same pixel in one device. It is expected that further work to be conducted after this dissertation will focus on optimizing the proper combination of materials and device designs to achieve the best device performance.

CHAPTER 4
DUAL ELECTROCHROMIC/ELECTROLUMINESCENT DISPLAYS

Conjugated conducting polymers are among a unique class of materials that exhibit a wide variety of useful properties. As was discussed in Chapter 1, these polymers are electrically conductive in the redox-doped state by either exposure to chemical oxidants/reductants or by electrochemical oxidation/reduction. Some of the applications in which doped polymers are used include antistatic coatings,[174] electrochromic windows/displays,[22] supercapacitors,[19] actuators,[24] and as transparent electrode materials.[40] On the other hand, there have been a large number of applications where the undoped form of conjugated polymers are useful as the polymer backbone allows for charge carrier (electron and hole) transport within the valence or conduction band. Some of these applications include photovoltaic devices,[23] field-effect transistors,[21] and light-emitting diodes.[20]

The discovery of electroluminescence in conjugated polymers has been one of the most important developments in the field as it has increased the interest of these materials for consumer display devices. Since then, there has been much interest in improving device lifetime and performance, and on producing colors that span the visible region by structural modification of the polymer backbone, along with a number of techniques that include guest-host blends, multi-layered structures, and others. Another development in the field of polymer light-emitting displays are the light-emitting electrochemical cells (LECs), as is also described in Chapter 1, that offer the advantage of device operation without the need for low work function, reactive electrode materials. Devices have even been demonstrated with the same metal as both anode and cathode where the electrodes are in a lateral arrangement with light emission occurring between electrode lines separated by up to 1 mm.[129]

The most extensively utilized display in consumer electronics today is that based on liquid crystal displays (LCDs).[175] Typical LCDs contain either a light-source (transmissive) or a reflective mirror behind the display elements (reflective). The transmissive devices operate by varying the amount of light allowed to pass through the device while the reflective LCDs contain a fully reflective mirror relying on ambient lighting or a front-light to provide illumination of the image. While the transmissive, back-lit displays have excellent image quality in low lighting situations, such as indoors, the quality is markedly diminished in situations where the brightness of the ambient lighting is higher than that of the back-light used in the display, such as outdoors in direct sunlight. A display able to be utilized in both low and high ambient lighting is that based on transmissive-reflective, called transreflective, technology. This device contains both a back-light and a reflective mirror. The mirror is partially reflecting, allowing some of the light from the back-light to pass when the ambient lighting is low and reflects when the ambient lighting is high. However, the brightness of the LCD indoors is not as high as with the transmissive display as the partially reflective mirror decreases the amount of light transmitted and the image quality is compromised in both modes compared to the fully transmissive or fully reflective displays. In addition, LCDs have the added disadvantage of reduced viewing angle and inability to fabricate mechanically flexible displays.

Another type of display is that based on microelectromechanical (MEMs) technology introduced by QUALCOMM and known as an Interferometric Modulator Display, or IMOD. This display is fabricated by placing a thin film mirror at a transparent substrate with a small gap between that is several hundred nanometers with the gap acting as an optically resonant cavity. Ambient light that strikes the display is reflected at the transparent substrate and the reflective mirror. Depending on the distance between the mirror and the substrate, light of various

wavelengths are produced by constructive and destructive interference. The distance between the thin film mirror and the transparent substrate is varied by the application of a voltage causing the deformable mirror to collapse towards the substrate by electrostatic forces.[176] As with other reflective displays, an external light source is required to illuminate the device. This is accomplished with either ambient lighting or a front-light.

A display that has been gaining interest is the electrophoretic display (EPD), also referred to as electronic paper. Electrophoretic displays were designed to imitate the appearance of ink on paper. Typically, the electronic ink is dark (blue or black) in color and is viewed against a white background, providing a higher optical contrast than achieved with other displays. The technology is based on a suspension of charged micron-sized white particles, such as titanium dioxide, dispersed in an oil that is dyed with a dark ink. The suspension is encapsulated in microparticles that are then placed between two parallel electrodes. When a positive potential is applied to the top electrode, the negatively charged white particles migrate to the top of the microcapsules and the viewer sees the white, highly reflecting, particles. A positive voltage is then applied to the bottom electrode and the white particles migrate to the bottom of the microcapsules, allowing the dark ink to now be seen by the viewer. This technology was developed by E Ink Corporation, a spin-off from MIT's Media Labs and through a partnership with Philips, these displays have appeared in several consumer electronic devices such as Sony's Reader[177] and Motorola's Motofone.[178] As with the other reflective displays, viewability relies on an external light source and a front-light is necessary to view the display in low ambient lighting.

This chapter details the design and operation of a device that, for the first time, demonstrates electrochromism and light-emission from a single active layer at the same pixel. In

low ambient lighting situations, the display could be operated in the emissive mode without the need for an additional light source. In high ambient lighting situations, as in direct sunlight, the display would be operated in the electrochromic mode. The electrochromic function of the display is modeled after the devices described in Chapter 3, while the emissive function of the device is described within this chapter. Before description and demonstration of the dual display, an investigation into the applicability of two types of polymer light-emitting displays (the PLED and PLEC) are detailed. PLEDs were first investigated as there is a long established history of these devices with published methods for fabrication and characterization data. This allowed for a model device to establish a prototype for construction and development of methods for device fabrication, analytical characterization, and materials performance along with protocols for obtaining electrooptical data. These materials and methods were then applied to the construction and characterization of PLECs, that are not as established in the literature and require an added level of complexity in device construction and operation.

Polymer LEDs

The operating principle of PLEDs is given in Chapter 1 and shown in Figures 1-5 and 1-6 with the schematic of a typical device given in Figure 1-7. The device in this research was constructed using a sandwich-type design with the ITO anode as the first layer. The ITO was patterned and cleaned as detailed in Chapter 5. A thin (40 nm) layer of PEDOT:PSS was then spin-coated onto the patterned ITO substrate and baked at 150ºC in a vacuum oven to remove residual water. The PEDOT:PSS layer is used as a hole transport layer as it lowers the barrier height for hole injection into the polymer layer.[43, 84, 85] The PEDOT:PSS-coated substrates were then transferred to an Argon atmosphere glove box with an oxygen content less than 0.5 ppm and water content less than 0.1 ppm. The active electroluminescent polymer layer was then spin-coated inside the glove box at various spin-rates for 30 seconds from a solution of 5 mg/mL of

MEH-PPV in chlorobenzene. The spin-rates used are 800, 1000, and 1200 rpm producing films of approximately 70 nm in thickness as measured by AFM. The invariability in film thickness is attributed to the low viscosity of the spin solution, and as has been shown previously, slight increases in spin-rate has less of an affect on film thickness for solutions of lower concentration.[179] The films were then loaded into a thermal evaporator and the entire chamber pumped down to 1 x 10^{-6} mbar for ~3 hours. The cathode material (10 nm calcium) was thermally evaporated onto the films followed by 150 nm of an aluminum capping layer to protect the cathode. Both metals are evaporated through a patterned shadow mask creating an active pixel area of 7.07 mm^2 with each device containing 8 pixels.

The electroluminescence of the devices were characterized by applying voltages across the pixel with the ITO connected as the anode and Ca connected as the cathode while light output was measured using the fiber-optic spectrometer, as described in Chapter 5, while inside the glove box. To allow for complete fabrication and characterization of PLED devices, an MBraum glove box system was established in which optical measurements are performed using a fiber-optic spectrometer that allows remote measurement of light output from inside the glove box. To accurately control the position of the fiber-optic cable relative to the device pixel, a X-Y-Z stage was utilized and all device measurements were performed in an enclosed dark box fabricated in-house. All optical measurements were taken normal to the device surface with the bare optical fiber having a fiber diameter of 400 μm. The distance from the fiber-optic tip to the pixel is chosen to allow the entire pixel area to be within the acceptance angle of the fiber-optic with an additional 2.19 mm on each side of the pixel to allow for slight variations in positioning the fiber-optic. This is shown schematically in Figure 4-1. The full acceptance angle (2 θ) of the fiber-optic is 24.8º. By defining the radius of the circular area to be measured as 3.69 mm

(radius of emitting area of pixel plus the 2.19 mm on each side) and the half angle of acceptance ,θ, as 12.4º a distance can be determined by taking the ratio of the defined radius to the tangent of the half angle, d = R'/tan θ, and is 16.8 mm.

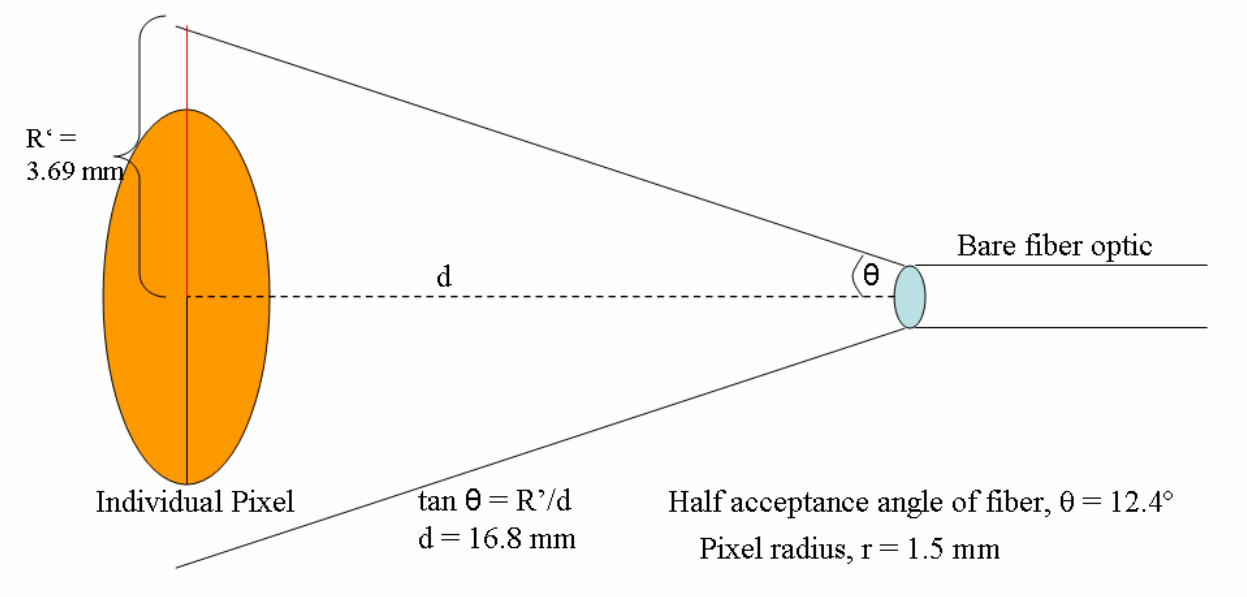

Figure 4-1. Schematic of measurement geometry between fiber-optic probe and PLED pixel.

The optical measurements were performed using an Ocean Optics USB4000 spectrometer as detailed in Chapter 5. The intensity of the light emitted from the pixel that is incident on the fiber-optic is measured for the wavelength range of 400 to 800 nm and is recorded as the spectral irradiance, E_λ. Spectral irradiance is defined as the radiance flux per unit area incident on a surface and per unit wavelength interval at the wavelength λ, and is given by the equation:

$$E_\lambda = \frac{dE}{d\lambda} = \frac{d^2\Phi}{ds_0\, d\lambda} \tag{4.1}$$

where Φ is the radiant flux (watts) and s_0 is the area, and is given in units of μW cm^{-2} nm^{-1}. As the radiation emitting from the pixel is incident on the fiber-optic tip surface, the area is defined by the fiber-optic tip area and is $1.26 \times 10^{-3} cm^2$. While the total power emitted from the pixel is constant and uniform in all directions and is distributed over an area that increases with the

distance from the pixel squared, the irradiance drops off in proportion to the distance from the pixel squared. Therefore, the distance between the pixel and fiber-optic tip, as defined in Figure 4-1, is kept constant for all measurements performed to allow comparison of irradiance measurements at different voltages and different pixels.

The spectral irradiance measured for an individual MEH-PPV pixel operated at increasing voltages is shown in Figure 4-2. At as low a voltage as 4 V, the spectral irradiance is 6.8×10^{-3} $\mu W\ cm^{-2}\ nm^{-1}$ at 585 nm. As the voltage is increased, the intensity of the light emitted increases to a maximum of 9.5×10^{-2} $\mu W\ cm^{-2}\ nm^{-1}$ with a shift in the peak wavelength of 13 nm to 572 nm while the visually observed color is a constant orange-yellow as shown in the inset to Figure 4-2.

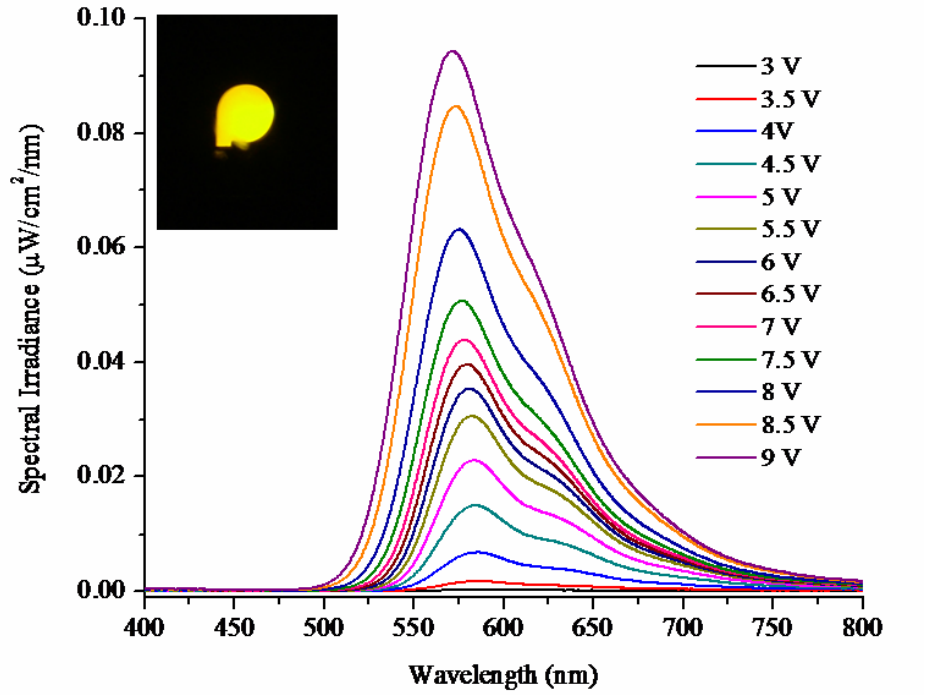

Figure 4-2. Spectral irradiance of an ITO/PEDOT:PSS/70 nm MEH-PPV/Ca/Al PLED pixel at different applied voltages. Inset shows photograph of pixel operated at 9V.

The blue-shift in peak wavelength can be attributed to the increased contribution to the electroluminescence spectra from shorter conjugation-length fractions in the polymer film that emit at shorter wavelengths as higher voltages are applied. This is further supported by the

shoulder in the spectra at longer wavelengths that decreases in relation to the peak wavelength at higher voltages. This longer wavelength emission is due to the longer conjugation-length fractions in the polymer film that are present at a lower concentration and have a lower turn-on voltage for emission. At higher voltages, the contribution from the higher concentration shorter conjugation-length fractions begins to dominate.

Spectral irradiance is a unit of measurement of radiation and can include not only the visible region of the spectra, but all electromagnetic radiation.[180] Quantities such as spectral irradiance, along with others not considered here, are defined as radiometric quantities. In the display field, it is necessary to consider the response of the human eye to this radiation in the visible region and therefore, a subset of radiometry has been defined that creates a relation between the radiometric measurements and the human eye response and is called photometry. A photometric quantity commonly used is luminance (L_v, units of cd m^{-2}) and is a measure of the subjective perception of brightness of a light source as a function of the area of the detector and is the photometric equivalent to radiance and given by the following equation:

$$L_v = 683 \int_{380}^{770} L_\lambda V(\lambda)\, d\lambda \tag{4.2}$$

The subscript, *v*, is used to indicate a photometric quantity, L_λ is spectral radiance and $V(\lambda)$ is the photopic spectral luminous efficiency as defined by the International Lighting Commission (CIE) in 1924 and given in the IES Lighting Handbook.[181] Spectral radiance is the area and solid angle density of radiant flux per unit wavelength interval and has the units of watt m^{-2} sr^{-1} nm^{-1}. The solid angle is calculated by taking the ratio of the area of the pixel to the square of the distance from the pixel to the fiber-optic tip (16.8 mm). This value is 0.025 sr for the measurements detailed in this work. The factor 683 in the equation for luminance is an additional constant necessary for the conversion of watts (radiometric) to lumens (photometric)

as V(λ) is a relative spectral response function of the eye. The luminous efficacy at 555 nm (the wavelength where the human eye is most sensitive) is 683 lm W^{-1} and accounts for the absolute magnitude of the conversion.

The average luminance for a PLED containing a 70 nm thick film of MEH-PPV at increasing voltages is shown in Figure 4-3 by the blue line. The luminance of the pixel is 79 cd/m^2 with as little as 4 V applied. The brightness of the pixel increases with increasing voltage until a maximum value of 1565 cd/m^2 at 9 V. As a comparison, typical computer monitors and color televisions have a luminance of 100 cd/m^2, and a typical fluorescent lamp has a luminance of $4x10^3$ cd/m^2. The current density also increases with applied voltage with a turn-on voltage of 3 V and a maximum current density of 767 mA/cm^2. Beyond an applied voltage of 9 V, the luminance and current decrease until the pixel ultimately burns-out and fails. The literature shows great variability in reported luminance values and is due to the variability in device fabrication methods, materials used and optical measurement methods as no standard methods for PLEDs have yet to be established.[20, 43, 82, 86, 92]

The PLED exhibits rectifying diode-like behavior with current flow and light emission occurring only in the positive voltage direction. As is shown in Figure 1-5, hole injection occurs at the anode to the valence band of the polymer while electron injection occurs at the cathode into the conduction band of the polymer. To minimize the barrier to charge carrier injection, the Fermi level of electrodes must be as closely matched as possible to the relevant energy levels of the luminescent polymer. This requires the use of a high work function anode, such as ITO, and a low work function cathode, such as calcium. Devices have been demonstrated with aluminum as the cathode with no calcium layer, but with low luminance values and a high turn-on voltage of over 12 V.[84] As the overall goal is to use electrochemical systems for the dual device, it is

desired not to use low work function metals as the high reactivity of the calcium layer is not well-suited for use in a device that is to function as both an electrochromic and electroluminescent device. In addition, doping of the electroactive polymer is known to quench electroluminescence in PLEDs and switching of the active layer between neutral and oxidized states during the electrochromic mode will not allow for further operation of the device in the luminescent mode. A type of electroluminescent device with conjugated conducting polymers as the active layer that would allow for operation without the need for low work-function metals and could tolerate repeated doping/dedoping of the polymer layer is the LEC as described in Chapter 1.

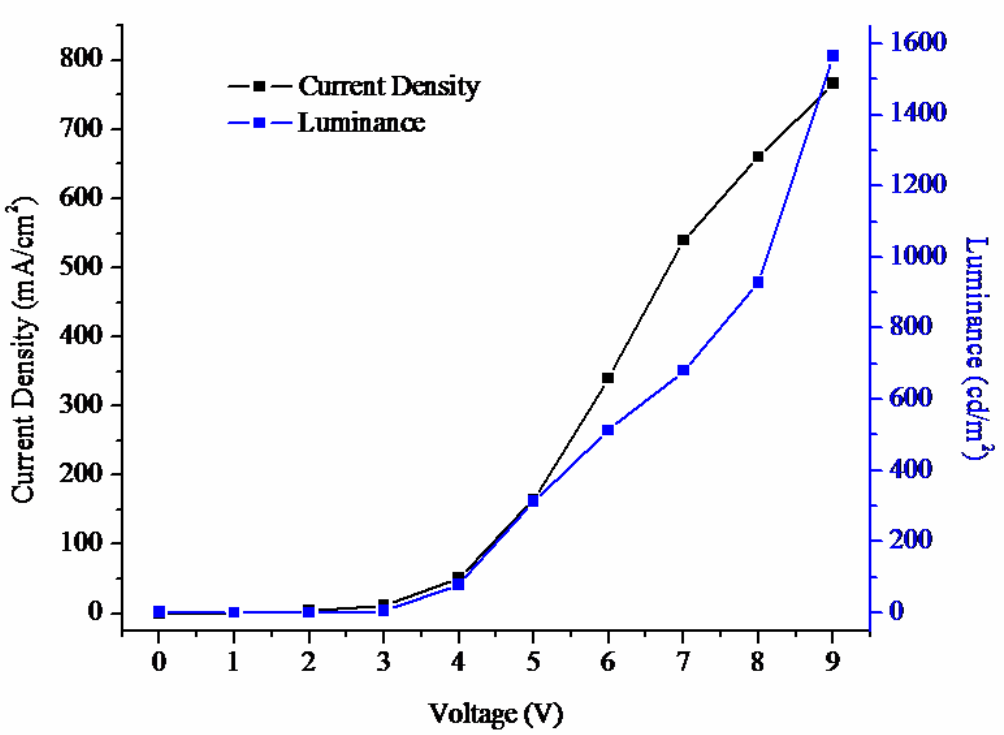

Figure 4-3. Current density (black) and luminance (blue) versus applied voltage for an average of 4 pixels of an ITO/PEDOT:PSS/70 nm MEH-PPV/Ca/Al PLED.

Polymer LECs

The operating principle for a polymer LEC is shown in Figure 1-8. The device layout is a sandwich-type of design as with the PLEDs. The ITO anode was patterned and cleaned in the

same manner as was described for construction of the LED devices. As no alignment of the electrode work function with the polymer conduction/valence bands are necessary, a PEDOT:PSS layer is not utilized in these devices. The active polymer layer contains a blend of the electroluminescent polymer, MEH-PPV, an ion solvating polymer, PEO, and a salt, LiOTf. Master solutions of each component were made by dissolving the material in cyclohexanone to a concentration of 10 mg/mL, 13 mg/mL, and 13 mg/mL for the MEH-PPV, PEO, and LiOTf, respectively. These solutions were allows to stir for 48 hours on a hotplate at a temperature of 40ºC to allow the solutes to completely incorporate into the solution. The blend solutions were then made by mixing each component in a weight ratio of 10:3:1 (MEH-PPV:PEO:LiOTf) and diluted with the appropriate amount of solvent so that the final MEH-PPV concentration is 5 mg/mL. This give a salt concentration of 3 mM. This weight ratio is one of the most commonly referenced in the literature for the best performing devices. Further future studies on the dual EC/EL displays would involve optimization of the blend components and relative weight ratios for the best performance in both EC and EL mode and will be highlighted in the last section.

The polymer films were cast by spin-coating at spin-rates of 800, 1000, and 1200 rpm to produce film thicknesses of 240, 170, and 75 nm, respectively. Given that this solution is relatively viscous, the spin-rate has a more pronounced effect on the final film thickness than that for the PLED device films. The most effective method for obtaining a film sufficiently thick for optimum device performance (between 100 and 200 nm thick) by spin-coating is to use a fairly concentrated solution. As the viscosity of this solution is higher than with the LED active layer solution (5 mg/mL MEH-PPV in chlorobenzene) care must be taken to ensure that there are no air bubbles remaining in the solution when it is dispensed onto the ITO substrate for spin-coating as the air bubbles will cause holes to be present in the film, creating shorts when the cathode

layer is deposited. To remove air bubbles in the solution, the tip of the pipet was dragged through the solution, across the substrate as the solution was dispensed. Lowering the viscosity of the solution by dilution is not a satisfactory option as this decreases the active polymer layer thickness on spin-coating to values that create devices that have a lower light output and a higher incidence of shorts between the anode and cathode. As with the PLED devices, the cathode layer (aluminum alone) was deposited by thermal evaporation through a shadow mask.

The devices were characterized in the same manner as the PLEDs with J-V measured using a Keithley SMU and the EL spectra and luminance measured using the Ocean Optics USB4000. The J-V and L-V curves for an average of 3 pixels for a MEH-PPV:PEO:LiOTf (10:3:1) LEC with an active layer thickness of 170 nm and with ITO as the anode and aluminum as the cathode is shown in Figure 4-4. An unexpected feature of these devices is that the light emission from the device is very low for positive voltages but high for negative voltages. While ambipolar light emission is expected, as has been shown in the literature and can be seen here with an onset for increase in current density and luminance at ±3 V, better device performance is expected with oxidation (p-doping) occurring at the ITO electrode and reduction (n-doping) occurring at the aluminum.[97]

To date, little has been reported on both the positively and negatively biased J-V and L-V characteristics of MEH-PPV:PEO:LiOTF LECs beyond the first paper to report these devices in 1995. On inspection of the results reported in that paper, it is actually unclear as to whether the device performed better at negative voltages relative to positive voltages as the luminance seems to level-off at the highest voltage they report (+4 V) while a leveling-off is not yet seen at the highest negative voltage shown (-4 V).[109] As seen in Figure 4-4, the maximum brightness in the positive voltage direction is 39 cd/m^2 with a current density of 170 mA/cm^2 at 5 V. In the

negative voltage direction, the maximum brightness is 227 cd/m^2 with a current density of -255 mA/cm^2 at -8 V.

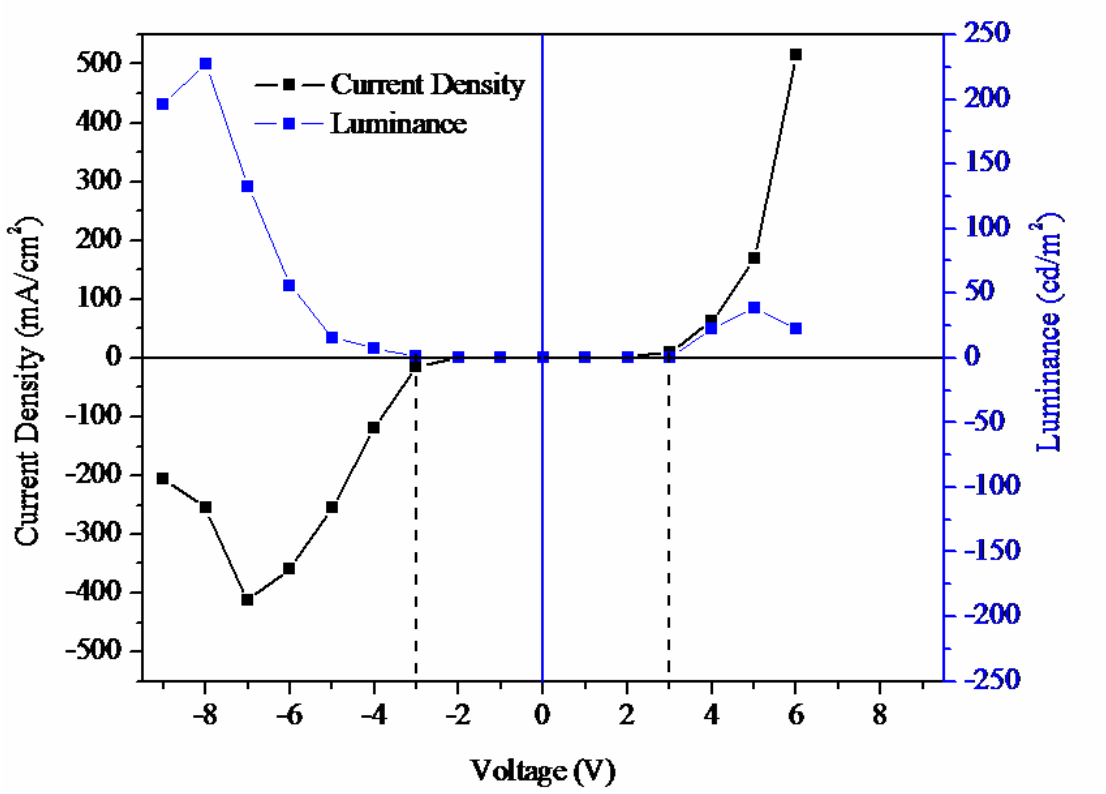

Figure 4-4. Current density (black) and luminance (blue) versus applied voltage for an ITO/blend/Al PLEC with an active layer of a blend of MEH-PPV:PEO:LiOTf in a weight ratio of 10:3:1 at 170 nm thick.

On comparison of the current density and luminance for low applied voltages in both the positive and negative directions, the luminance is higher for positive voltages up to ±5 V with lower current densities. From the applied voltage of +5 to +6 V, the luminance decreases and the current density more than doubles. On increasing the negative voltage, the luminance increases and continues to do so until -8 V after which it decreases, possibly due to degradation of the polymer blend at more negative voltages. A possible explanation for the cross-over in higher luminance for positive voltages below 4 V to higher luminance for negative voltages greater than -4 V is alteration of the aluminum contact to the polymer at these higher positive voltages. A

similar effect was observed as discussed in Chapter 3 for the aluminum-coated membranes used in the reflective ECDs. The elucidation of the mechanism here is beyond the scope of this work.

It is also noticed that the current density peaks at a lower voltage, -7 V, than the luminance and then begins to decrease. This can also be seen in Figure 4-5 for an average of three pixels in a separate device with a 170 nm thick active layer. At voltages greater than -5 V, the current essentially levels off. This can be attributed to the near-thin layer cell behavior of a PLEC device. Between the voltages of -3 and -5 V, the majority of the current is devoted to setting up of the p- and n-doped polymer junction. At voltages more negative than -5 V, the majority of the current is devoted to maintaining the high concentration of doped polymer within the cell and regenerating charge carriers as holes and electrons recombine within the p-i-n junction.

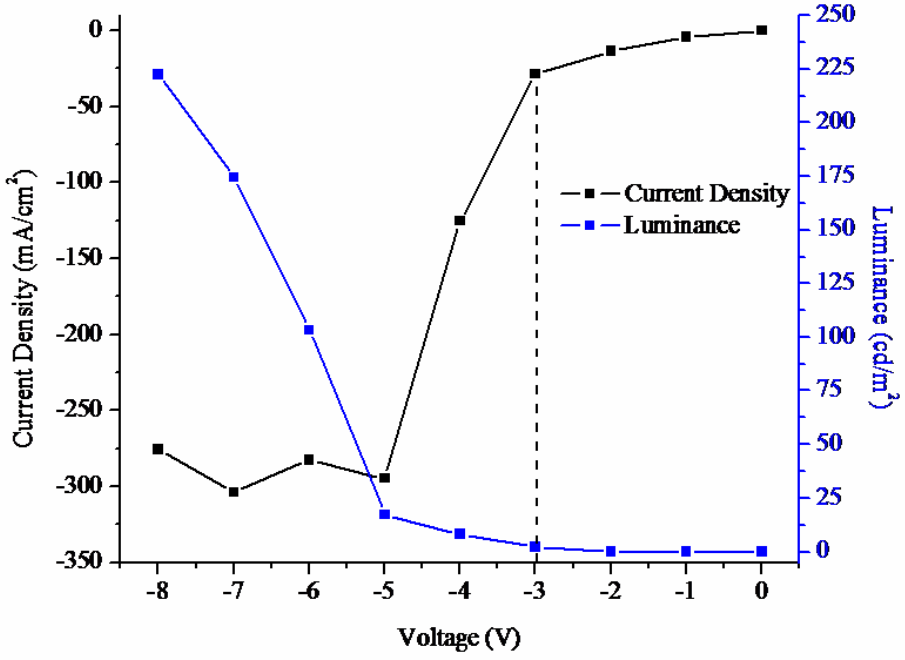

Figure 4-5. Current density (black) and luminance (blue) versus applied voltage for an average of 3 pixels of an ITO/blend/Al PLEC with an active layer of a blend of MEH-PPV:PEO:LiOTf in a weight ratio of 10:3:1 at 170 nm thick.

The spectral irradiance of a pixel of a MEH-PPV LEC device with an active layer of 170 nm at increasingly negative voltages is shown in Figure 4-6. The spectra are very similar to that

for the PLED device shown in Figure 4-2; however, the peak wavelength does not shift to shorter wavelengths as was observed in the PLEDs. While applying higher voltages to the PLED device allows access to the energy levels of the shorter-conjugation length fractions of the polymer, these higher energy levels are not able to be accessed in the PLECs. This is due to the different mechanism for charge carrier injection of PLEDs vs. PLEC (carrier tunneling vs. oxidation/reduction). While the voltages applied across the PLEC device are sufficient to cause p-doping and n-doping of the polymer bulk, the voltages are not sufficient to dope the shorter chain-length fractions as their oxidation/reduction potentials are higher than that of the bulk film. As can be seen in the inset photograph, the emission color is the same for the PLEC as the PLED based on MEH-PPV as emission is from the same excited state with the PLED light intensity ~5 times brighter.

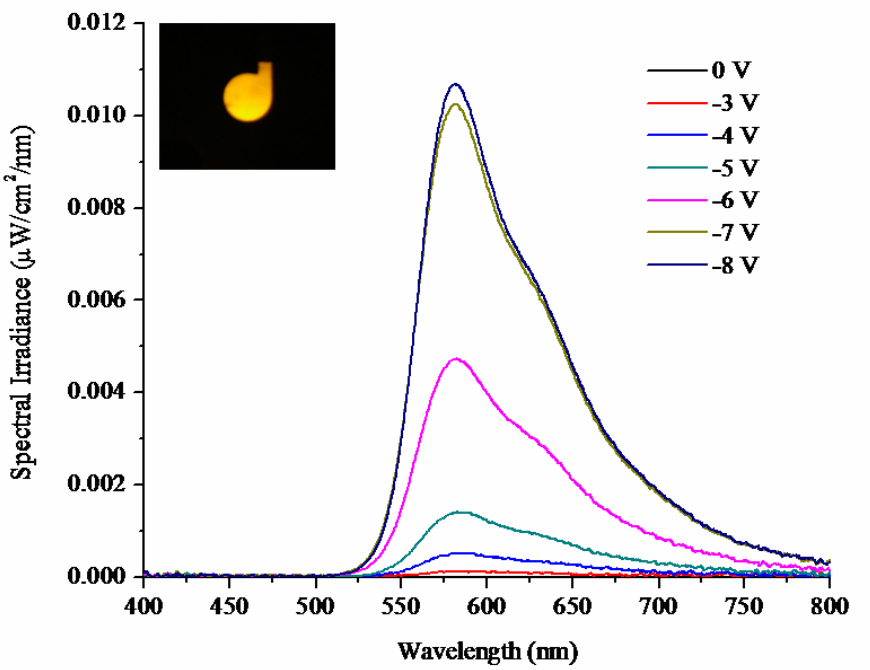

Figure 4-6. Spectral irradiance of a ITO/170 nm MEH-PPV:PEO:LiOTf blend/Al PLEC pixel at different applied voltages. Inset shows photograph of pixel operated at -6 V.

In addition to device brightness and current density, relative device stability will be another important factor for the device performance when incorporated into the dual EC/EL display. Figure 4-7, shows that after an initial break-in cycle, the device shows little hysteresis when cycling between 0 and -8 V and only an 8% drop in luminance between the 2nd and 3rd cycles. While there will continue to be a slow decay, the rate of decay lessens. This is encouraging as these devices were characterized without any form of packaging, allowing the polymer layer and contacts to be fully exposed.

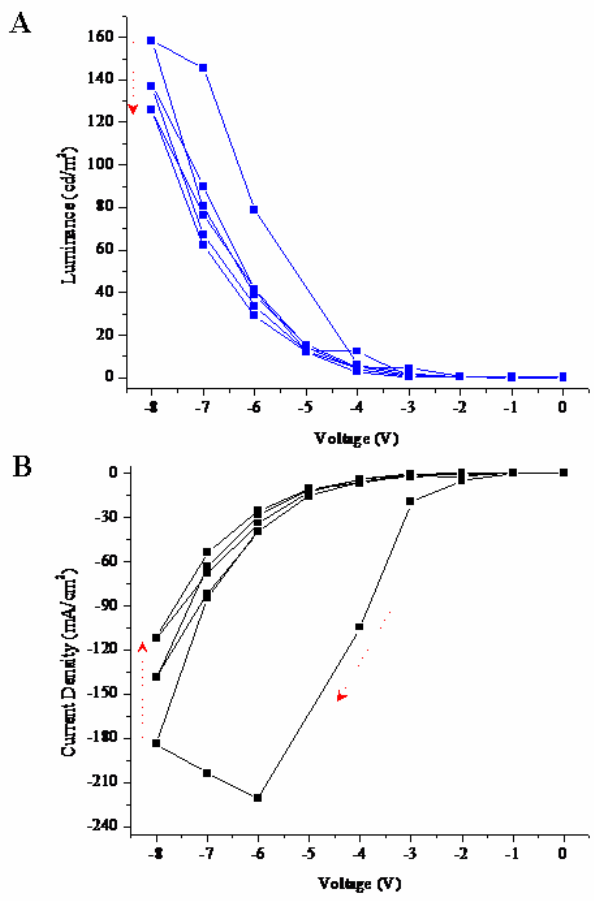

Figure 4-7. Luminance (A) and current density (B) as a function of applied voltage for an ITO/blend/Al PLEC with an active layer of a blend of MEH-PPV:PEO:LiOTf in a weight ratio of 10:3:1 at 170 nm thick cycled between 0V and -8 V for three cycles.

Another indication of device stability is a measurement of pixel lifetime at a constant voltage as is shown in Figure 4-8. The pixel was cycled between 0 V and -8 V five times and then held at -6 V for 13 hours. During this time the spectral irradiance integrated from 400 to 800 nm was monitored. As can be seen in the inset in Figure 4-8, the pixel reached maximum brightness within 7 seconds of initial turn-on after having the initial cycling break-in. At this time, the luminance was 54.5 cd/m^2 and the current density was under -200 mA/cm^2. After 4 minutes, the luminance dropped 24% from the initial value. At 1.5 hours a minimum in light output reaches a value of 1.5 cd/m^2. However, the light output began to increase again and did so for the next 8.5 hours and again decreased.

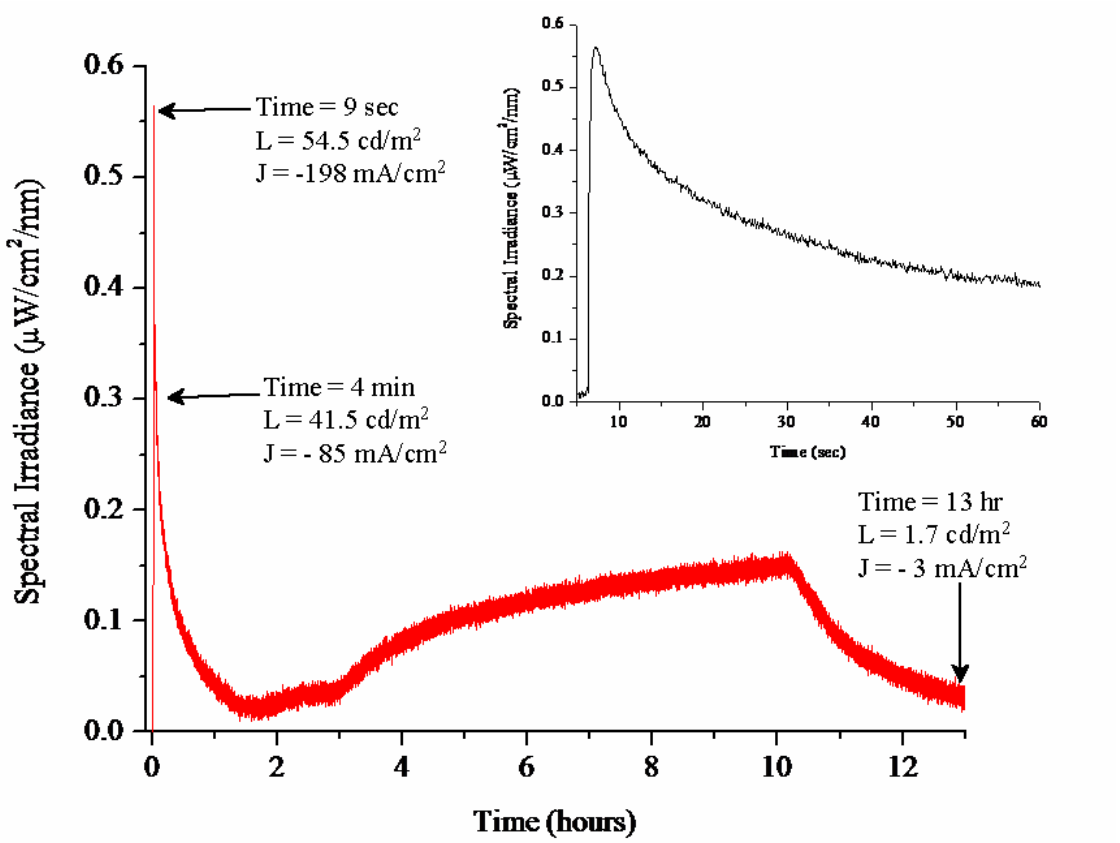

Figure 4-8. Integrated spectral irradiance over the wavelength range of 400 and 800 nm for a LEC pixel operated for 13 continuous hours at -6V. The inset shows the spectral response in the first 2 minutes of operation. The device consisted of ITO/blend/Al PLEC with an active layer of a blend of MEH-PPV:PEO:LiOTf in a weight ratio of 10:3:1 at 170 nm thick.

Previous researchers have also noticed a second increase in light emission after an initial decline during lifetime measurements and attributed this to self-heating of the device.[182] PEO is a semicrystalline polymer at room temperature and these crystalline regions (60% of the bulk) present barriers for ion diffusion with the ion transport preferentially occurring in the amorphous phases.[183] These crystalline regions begin melting at temperatures above room temperature depending on the water content present in the PEO. Since great care was taken to effectively remove the water from the PEO and handle the polymer in a dry atmosphere, it is expected that the water content is minimal. The melting of the crystalline regions in PEO with weight fractions of water less than 0.05 begins to occur at 30ºC.[184] As these crystalline regions begin to melt, the ionic conductivity of PEO then increases. This could then lead to the higher light output after the initial decrease in device brightness as the charge carrier mobility is increased. After several hours of operating at this higher temperature, the device inevitably begins to fail with light output and current density decreasing to a minimum as seen in the lifetime experiment.

The work described here is the first in which the PEO component of the LEC blend is dried to this extent. The technique used was lyophilization, a method to effectively remove water from biological and pharmaceutical samples without destroying the sample as high temperature techniques can do. With lyophilization, the sample, in this case PEO, was dissolved in the low boiling point solvent, acetonitrile, that forms an azeotrope with water. The solution was then quickly frozen in liquid nitrogen and placed under vacuum. As the sample is allowed to slowly warm to room temperature, the acetonitrile/water azeotrope sublimes and collects at a water-cooled condenser. LEC active layer blends made with this PEO were compared to PEO "dried" as has been previously done throughout the literature by heating the sample in a vacuum oven to

40ºC. Figure 4-9 shows the L-V and J-V curves for the device containing the lyophilized PEO (A) and the non-lyophilized PEO (B).

While both devices exhibit the same turn-on voltage at 3 V, the non-lyophilized PEO device initially has a higher luminance and higher current density. At -6 V the non-lyophilized PEO device has a luminance of 113 cd/m^2 while the device containing the lyophilized PEO has a luminance of 45 cd/m^2 at that same voltage. However, the device with the non-lyophilized PEO begins to fail with a drop in luminance and current density at voltages beyond -6 V while the device containing the dry PEO continues to exhibit an increase in luminance at increasing negative voltages until -10 V. The degree of crystallinity is dependent on the amount of water present with PEO containing a higher weight fraction of water exhibiting a lower degree of crystallinity. These results show that while the drier PEO may have a lower ionic mobility (exhibited by the lower luminance) than the PEO with a higher percent of water present, the device with the drier PEO shows a higher stability, operating efficiently to higher negative voltages due to the absence of water that can have a detrimental effect on device performance.

It has been demonstrated that blends of MEH-PPV/PEO/LiOTf cast as thin films can be utilized as the active layer in reflective electrochromic displays (Chapter 3) with ITO as the working electrode and containing an aluminum-coated porous membrane as the reflective layer. This chapter demonstrates that these blends of MEH-PPV with the solid electrolyte PEO/LiOTf can also be utilized as the active layer in light-emitting electrochemical cells with light emission occurring by n-doping at the ITO electrode and p-doping at the aluminum electrode. A device is then constructed that is a combination of both of these devices, showing electroluminescence and electrochromism from MEH-PPV at the same pixel.

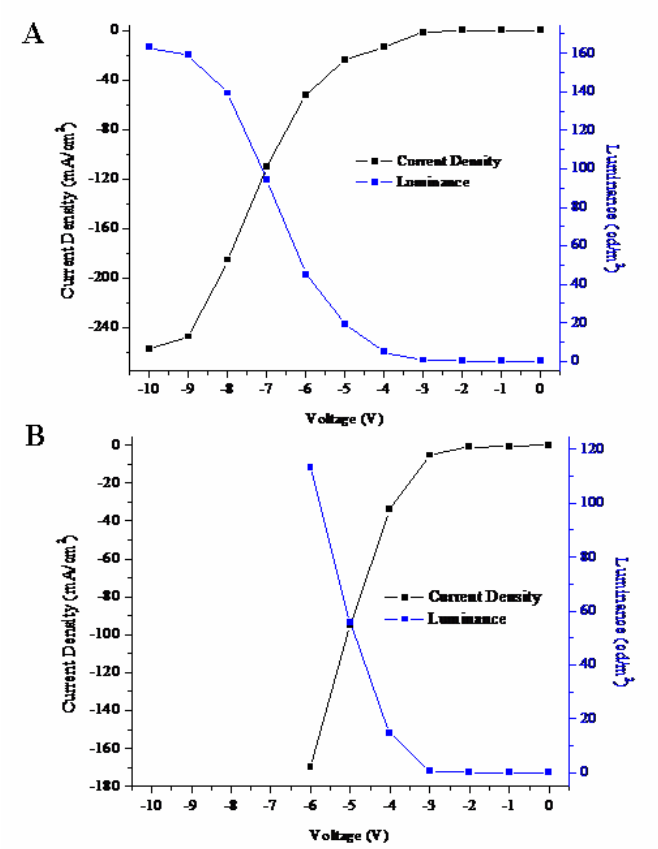

Figure 4-9. Comparison of the J-V and L-V response of two LECs constructed with PEO dried to different extent. A) PEO dried by lyophilization, B) PEO dried in a vacuum oven at 40ºC.

Dual EC/EL

As was discussed earlier in this chapter, there are currently a large variety of device designs for visual displays, some of which operate in a reflective mode, while others operate in an emissive mode. Reflective displays operate at an advantage in situations in which ambient light is sufficient to provide contrast when the device or pixel is switched, but need an external light source in dark situations while light-emitting displays operate efficiently in low ambient light situations, yet have poor image quality in highly lit environments. Many devices that are utilized in displays and consumer electronics commonly operate in environments where the ambient lighting varies significantly. This includes cell phones, personal digital assistants (PDA's), laptop computers, iPods and related entertainment devices, and many Department of

Defense oriented displays (such as those in aircraft cockpits). A display that could effectively function in a variety of lighting conditions by switching between a full color reflective electrochromic operation and a light-emitting operation would be advantageous.

Here, it is demonstrated for the first time advances on just such a device. A combination of both an ECD and a LEC was utilized, which operates as a reflective ECD when one set of electrodes are biased, and as a LEC when another set of electrodes are biased. The dual EC-EL effect is generated from a single active film material as desired for ultimate ease of production. As shown schematically in Figure 4-10A and by the photograph in Figure 4-10B, the device consisted of the active polymer layer coated onto a patterned ITO substrate. The next layer was a metallized porous membrane followed by a porous separator and finally with the electroactive polymer-coated counter electrode. Light emission occurred when the front ITO (electrode I) and metallized membrane (electrode II) were connected as anode and cathode. Electrochromism occurred when the ITO (electrode I) was connected as the working electrode and the back electrode (electrode III) was connected as the counter electrode as in an ECD.

In the device construction, ITO-coated glass with the polymer blend was used as both the anode for light-emission and the working electrode for electrochromism. The ITO for the top anode (electrode I) was patterned as two parallel strips 5 mm wide, 2 mm apart, forming two transparent electrodes. The device was assembled using a blend solution as the active polymer layer. The blend contained MEH-PPV, PEO, and LiOTf in a weight ratio of 10:3:1, respectively, dissolved in cyclohexanone as with the LEC devices described previously. The polymer blend was cast onto electrode I by spin-coating 400 μL of the solution at 1000 rpm.

A metallized porous membrane was then placed on top with the metal side facing the active polymer layer. This electrode was a porous polycarbonate membrane that has been

patterned with a 60 nm layer of aluminum by thermal evaporation deposited in a pattern of two parallel strips that were 5 mm wide and separated from each other by 2 mm. These strips were patterned such that they lay perpendicular to the ITO-patterned strips, forming 4 separate pixels that are 25 mm^2 in area. This electrode acts as the cathode when the device is operated as a light-emitting electrochemical cell.

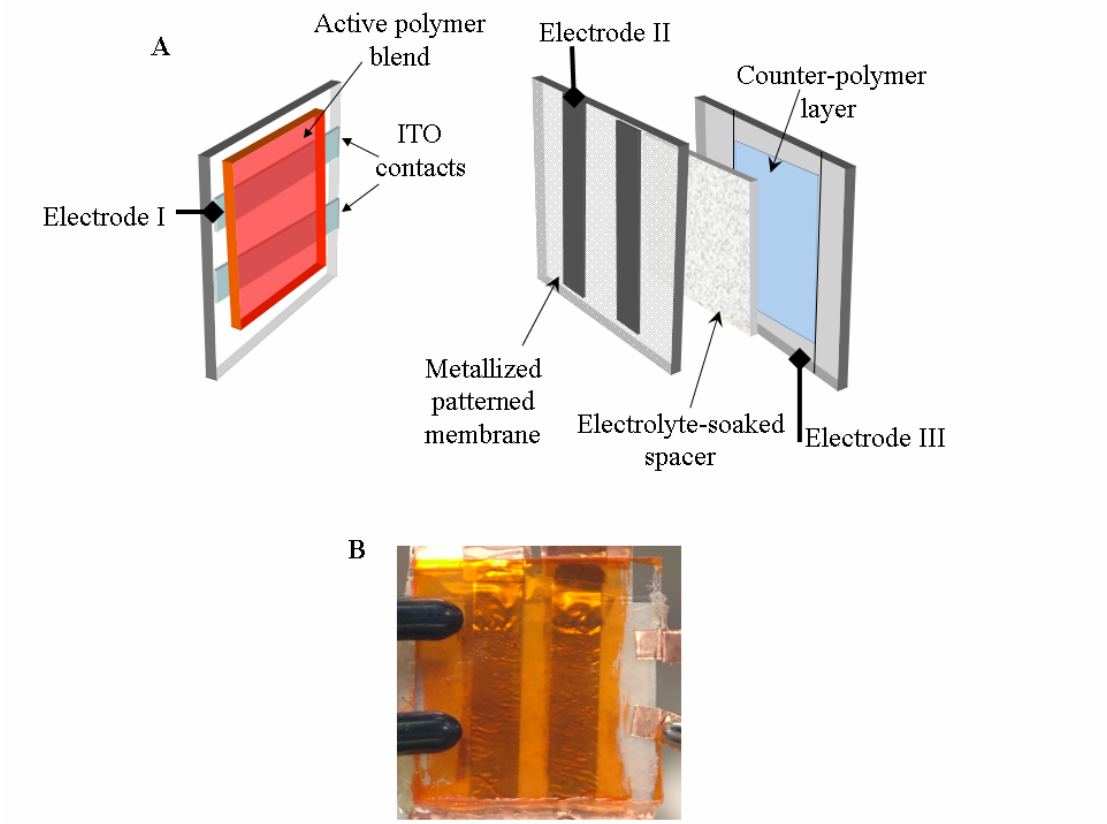

Figure 4-10. Schematic of dual EC/EL device (A). Photograph of actual device (B).

The back electrode (electrode III) was ITO-coated glass on which PEDOT had been electrochemically deposited as described in Chapter 3. This electrode acts as the counter electrode when the device is operated as an electrochromic display. A separator paper, soaked in electrolyte, was used to isolate the back of the metallized membrane from the counter polymer layer as some of the metal can penetrate the membrane and short with the counter electrode. The electrolyte consisted of 5 mg/mL PEO and 0.9 mg/mL LiOTf dissolved in ACN.

Before assembly, the solvent was allowed to evaporate, leaving behind a solid electrolyte. In addition, a layer of the solid electrolyte was also deposited onto the PEDOT layer and allowed to dry before device construction. This was to ensure a sufficient concentration of ions for electrochromic operation of the device. All electrodes were contacted with copper tape and the device was sealed with epoxy on the edges. With this design, only the active polymer layer is responsible for the light-emission and electrochromism observed, while the counter electrode polymer is used for charge balance during electrochromic switching.

As the top ITO anode and the middle metallized porous cathode are connected to a voltage source, light emission occurs from the active polymer layer. After the addition of a small amount of ACN to improve ion mobility (~250 μL), the front ITO electrode was connected to a potentiostat as the working electrode and the back PEDOT-coated ITO electrode was connected as the counter electrode. When the device was biased with positive voltages applied to the working electrode, the active polymer layer electrochromically switched between a neutral orange-red color to an oxidized blue color. The device was then biased with negative voltages applied to the working electrode and the active polymer layer switched back to the orange-red neutral state. It should be noted that the utilization of a lower viscosity electrolyte should improve ion mobility during electrochromic switching, thereby eliminating the need for the addition of small amounts of solvent during electrochromic switching.

As is shown in the photographs in Figure 4-11A (entire device) and D (close-up of a pixel from a different device), when the ITO electrodes were connected as the anode and the porous aluminum electrodes connected as the cathode, the pixels emitted light when -21 V was applied. This high voltage for light emission is expected as there is poor contact between the polymer film and the aluminum electrode. This can be improved in further studies by evaporation of a

thin layer of aluminum directly onto the polymer film. The light emitted was orange, with a peak wavelength centered around 600nm. This light-emission was relatively steady and sustained as long as the voltage is continuously applied.

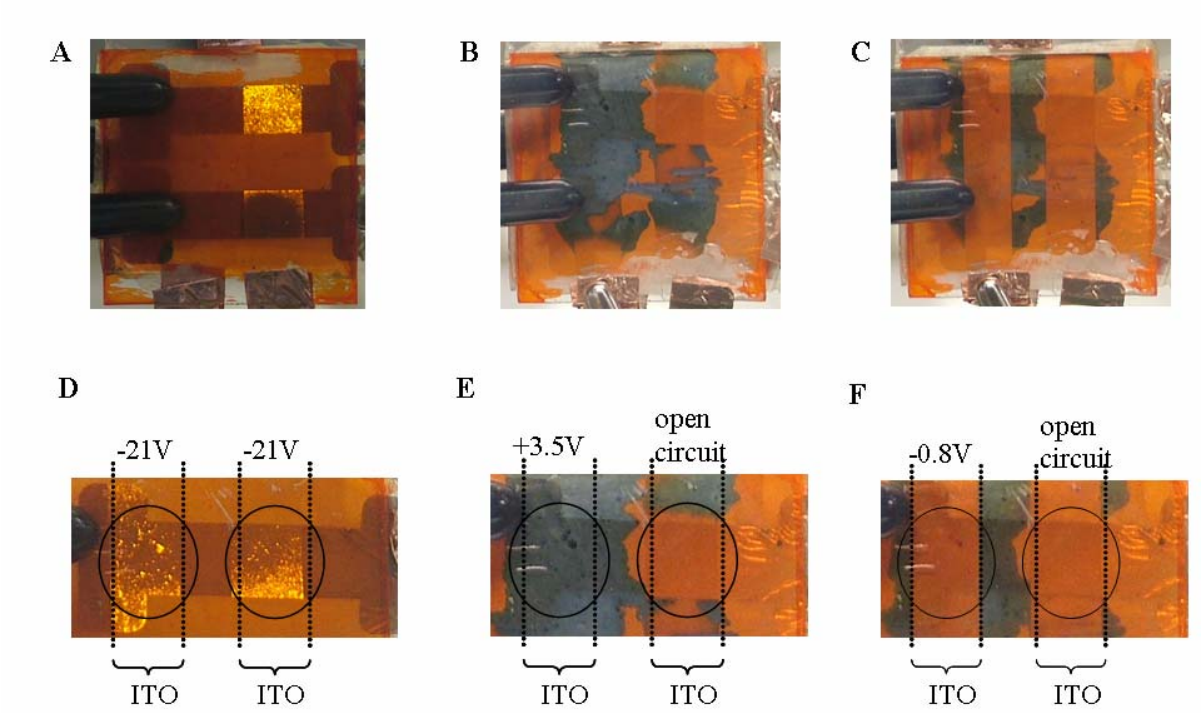

Figure 4-11. Photographs of a dual electrochromic and light-emitting device with MEH-PPV as the active material. A) shows a device when it is operating in the light-emitting mode. B) and C) show a separate device when it is operating in the electrochromic mode with the polymer oxidized in B) and reneutralized in C). A close-up of a device operated in light-emitting (D), and electrochromic (E and F) mode.

The top ITO electrode was then connected as the working electrode and the back ITO electrode (hidden) connected as the counter electrode after addition of 250 μL of ACN to the cell. When +3.5 V was applied across the cell, the color of the active polymer layer at the ITO electrode changed color from its neutral orange-red state to its oxidized blue state. In the photograph in Figure 4-11B (Figure 4-11E shows a close-up of the same pixel), the pixel on the left was connected to the potentiostat while the pixel on the right left at open circuit. Therefore, only the left pixel changed color while the right pixel remained in the neutral state. When -0.8 V was applied to the left pixel, the polymer was neutralized and returned to its orange-red color.

This can be seen in Figure 4-11C (and the close-up of the same pixel in Figure 4-11F), where the pixel on the left is again orange-red. The pixel on the right is still at open circuit. These pixels can be repeatedly switched between the two color states.

Overview and Future Directions

While the ultimate goal of this chapter to demonstrate a dual electrochromic/ electroluminescent device has been attained, many key concepts and methods were also demonstrated and established. Many device construction and measurement methods were established with the fabrication of standard MEH-PPV PLEDs with complete fabrication in an inert atmosphere glovebox along with optical characterization using a new fiber-optic system. This allowed for the creation of a protocol for further analytical characterization of materials and devices of the more complicated PLECs. These PLEC devices, never before demonstrated in our laboratory, were constructed with a MEH-PPV/PEO/LiOTf active blend layer with the onset for light-emission occurring at ±3V and maximum luminance values on par with those reported in the literature. As the operational behavior of this type of device was observed with reproducible results, it allowed the incorporation of the LEC concept into the dual EC/EL device. The reflective electrochromic and light-emitting cell designs were then integrated into a single device where both electrochromism and electroluminescence were shown.

While this is the first time it has been demonstrated for a display device to exhibit both electrochromism and electroluminescence from the same pixel, there are yet a number of future modifications to the device components or design that could be made to improve device performance, as with any proof-of-concept. A possible alternative would be to investigate the possibility of other solid electrolytes by varying the salt and/or the ionically conducting polymer. As was also mentioned, PEO is a semicrystalline polymer and the presence of crystalline regions inhibits ionic mobility within this phase. Other ion-solvating polymers that have a higher

amorphous content at room temperature could possibly offer an improvement over PEO. However, care must be taken to choose a salt that is easily solvated by the ionically conducting polymer and both the salt and ion-solvating polymer would need to be soluble in a common solvent with the emissive polymer and this requirement further limits the choice in solid electrolyte. Several researchers have shown that either salts complexed with crown ether-based systems or ionic liquids as attractive choices in LEC devices.[115, 120]

There also exists the possibility of utilizing other electroluminescent polymers in the dual EC/EL to achieve a wide range of colors not only for light emission, but also electrochromism. The requirement for a polymer to be utilized in this device is that it exhibit emission in the solid state, have a HOMO level high enough to allow oxidation of the polymer during electrochromic switching at readily accessible potentials, and have an accessible reduction potential.

In addition, alternative device designs are another possibility to overcome some of the limitations encountered and improve device performance. One such device would be the planar/lateral device. This device would be comprised of an interdigitated microelectrode (IME) on a substrate that has been coated with the active blend layer. This is then followed by a porous separator and a counter electrode coated with a counter polymer layer as is shown in the schematic in Figure 4-12. For light emission, the interdigitated electrodes I and II are contacted as the anode and cathode with light emission occurring between the fingers. For electrochromism, both interdigitated electrodes I and II are shorted together as the working electrode and the polymer-coated back electrode III is connected as the counter electrode.

For initial experiments, the IMEs could be purchased from a commercial source that offers line widths and line spacings from 5 to 20 μm with electrode materials such as gold, platinum, and ITO on glass. Previous research by Heeger et al., has demonstrated the concept of a lateral

LEC with electrode line spacings of 15µm;[109] however, it has been recently shown that line spacings of up to 1mm are possible while maintaining efficient device operation.[185] Macro-interdigitated electrodes could be fabricated in-house of various electrode materials using photolithography, shadow masking, or line patterning. This would also lend well to the patterning of PEDOT-PSS onto glass or plastic as the aqueous polymer solution can be printed allowing for a flexible, all-plastic dual device.[186]

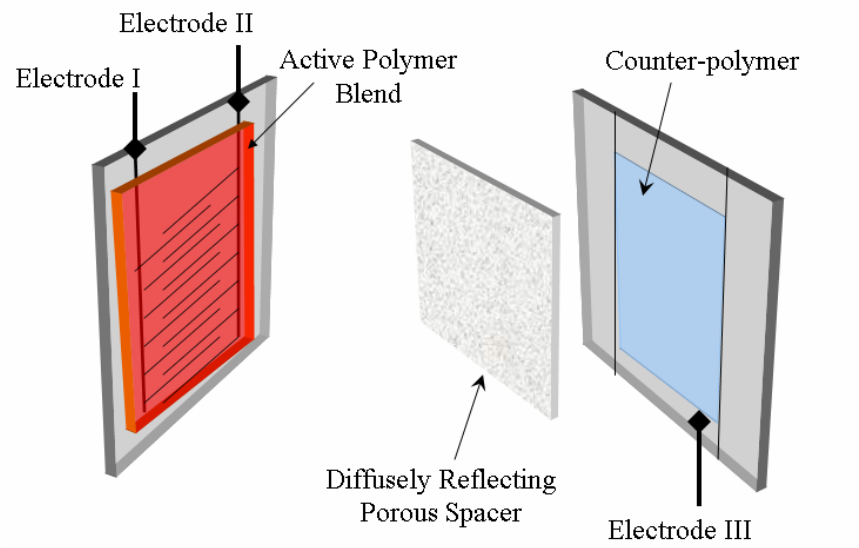

Figure 4-12. Schematic of proposed lateral dual EC/EL device.

As can be seen, there are a large number of possibilities for future direction for these devices, many of which lie outside the scope of this research to develop and demonstrate a new type of device. However, throughout this dissertation, new device designs and applications for these designs have been established and add to the growing list of uses and applications for conjugated conducting polymers.

CHAPTER 5
INSTRUMENTATION AND EXPERIMENTAL TECHNIQUES

As this dissertation covers various, differing, applications of conjugated electroactive polymers, a large variety of techniques have been utilized in fabrication of devices and their subsequent characterization. This chapter sets forth to present an overview of the materials, techniques, and instrumentation used during the course of this research.

Chemicals and Materials

Reagent grade acetonitrile (ACN), propylene carbonate (PC), and cyclohexanone in Sure Seal® bottles were purchased from Aldrich. Chloroform (Aldrich) and ACN were distilled over CaH_2. PC was percolated through activated type 3A molecular sieves, followed by fractional distillation under reduced pressure. Cyclohexanone was directly transferred to a Schlenk flask under Argon by cannula, followed by freeze-pump-thaw for three cycles and stored in the glovebox. Solvents used in the glovebox were deoxygenated by freeze-pump-thaw before being transferred into the glovebox. Solvents used on the bench were stored under Argon and purged for a minimum of 10 minutes prior to use.

Tetrabutylammonium hexafluorophosphate ($TBAPF_6$- Fluka), lithium perchlorate ($LiClO_4$ - Alrich), and lithium trifluoromethanesulfonate ($LiCF_3SO_3$ – Aldrich) were dried under vacuum at 150ºC for 24 hours prior to use. Poly(methyl methacrylate) (PMMA) (M_w 85,000 g/mol, PDI 2.4) was purchased from Aldrich and used without further purification. Poly(ethylene oxide) (PEO - Aldrich) (M_w 1,000,000 g/mol) was dried by lyophilization (as detailed in Chapter 4) from ACN prior to use. Poly(3,4-ethylenedioxythiophene)/poly(styrene sulfonate) (PEDOT:PSS) (Baytron P VP Al 4083) was purchased from H.C. Starck and syringe filtered through a 0.45 micron Nylon filter followed by filtering through a 0.2 micron Nylon filter prior before use. The monomer, EDOT (Baytron M V2) was purchased from H.C. Starck and distilled

under vacuum from CaH_2. Poly[2-methoxy-5-(2-ethylhexyloxy)-1,4-phenylenevinylene], MEH-PPV (OPA6345) (M_w 175,000 g/mol, PDI 1.3) was purchased from H.W.Sands and used as received. Poly(3,3-bis(2-ethylhexyloxymethyl)-3,4-dihydro-2*H*-thieno[3,4-*b*][1,4]dioxepine) (PProDOT-$(CH_2OEtHx)_2$) (M_w 75,000, PDI 1.6), and poly(3,3-dihexyl-3,4-dihydro-2*H*-thieno[3,4-*b*][1,4]dioxepine) (PProDOT-Hx_2) (M_w 66,000 g/mol, PDI 1.7) were prepared as previously reported.[48] Poly[(9,9-bis(methoxyethoxyethyl)-2,7-fluorene)-*alt*-(*N*-(methoxyethoxyethyl)-3,6-carbazole)] (Cbz2-Fl2), and poly[(1,4-bis(methoxyethoxyethoxyethoxy)-2,5-phenylene)-alt-(*N*-(methoxyethoxyethyl)-3,6-carbazole)] (Cbz2-Ph3) ,whose structures are shown in Figure 3-2, were synthesized specifically for this study.[187] Briefly, the polymers were synthesized by Suzuki coupling between the diboronate of the carbazole monomer and the corresponding aromatic dihalide (phenyl or fluorene) monomer. The polymerizations required equimolar amounts of 3,6-di(dioxaborolanyl)-*N*-methoxyethoxyethyl-carbazole and the aromatic dihalide (1,4-dibromo-2,5-bis(methoxyethoxyethoxyethoxy)benzene or 2,7-dibromo-9,9-bis(methoxyethoxyethyl)fluorene) were added to a solution of Aliquat 336 in toluene and bubbled with Argon. To this, a 2M aqueous solution of sodium carbonate was added with freshly prepared palladium tetrakis(triphenyl phosphine) and refluxed at ~105^oC for three days. The organic layer was collected, concentrated by evaporation and the product isolated by dissolving in dichloromethane followed by precipitation into methanol. The polymer was collected by filtration and dried under vacuum.

ITO-coated glass slides were purchased from Delta Technologies (CG-50IN-CUV and CB-50IN-0111). Prior to use, the ITO slides were cleaned by light mechanical rubbing with a cotton swab soaked in a surfactant solution (aqueous sodium dodecylsulfate). This was followed by

rinsing in a stream of distilled water, then acetone and isoproanol, then air dried. Track-etched polycarbonate membranes were purchased from GE Osmonics Inc. Membranes are 10 microns thick with 10 micron diameter cylindrical pores. Gold (99.99% pure) was purchased locally (National Coin Investors, Inc.). Platinum wire and sheets, silver wire, and aluminum slugs were purchased from Alfa Aesar. Platinum button electrodes were purchased from BAS. ITO/glass interdigitated microelectrodes (IME 1050.5-M-ITO-U) were purchased from AbTech Scientific. The digit length was 5 mm with 10 micron line width and 10 micron spacing between digits. Gold-coated Kapton® (100 nm thick gold layer on 1 mm thick Kapton® sheets) was purchased from Astral Technologies and cut to size with scissors. Copper tape, used to contact ITO and Au-coated membrane electrodes was purchased from 3M electronics division.

Device Construction

Electrochromic Displays

The gel electrolyte used in the devices was composed of either 1 g of $TBAPF_6$ or 0.4 g of LiOTf , dissolved with 2.3 g of PMMA, in 5.6 mL of PC giving a salt concentration of 0.46 M. The gel was prepared by dissolving the salt in PC, followed by slowly adding PMMA while stirring and heating to 60ºC until all components were incorporated to form a highly viscous clear gel. Gold- or aluminum-coated polycarbonate membranes were prepared by thermally evaporating the metal using a high vacuum thermal evaporator (Denton DV-502A) operated at $1x10^6$ mbar. The membranes were sandwiched between an aluminum plate and a patterned mask. The metals were deposited to a final thickness of 60 nm at a deposition rate of 4 Å/sec.

The reflective ECDs as described in Chapter 2, were fabricated by sandwiching together several layers. The fabrication, from bottom to top, began with an acetate (3M transparency film, PP2500) support onto which the counter electrode was placed. The counter electrode consists of a gold-coated Kapton® electrode (contacted with copper tape) with an

electropolymerized layer of PEDOT. The PEDOT was polymerized using potentiostatic conditions at 1.6 V vs. Ag wire until a deposition charge of 200 mC has passed. The monomer solution contained 10 mM EDOT and 0.2 M $TBAPF_6$ in PC. This layer is left in the oxidized form for device construction. The next layer is three pieces of filter paper (Fisherbrand, 09-803-5A) that are soaked in the gel electrolyte. This is followed by the outward facing working electrode, which is the gold-coated polycarbonate membrane.

The active electrochromic polymer layer is applied to this electrode by either spray-casting or electropolymerization. Spray-casting was performed using a 5 mg/mL solution of the desired polymer in toluene that is sprayed from a commercial airbrush (Testors Corp., Aztek TS28) operated at an air pressure 20 psi. Electrochemical polymerization was performed by applying a potential high enough to oxidize the monomer (typically 1.2 to 1.6 V vs. Ag wire) in a solution of 10 mM monomer, 0.2 M $TBAPF_6$. This potential was held until the desired polymer thickness was achieved as determined by passed charge density, with values typically ranging from 3 to 17 mC/cm^2. The active polymer layer thickness was typically equal to or less than the PEDOT counter layer thickness, which ensured full switching of the working electrode. A transparent window (3M transparency film, PP2500) was placed on top and the entire device sealed on all four edges using transparent tape. The device schematic and photographs can be seen in Figure 2-1A and B.

The ECDs described in Chapter 3 were fabricated similarly; differing in the type of reflector and working electrode. The counter electrode was the same as described above (PEDOT on Au-Kapton®). For the device containing the aluminum reflector, the counter electrode was followed by two pieces of gel electrolyte-soaked filter paper. The next layer was an aluminum-coated polycarbonate membrane that is outward facing (as shown in Figure 3-9B).

The working electrode is ITO/glass on which the active electrochromic layer was spin-cast. The working and counter electrodes were contacted with copper tape and the entire device sealed with epoxy on all four edges. For the device containing the white paper reflector (Figure 3-9A), the counter electrode was followed by three pieces of gel electrolyte-soaked filter paper. The working electrode is again ITO/glass coated with the active electrochromic layer by spin-casting.

Polymer Light-Emitting Diodes

Polymer LEDs were prepared by first etching the ITO/glass (25 x 25 mm) to create an anode pattern. The pattern for ITO etching can be found in the dissertation by a previous doctoral student in the Reynolds group.[188] The ITO was covered with clear packing tape (Scotch™ Brand) and the pattern cut out using a razor blade. The unmasked areas of ITO were etched by exposure to aqua regia vapors (3:1 $HCl:HNO_3$) for ten minutes. The etched ITO was cleaned as described previously. The electrodes were placed in an oxygen plasma cleaner for 30 minutes. The PEDOT:PSS hole transport layer was spin-coated onto the ITO electrodes at 4000 rpm to a final thickness of 40 nm. The electrodes were baked in a vacuum oven at 150ºC for 12 hours. The substrates were transferred to an Argon atmosphere drybox where the remaining device fabrication and characterization took place. The active electroluminescent layer was applied by spin-coating a solution of 5 mg/mL MEH-PPV in chlorobenzene at various spin rates for 60 seconds. The devices were transferred to a thermal evaporator and the cathodes were deposited at a pressure of 1×10^{-6} mbar. The first layer was calcium deposited to 10 nm followed by 150 nm of aluminum through a shadow mask giving an active pixel area of ~7.07 mm^2. The pattern for the shadow mask is as previously described.[188]

Polymer Light-Emitting Electrochemical Cells

Polymer LECs were fabricated in a similar manner as the LEDs. The ITO/glass anodes were patterned and cleaned by the same methods. The difference being that there is no

PEDOT:PSS hole transport layer. After cleaning, the electrodes were immediately transferred to the glovebox. The electroluminescent layer was spin-cast onto the ITO anodes at various spin rates for 60 seconds. The LECs master solutions contained the electroluminescent polymer, PEO, and LiOTf each at a concentration of 10 mg/mL, 13 mg/mL, and 13 mg/mL in cyclohexanone, respectively. The MEH-PPV blend was prepared by combining each component in a weight ratio of 10:3:1 and diluted to a MEH-PPV concentration of 5 mg/mL. The carbazole copolymer blend solutions were prepared by adding LiOTf to the polymer master solution to form a weight ratio of 20:4 with a final copolymer concentration of 10 mg/mL. The films were then transferred to the thermal evaporator and an aluminum cathode was thermally evaporated to a thickness of 150 nm through the same shadow mask described for the PLEDs.

Dual Electrochromic/Electroluminescent Devices

The layered dual EC/EL devices (as shown in Figure 4-10) were fabricated based on the combination of the standard LEC device and the aluminum reflector electrochromic device design. The first layer of this device is comprised of a PEDOT-coated gold/Kapton® counter electrode on a glass support. The next layer is two pieces of filter paper soaked with a LiOTf-based gel electrolyte. On that layer is the aluminum-coated porous membrane that acts as both a cathode for light-emitting operation and a reflective metal for the electrochromic operation. The deposited aluminum is patterned in two strips that are 5 mm in width and 10 mm apart. The active layer is comprised of MEH-PPV:PEO:LiOTf in a weight ratio of 10:3:1 in cyclohexanone (as with the LECs) spin-cast on the ITO anode. The ITO is patterned on the anode in two strips that are 5 mm in width and 10 mm apart (as with the cathode). The strips are arranged perpendicular to the aluminum strips such that the active light-emitting pixel area is defined by the overlap between the aluminum and ITO electrodes and is 25 mm^2. The entire device was sealed with epoxy on all four edges. Operation of the device is described in detail in Chapter 4.

Electrochemical Methods

The electrochemical methods used in polymer electrochemistry have been extensively reviewed by previous researchers in the Reynolds group.[189, 190] Therefore, the methods specific to this work will briefly be covered here. All electrochemical measurements were performed with an EG&G PAR model 273A potentiostat controlled using CorrWare software (Scribner Associates)

Electropolymerization

The potential for electropolymerization of a monomer is typically determined by cycling the potential of a working electrode and monitoring the resulting current. Once the peak current for monomer oxidation is determined, that potential is used for subsequent potentiostatic electropolymerization experiments. The typical electrochemical cell setup is comprised of a working electrode, reference electrode, and counter electrode in a glass cell. The working electrodes used in this work include ITO/glass, gold-coated polycarbonate membranes, and gold-coated Kapton®. Electrical contact to these electrodes was made with copper tape. The electrode is immersed in the monomer solution in the glass cell. The setup also includes a counter electrode that is a platinum flag made by spot-welding platinum wire to platinum foil. The size of the foil is such that the area of the counter electrode is always larger than the area of the working electrode to be used. The reference electrode is a silver wire pseudoreference that is frequently (every half-hour) calibrated with a standard ferrocene solution (5 mmM ferrocene, 0.2 M $LiClO_4$, ACN). Monomer solutions are composed of 10 mM monomer in 0.2 M salt (either $TBAPF_6$ or LiOTf) in propylene carbonate and are bubbled with Ar for at least ten minutes.

During the potentiostatic electropolymerization, the oxidizing potential is applied to the working electrode. This polymerization is terminated when a specific charge has passed where the charge is determined in previous experiments in which a calibration plot of charge versus

final film thickness is prepared for each monomer. By this method the resulting polymer film thickness can be chosen by setting the potential to be applied until the necessary charge has passed. The polymer films are then rinsed with fresh solvent and electrochemically switched in monomer-free electrolyte.

Polymer Electrochemistry

Electrochemistry of polymer films, whether prepared by spray-casting, drop-casting, or electropolymerization, is performed in a three-electrode cell. This cell is described as above with the polymer-coated electrode as the working electrode, a platinum flag as the counter electrode, and a Fc/Fc^{+}-calibrated silver wire as the reference electrode. The film is switched by cycling the electrode potential using cyclic voltammetry (CV) in an electrolyte solution of 0.2 M salt in either PC, ACN, or water that has been bubbled with Argon for ten minutes. An Argon blanket is kept over the solution during the measurements. The potential applied to the working electrode is scanned to a value sufficient to oxidize the polymer and cycled back to the beginning while the current is measured. Polymer films typically require a break-in of at least five scans before repeated cycling of the potential is stable to ion and solvent diffusion in and out of the film. If an anodic and cathodic peak are clearly visible, the $E_{1/2}$ of the polymer is then determined by summing the peak cathodic current with the peak anodic current and dividing their sum by 2. If an anodic peak current is not clear, the onset for the current increase on oxidation is determined and reported.

Optical Methods

Spectroelectrochemistry

Benchtop spectroelectrochemical measurements were performed with a Varian Cary 500 UV/Vis-NIR spectrophotometer. Polymer films to be measured on ITO/glass were placed in a standard 1 cm cuvette fitted with a Teflon cap to hold the ITO/glass in place along with the

reference and counter electrode wires. These wires were placed on either side of the cuvette so as to not block the source beam or come into contact with the working electrode. The cuvette was filled with the appropriate electrolyte solution that has been purged with Argon for 10 minutes. The baseline is taken as an identical cell to the one to be measured minus the polymer film. The electrodes were connected to a potentiostat and the desired potential applied to the working electrode and held while the wavelength region of interest was being scanned. An electrochemical break-in scan of the film is performed before the spectroelectrochemical series is performed, except where noted. Spectroelectrochemical measurements performed in the glovebox were done using a StellarNet EPP2000 Vis-NIR fiber-optic spectrophotometer. The instrument contains a SL1 calibrated light source and a photo diode array detector. The fiber-optic cables allowed remote measurement of the polymer spectra from inside the glovebox.

Benchtop reflectance spectroelectrochemistry of ECDs was performed using the Cary 500 spectrophotometer with an integrating sphere attachment mounted to the instrument. The inside of the sphere is coated with highly reflective BaO and has a sample and reference port. The device is placed at the sample port while a BaO standard is placed at the reference port. The baseline is taken using a reference device that is constructed with the same components as the sample device, except for the active polymer layer. The reflectance measured is total reflectance and is comprised of both specular and diffuse light. The device is connected to a potentiostat with the working electrode connection to the active electrode. The reference and counter connections are shorted together and connected to the counter electrode of the device. A potential is applied across the device and held while the wavelength region of interest is scanned.

Reflectance measurements using the fiber-optic spectrometer were performed using the setup described in Chapter 2. The device is placed (face up) between the two plates of the

sample holder and the input and output fibers are attached. The light measured from the device is specular only at a 45º angle. The schematic and photograph of the device holder is shown in Figure 2-12.

Electroluminescence Measurements

Electroluminescence of PLEDs and PLECs was measured using an Ocean Optics USB4000 fiber-optic spectrometer containing linear CCD array detector. The response of the detector is calibrated on a monthly basis using a standard LS-1-CAL light source. This allowed measurements to be performed in the glovebox under an Argon atmosphere. Voltages were applied to the device using a Keithley 2400 source measurement unit (SMU) with the positive bias applied to the ITO contacts and negative bias applied to the aluminum contacts and resulting current measured. Optical measurements were made normal to the device surface using the bare fiber-optic of the USB4000. The position of the fiber-optic probe was controlled, relative to the device pixel, using a X-Y-Z stage while the device is enclosed in a dark box, to not allow for stray light. The spectrometer was controlled using the SpectraSuite software. Electroluminescence measurements were made by applying a voltage to the desired pixel and measuring the spectral irradiance ($\mu W/cm^2/nm$) from 350 to 800 nm as detailed more fully in Chapter 4.

APPENDIX A
POLYMER STRUCTURES

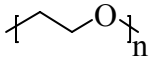

PEO

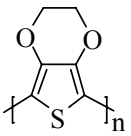

PEDOT

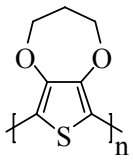

PProDOT

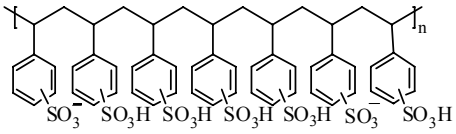

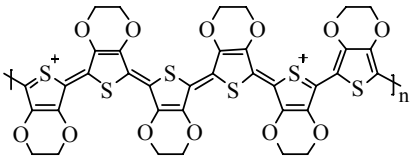

PEDOT:PSS

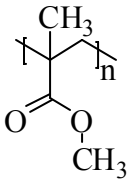

PMMA

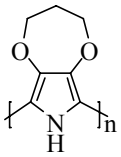

PProDOP

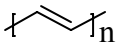

PAc

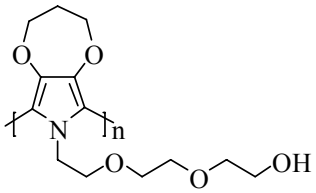

PProDOP-*N*-Gly

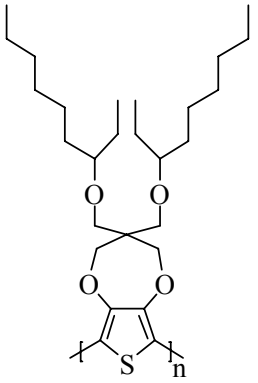

PProDOT-$(CH_2OEtHx)_2$

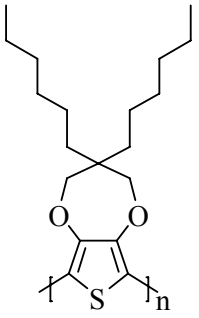

PProDOT-Hx_2

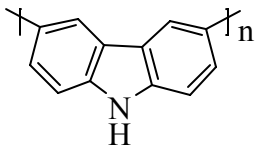

PCbz

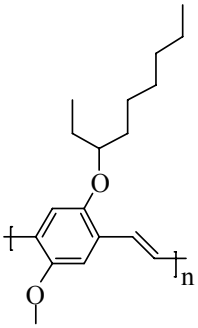

MEH-PPV

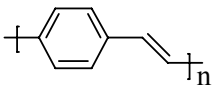

PPV

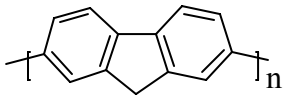

PFl

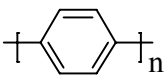

PPP

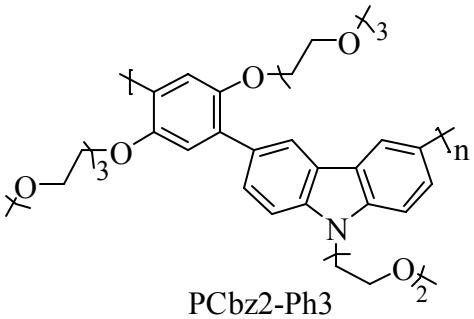

PCbz2-Ph3

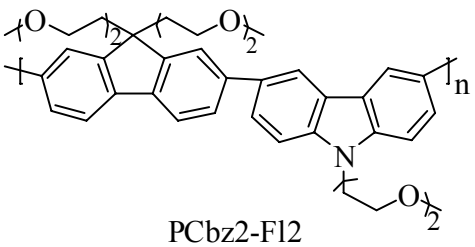

PCbz2-Fl2

LIST OF REFERENCES

1. Letheby, H. *XXIX--On the production of a blue substance by the electrolysis of sulfate of aniline*; 1862; 161.

2. Natta, G.; Mazzanti, G.; Corradini, P. *Atti accad. nazl. Lincei Rend. Classe sci. fis. mat. e nat.* **1958,** *25*, 3.

3. Watson, W. H., Jr.; McMordie, W. C., Jr.; Lands, L. G. *J. Polym. Sci.* **1961,** *55*, 137.

4. Hatano, M.; Kambara, S.; Shigeharu, O. *J. Polym. Sci.* **1961,** *51*, S26.

5. Berets, D. J.; Smith, D. S. *Trans. Farad. Soc.* **1968,** *64*, 823.

6. Kleist, F. D.; Byrd, N. R. *J. Polym. Sci., Polym. Chem. Ed.* **1969,** *7*, 3419.

7. Ito, T.; Shirakawa, H.; Ikeda, S. *J. Polym. Sci., Polym. Chem. Ed.* **1974,** *12*, 11.

8. Shirakawa, H.; Ito, T.; Ikeda, S. *Makromol. Chem.* **1978,** *179*, 1565.

9. Shirakawa, H.; Louis, E. J.; MacDiarmid, A. G.; Chiang, C. K.; Heeger, A. J. *J. Chem. Soc., Chem. Commun.* **1977**, 578.

10. Chiang, C. K.; Park, Y. W.; Heeger, A. J.; Shirakawa, H.; Louis, E. J.; MacDiarmid, A. G. *J. Chem. Phys.* **1978,** *69*, 5098.

11. Chiang, C. K.; Gau, S. C.; Fincher, C. R., Jr.; Park, Y. W.; MacDiarmid, A. G.; Heeger, A. J. *Appl. Phys. Lett.* **1978,** *33*, 18.

12. Chiang, C. K.; Druy, M. A.; Gau, S. C.; Heeger, A. J.; Louis, E. J.; MacDiarmid, A. G.; Park, Y. W.; Shirakawa, H. *J. Am. Chem. Soc.* **1978,** *100*, 1013.

13. Reynolds, J. R.; Chien, J. C. W.; Karasz, F. E.; Lillya, C. P.; Curran, D. J. *J. Phys., Coll.* **1983**, 171.

14. Rolland, M.; Bernier, P.; Disi, M.; Linaya, C.; Sledz, J.; Schue, F.; Fabre, J. M.; Giral, L. *J. Phys., Lett.* **1980,** *41*, 165.

15. Nigrey, P. J.; MacDiarmid, A. G.; Heeger, A. J. *J. Chem. Soc., Chem. Commun.* **1979**, 594.

16. Diaz, A. F.; Kanazawa, K. K.; Gardini, G. P. *J. Chem. Soc., Chem. Commun.* **1979**, 635.

17. Kanazawa, K. K.; Diaz, A. F.; Geiss, R. H.; Gill, W. D.; Kwak, J. F.; Logan, J. A.; Rabolt, J. F.; Street, G. B. *J. Chem. Soc., Chem. Commun.* **1979**, 854.

18. Dall'Olio, A.; Dascola, G.; Varacca, V.; Bocchi, V. *Comptes Rendus des Seances de l'Academie des Sciences, Serie C: Sciences Chimiques* **1968,** *267*, 433.

19. Irvin, J. A.; Irvin, D. J.; Stenger-Smith, J. D., Electroactive Polymers for Batteries and Supercapacitors. In *Handbook of Conducting Polymers*, 3 ed.; Reynolds, J. R.; Skotheim, T. A., Ed. CRC Press: Boca Raton, FL, 2006; Chapter 9.

20. Burroughes, J. H.; Bradley, D. D. C.; Brown, A. R.; Marks, R. N.; Mackay, K.; Friend, R. H.; Burns, P. L.; Holmes, A. B. *Nature* **1990,** *347*, 539.

21. Koezuka, H.; Tsumura, A.; Ando, T. *Synth. Met.* **1987,** *18*, 699.

22. Dyer, A. L.; Reynolds, J. R., Electrochromism of Conjugated Conducting Polymers. In *Handbook of Conducting Polymers*, ed.; Skotheim, T. A.; Reynolds, J. R., Ed. CRC Press: Boca Raton, FL, 2006; Chapter 20.

23. Wallace, G. G.; Dastoor, P. C.; Officer, D. L.; Too, C. O. *Chemical Innovation* **2000,** *30*, 14.

24. Smela, E. *Advanced Materials* **1999,** *11*, 1343.

25. Platt, J. R. *J. Chem. Phys.* **1961,** *34*, 862.

26. Rose, T. L.; D'Antonio, S.; Jillson, M. H.; Kon, A. B.; Suresh, R.; Wang, F. *Synth. Met.* **1997,** *85*, 1439.

27. Franke, E. B.; Trimble, C. L.; Hale, J. S.; Schubert, M.; Woollam, J. A. *J. Appl. Phys.* **2000,** *88*, 5777.

28. Topart, P.; Hourquebie, P. *Thin Solid Films* **1999,** *352*, 243.

29. Monk, P. M. S.; Mortimer, R. J.; Rosseinsky, D. R., *Electrochromism: Fundamentals and Applications*. ed.; Wiley-VCH: Weinheim, Germany, 1995.

30. Deb, S. K. *Appl. Opt., Suppl.* **1969,** *No. 3*, 192.

31. Deb, S. K. *Philosophical Magazine* **1973,** *27*, 801.

32. Granqvist, C. G. *Electrochim. Acta* **1999,** *44*, 3005.

33. Granqvist, C. G. *Sol. Energy Mater. Sol. Cells* **2000,** *60*, 201.

34. Mortimer, R. J. *Electrochim. Acta* **1999,** *44*, 2971.

35. Mortimer, R. J.; Reynolds, J. R. *J. Mater. Chem.* **2005,** *15*, 2226.

36. Garnier, F.; Tourillon, G.; Gazard, M.; Dubois, J. C. *J. Electroanal. Chem.* **1983,** *148*, 299.

37. Gazard, M.; Dubois, J. C.; Champagne, M.; Garnier, F.; Tourillon, G. *J. Phys., Coll.* **1983**, 537.

38. Alkan, S.; Cutler, C. A.; Reynolds, J. R. *Adv. Func. Mater.* **2003,** *13*, 331.

39. Druy, M. A.; Seymour, R. J. *J. Phys., Coll.* **1983**, 595.

40. Argun, A. A.; Cirpan, A.; Reynolds, J. R. *Advanced Materials* **2003,** *15*, 1338.

41. Groenendaal, L. B.; Jonas, F.; Freitag, D.; Pielartzik, H.; Reynolds, J. R. *Advanced Materials* **2000,** *12*, 481.

42. Heywang, G.; Jonas, F. *Advanced Materials* **1992,** *4*, 116.

43. Cao, Y.; Yu, G.; Zhang, C.; Menon, R.; Heeger, A. J. *Synth. Met.* **1997,** *87*, 171.

44. Kirchmeyer, S.; Reuter, K. *J. Mater. Chem.* **2005,** *15*, 2077.

45. Welsh, D. M.; Kloeppner, L. J.; Madrigal, L.; Pinto, M. R.; Thompson, B. C.; Schanze, K. S.; Abboud, K. A.; Powell, D.; Reynolds, J. R. *Macromolecules* **2002,** *35*, 6517.

46. Mishra, S. P.; Krishnamoorthy, K.; Sahoo, R.; Kumar, A. *J. Polym. Sci., Part A: Polym. Chem.* **2004,** *43*, 419.

47. Cirpan, A.; Argun, A. A.; Grenier, C. R. G.; Reeves, B. D.; Reynolds, J. R. *J. Mater. Chem.* **2003,** *13*, 2422.

48. Reeves, B. D.; Grenier, C. R. G.; Argun, A. A.; Cirpan, A.; McCarley, T. D.; Reynolds, J. R. *Macromolecules* **2004,** *37*, 7559.

49. Thomas, C. A.; Zong, K.; Schottland, P.; Reynolds, J. R. *Advanced Materials* **2000,** *12*, 222.

50. Walczak, R. M.; Reynolds, J. R. *Advanced Materials* **2006,** *18*, 1121.

51. Zong, K.; Reynolds, J. R. *J. Org. Chem.* **2001,** *66*, 6873.

52. Sönmez, G.; Schwendeman, I.; Schottland, P.; Zong, K.; Reynolds, J. R. *Macromolecules* **2003,** *36*, 639.

53. Schwendeman, I.; Hickman, R.; Sönmez, G.; Schottland, P.; Zong, K.; Welsh, D. M.; Reynolds, J. R. *Chem. Mater.* **2002,** *14*, 3118.

54. Gaupp, C. L.; Zong, K.; Schottland, P.; Thompson, B. C.; Thomas, C. A.; Reynolds, J. R. *Macromolecules* **2000,** *33*, 1132.

55. Schottland, P.; Zong, K.; Gaupp, C. L.; Thompson, B. C.; Thomas, C. A.; Giurgiu, I.; Hickman, R.; Abboud, K. A.; Reynolds, J. R. *Macromolecules* **2000,** *33*, 7051.

56. Reynolds, J. R.; Zong, K.; Schwendemann, I.; Sönmez, G.; Schottland, P.; Argun, A. A.; Aubert, P. H. Electrochromic polymers and polymer electrochromic devices. United States Patent 6,791,738, 2003.

57. Schwendeman, I.; Hwang, J.; Welsh, D. M.; Tanner, D. B.; Reynolds, J. R. *Advanced Materials* **2001,** *13*, 634.

58. Rosseinsky, D. R.; Mortimer, R. J. *Advanced Materials* **2001,** *13*, 783.

59. Somani, P. R.; Radhakrishnan, S. *Mater. Chem. Phys.* **2003,** *77*, 117.

60. Panero, S.; Passerini, S.; Scrosati, B. *Molecular Crystals and Liquid Crystals Science and Technology, Section A: Molecular Crystals and Liquid Crystals* **1993,** *229*, 97.

61. Argun, A. A.; Aubert, P.-H.; Thompson, B. C.; Schwendeman, I.; Gaupp, C. L.; Hwang, J.; Pinto, N. J.; Tanner, D. B.; MacDiarmid, A. G.; Reynolds, J. R. *Chem. Mater.* **2004,** *16*, 4401.

62. Leventis, N.; Chung, Y. C. *Chem. Mater.* **1992,** *4*, 1415.

63. Granqvist, C. G.; Avendano, E.; Azens, A. *Thin Solid Films* **2003,** *442*, 201.

64. Jelle, B. P.; Hagen, G. *Journal of Applied Electrochemistry* **1998,** *28*, 1061.

65. Girotto, E. M.; De Paoli, M.-A. *Advanced Materials* **1998,** *10*, 790.

66. Shimidzu, T.; Ohtani, A.; Aiba, M.; Honda, K. *Journal of the Chemical Society, Faraday Transactions. 1* **1988,** *841*, 3941.

67. Lu, W.; Fadeev, A. G.; Qi, B.; Smela, E.; Mattes, B. R.; Ding, J.; Spinks, G. M.; Mazurkiewicz, J.; Zhou, D.; Wallace, G. G.; MacFarlane, D. R.; Forsyth, S. A.; Forsyth, M. *Science* **2002,** *297*, 983.

68. Vondrik, J.; Sedlaiikova, M.; Reiter, J.; Hodal, T. *Electrochim. Acta* **1999,** *44*, 3067.

69. Pawlicka, A.; Dragunski, D.; Guimaraes, K.; Avellaneda, C. *Molecular Crystals and Liquid Crystals* **2004,** *416*, 105.

70. Lu, W.; Fadeev, A. G.; Qi, B.; Mattes, B. R. *Journal of the Electrochemical Society* **2004,** *151*, H33.

71. Lu, W.; Mattes, B. R.; Fadeev, A. G. Long-lived conjugated polymer electrochemical devices incorporating ionic liquids. United States Patent 6,828,062, 2002.

72. Chandrasekhar, P.; Zay, B. J.; Birur, G. C.; Rawal, S.; Pierson, E. A.; Kauder, L.; Swanson, T. *Adv. Func. Mater.* **2002,** *12*, 95.

73. Bennett, R. N.; Kokonaski, W. E.; Hannan, M. J.; Boxall, L. G. Electrode for display devices. United States Patent 5,446,577, 1994.

74. Chandrasekhar, P. Electrochromic display device. United States Patent 5,995,273, 1999.

75. Argun, A. A.; Cirpan, A.; Reynolds, J. R. *Advanced Materials* **2003,** *15*, 1338.

76. Wu, Z.; Chen, Z.; Du, X.; Logan, J. M.; Sippel, J.; Nikolou, M.; Kamaras, K.; Reynolds, J. R.; Tanner, D. B.; Hebard, A. F.; Rinzler, A. G. *Science* **2004,** *305*, 1273.

77. Brotherston, I. D.; Mudigonda, D. S. K.; Osborn, J. M.; Belk, J.; Chen, J.; Loveday, D. C.; Boehme, J. L.; Ferraris, J. P.; Meeker, D. L. *Electrochim. Acta* **1999,** *44*, 2993.

78. Aubert, P.-H.; Argun, A. A.; Cirpan, A.; Tanner, D. B.; Reynolds, J. R. *Chem. Mater.* **2004,** *16*, 2386.

79. Argun, A. A.; Reynolds, J. R. *J. Mater. Chem.* **2005,** *15*, 1793.

80. Argun, A. A.; Berard, M.; Aubert, P.-H.; Reynolds, J. R. *Advanced Materials* **2005,** *17*, 422.

81. Tang, C. W.; VanSlyke, S. A. *Appl. Phys. Lett.* **1987,** *51*, 913.

82. Friend, R. H.; Gymer, R. W.; Holmes, A. B.; Burroughes, J. H.; Marks, R. N.; Taliani, C.; Bradley, D. D. C.; Dos Santos, D. A.; Bredas, J. L.; Logdlund, M.; Salaneck, W. R. *Nature* **1999,** *397*, 121.

83. Fowler, R. H.; Nordheim, L. *Proc. Roy. Soc.* **1928,** *A119*, 173.

84. Brown, T. M.; Cacialli, F. *J. Polym. Sci., Part B: Polym. Phys.* **2003,** *41*, 2649.

85. Kugler, T.; Salaneck, W. R.; Rost, H.; Holmes, A. B. *Chem. Phys. Lett.* **1999,** *310*, 391.

86. Parker, I. D. *J. Appl. Phys.* **1994,** *75*, 1656.

87. Campbell, I. H.; Hagler, T. W.; Smith, D. L.; Ferraris, J. P. *Phys. Rev. Lett.* **1996,** *76*, 1900.

88. Salaneck, W. R.; Bredas, J. L. *Advanced Materials* **1996,** *8*, 48.

89. Dannetun, P.; Logdlund, M.; Fredriksson, C.; Lazzaroni, R.; Fauquet, C.; Stafstroem, S.; Spangler, C. W.; Bredas, J. L.; Salaneck, W. R. *J. Chem. Phys.* **1994,** *100*, 6765.

90. Gustafsson, G.; Cao, Y.; Treacy, G. M.; Klavetter, F.; Colaneri, N.; Heeger, A. J. *Nature* **1992,** *357*, 477.

91. Heeger, A. J. *Solid State Commun.* **1998,** *107*, 673.

92. Kraft, A.; Grimsdale, A. C.; Holmes, A. B. *Angewandte Chemie, International Edition* **1998,** *37*, 403.

93. Thompson, B. C.; Madrigal, L. G.; Pinto, M. R.; Kang, T.-S.; Schanze, K. S.; Reynolds, J. R. *J. Polym. Sci., Part A: Polym. Chem.* **2005,** *43*, 1417.

94. Reddinger, J. L.; Reynolds, J. R. *Macromolecules* **1997,** *30*, 479.

95. Zhou, X.-H.; Niu, Y.-H.; Huang, F.; Liu, M. S.; Jen, A. K. Y. *Macromolecules* **2007,** *40*, 3015.

96. Zhang, Y.; Yang, J.; Hou, Q.; Mo, Y.; Peng, J.; Cao, Y. *Chin. Sci. Bull.* **2005,** *50*, 957.

97. Pei, Q.; Yu, G.; Zhang, C.; Yang, Y.; Heeger, A. J. *Science* **1995,** *269*, 1086.

98. deMello, J. C.; Halls, J. J. M.; Graham, S. C.; Tessler, N.; Friend, R. H. *Phys. Rev. Lett.* **2000,** *85*, 421.

99. Armstrong, N. R.; Wightman, R. M.; Gross, E. M. *Annu. Rev. Phys. Chem.* **2001,** *52*, 391.

100. Edman, L. *Electrochim. Acta* **2005,** *50*, 3878.

101. Gao, J.; Heeger, A. J.; Campbell, I. H.; Smith, D. L. *Phys. Rev. B: Condens. Matter* **1999,** *59*, R2482.

102. Gao, J.; Dane, J. *Appl. Phys. Lett.* **2004,** *84*, 2778.

103. Dick, D. J.; Heeger, A. J.; Yang, Y.; Pei, Q. *Advanced Materials* **1996,** *8*, 985.

104. Edman, L.; Summers, M. A.; Buratto, S. K.; Heeger, A. J. *Phys. Rev. B: Condens. Matter* **2004,** *70*, 115212/1.

105. Holzer, L.; Wenzl, F. P.; Sotgiu, R.; Gritsch, M.; Tasch, S.; Hutter, H.; Sampietro, M.; Leising, G. *Synth. Met.* **1999,** *102*, 1022.

106. Manzanares, J. A.; Reiss, H.; Heeger, A. J. *J. Phys. Chem. B* **1998,** *102*, 4327.

107. Neher, D.; Gruner, J.; Cimrova, V.; Schmidt, W.; Rulkens, R.; Lauter, U. *Polym. Adv. Tech.* **1998,** *9*, 461.

108. Pei, Q.; Yang, Y. *Synth. Met.* **1996,** *80*, 131.

109. Pei, Q.; Yang, Y.; Yu, G.; Zhang, C.; Heeger, A. J. *Journal of the American Chemical Society* **1996,** *118*, 3922.

110. Smith, D. L. *J. Appl. Phys.* **1997,** *81*, 2869.

111. Xu, Z.; Liu, M.; Chen, X.; Hou, Y.; Teng, F.; Meng, L.; Xu, X. *Displays* **2006,** *27*, 45.

112. Cao, Y.; Yu, G.; Heeger, A. J.; Yang, C. Y. *Appl. Phys. Lett.* **1996,** *68*, 3218.

113. Ryan, A. J. *Nature Materials* **2002,** *1*, 8.

114. Wenzl, F. P.; Pachler, P.; Suess, C.; Haase, A.; List, E. J. W.; Poelt, P.; Somitsch, D.; Knoll, P.; Scherf, U.; Leising, G. *Adv. Func. Mater.* **2004,** *14*, 441.

115. Cao, Y.; Pei, Q.; Andersson, M. R.; Yu, G.; Heeger, A. J. *Journal of the Electrochemical Society* **1997,** *144*, 317.

116. Edman, L.; Pauchard, M.; Liu, B.; Bazan, G.; Moses, D.; Heeger, A. J. *Appl. Phys. Lett.* **2003,** *82*, 3961.

117. Kong, F.; Zhang, S. Y.; Zheng, Y.; Ou, C. G.; Yang, C. Z.; Yuan, R. K. *J. Appl. Polym. Sci.* **2006,** *101*, 4253.

118. Wenzl, F. P.; Poelt, P.; Haase, A.; Patil, S.; Scherf, U.; Leising, G. *Solid State Ionics* **2005,** *176*, 1747.

119. Pachler, P.; Wenzl, F. P.; Scherf, U.; Leising, G. *J. Phys. Chem. B* **2005,** *109*, 6020.

120. Yang, C.; Sun, Q.; Qiao, J.; Li, Y. *J. Phys. Chem. B* **2003,** *107*, 12981.

121. Sun, Q.; Wang, H.; Yang, C.; Li, Y. *Synth. Met.* **2003,** *137*, 1087.

122. Sun, Q. J.; Wang, H. Q.; Yang, C. H.; Wang, X. G.; Liu, D. S.; Li, Y. F. *Thin Solid Films* **2002,** *417*, 14.

123. Yang, Y.; Pei, Q. *J. Appl. Phys.* **1997,** *81*, 3294.

124. Holzer, L.; Winkler, B.; Wenzl, F. P.; Tasch, S.; Dai, L.; Mau, A. W. H.; Leising, G. *Synth. Met.* **1999,** *100*, 71.

125. Morgado, J.; Cacialli, F.; Friend, R. H.; Chuah, B. S.; Rost, H.; Holmes, A. B. *Macromolecules* **2001,** *34*, 3094.

126. Morgado, J.; Friend, R. H.; Cacialli, F.; Chuah, B. S.; Rost, H.; Moratti, S. C.; Holmes, A. B. *Synth. Met.* **2001,** *122*, 111.

127. Gao, J.; Dane, J. *Appl. Phys. Lett.* **2003,** *83*, 3027.

128. Leger, J. M.; Carter, S. A.; Ruhstaller, B. *J. Appl. Phys.* **2005,** *98*, 1.

129. Shin, J.-H.; Edman, L. *J. Am. Chem. Soc.* **2006,** *128*, 15568.

130. Shin, J. H.; Matyba, P.; Robinson, N. D.; Edman, L. *Electrochim. Acta* **2007,** *52*, 6456.

131. Andersson, P.; Nilsson, D.; Svensson, P.-O.; Chen, M.; Malmstrom, A.; Remonen, T.; Kugler, T.; Berggren, M. *Advanced Materials* **2002,** *14*, 1460.

132. Cravino, A.; Leriche, P.; Aleveque, O.; Roquet, S.; Roncali, J. *Advanced Materials* **2006,** *18*, 3033.

133. Kim, H.; Kim, J. Y.; Park, S. H.; Lee, K.; Jin, Y.; Kim, J.; Suh, H. *Appl. Phys. Lett.* **2005,** *86*, 1.

134. Yang, C.-J.; Cho, T.-Y.; Lin, C.-L.; Wu, C.-C. *Appl. Phys. Lett.* **2007,** *90*, 1.

135. Yang, C.-Y.; Cho, T.-Y.; Chen, Y.-Y.; Yang, C.-J.; Meng, C.-Y.; Yang, C.-H.; Yang, P.-C.; Chang, H.-Y.; Hsueh, C.-Y.; Wu, C.-C.; Lee, S.-C. *Appl. Phys. Lett.* **2007,** *90*, 1.

136. Wang, X. J.; Lau, W. M.; Wong, K. Y. *Appl. Phys. Lett.* **2005,** *87*, 1.

137. Johansson, T.; Persson, N.-K.; Inganaes, O. *Journal of the Electrochemical Society* **2004,** *151*, E119.

138. Lacroix, J. C.; Fraoua, K.; Lacaze, P. C. *Journal of Electroanalytical Chemistry* **1998,** *444*, 83.

139. Aoki, K.; Cao, J.; Hoshino, Y. *Electrochim. Acta* **1993,** *38*, 1711.

140. Aoki, K.; Teragishi, Y. *Journal of Electroanalytical Chemistry* **1998,** *441*, 25.

141. Tezuka, Y.; Aoki, K. *Journal of Electroanalytical Chemistry* **1989,** *273*, 161.

142. Tezuka, Y.; Aoki, K.; Yajima, H.; Ishii, T. *Journal of Electroanalytical Chemistry* **1997,** *425*, 167.

143. Tezuka, Y.; Kimura, T.; Ishii, T.; Aoki, K. *Journal of Electroanalytical Chemistry* **1995,** *395*, 51.

144. Wemple, S. H.; Seman, J. A. *Applied Optics* **1973,** *12*, 2947.

145. Cohen, S. *Laser Focus World* **2000,** *36*, 139.

146. O'Brien, N. A.; Mathew, J. G. H.; Cumbo, M. J.; Hichwa, B. P.; Adair, R. W. Variable optical attenuator device. United States Patent 6,625,378, 2003.

147. Sato, K.; Aoki, T.; Watanabe, Y.; Oguri, Y.; Shibata, N.; Nishiwaki, T.; Oike, M.; Ota, T. *Furukawa Review* **2001,** *20*, 15.

148. Uetsuka, H.; Hasegawa, T.; Ohkawa, M.; Takasugi, S.; Kitano, N.; Tanaka, K. *Hitachi Cable Review* **2001,** *20*, 15.

149. Pan, J.-J. Polarization-independent optical switch/attenuator. United States Patent 5,276,747, 1994.

150. Loukina, T.; Chevallier, R.; de Bougrenet de la Tocnaye, J. L.; Barge, M. *J. Lightwave Technol.* **2003,** *21*, 2067.

151. Khalil, D.; Maaty, H.; Bashir, A.; Saadany, B. *Microw. Optic. Tech. Lett.* **2003,** *36*, 110.

152. Morimoto, M.; Morimoto, K.; Sato, K.; Iizuka, S. i. *Furukawa Review* **2003,** *23*, 26.

153. Liu, A. Q.; Zhang, X. M.; Lu, C.; Wang, F.; Lu, C.; Liu, Z. S. *J. Micromech. Microeng.* **2003,** *13*, 400.

154. Barber, B.; Giles, C. R.; Askyuk, V.; Ruel, R.; Stulz, L.; Bishop, D. *IEEE Photonics Technology Letters* **1998,** *10*, 1262.

155. Ford, J. E.; Walker, J. A.; Greywall, D. S.; Goossen, K. W. *J. Lightwave Technol.* **1998,** *16*, 1663.

156. Cowin, M. A.; Varrazza, R.; Morgan, C.; Penty, R. V.; White, I. H.; McDonagh, A. M.; Bayly, S.; Riley, J.; Ward, M. D.; McCleverty, J. A. *Trends in Optics and Photonics* **2001,** *54*, WR6/1.

157. Franke, E. B.; Trimble, C. L.; Hale, J. S.; Schubert, M.; Woollam, J. A. *J. Appl. Phys.* **2000,** *88*, 5777.

158. MacPherson, C. D.; Anderson, K.; McGarry, S. P. Electrochromic optical attenuator. U.S. Patent Appl. US 2002/0067905 A1, 2002.

159. McDonagh, A. M.; Bayly, S. R.; Riley, D. J.; Ward, M. D.; McCleverty, J. A.; Cowin, M. A.; Morgan, C. N.; Varrazza, R.; Penty, R. V.; White, I. H. *Chem. Mater.* **2000,** *12*, 2523.

160. Qi, Y.; Wang, Z. Y. *Macromolecules* **2003,** *36*, 3146.

161. Qi, Y. H.; Desjardins, P.; Meng, X. S.; Wang, Z. Y. *Optic. Mater.* **2002,** *21*, 255.

162. Qi, Y.-h.; Desjardins, P.; Birau, M.; Wu, X.-g.; Wang, Z.-y. *Chin. J. Polym. Sci.* **2003,** *21*, 147.

163. Vergaz, R.; Barrios, D.; Sánchez-Pena, J. M.; Vázquez, C.; Pozo-Gonzalo, C.; Mecerreyes, D.; Pomposo, J. *Proceedings of SPIE: Photonic materials, devices, and applications* **2005,** *5840*, 389.

164. Wang, Z. Y.; Zhang, J. D.; Wu, X. G.; Birau, M.; Yu, G.; Yu, H. A.; Qi, Y.; Desjardins, P.; Meng, X. S.; Gao, J. P.; Todd, E.; Song, N.; Bai, Y.; Beaudin, A. M. R.; LeClair, G. *Pure Appl. Chem.* **2004,** *76*, 1435.

165. Ward, M. D. *Journal of Solid State Electrochemistry* **2005,** *9*, 778.

166. Zhang, J. D.; Lu, F.; Huang, H.; Wang, J.; Yu, H. a.; Jiang, J.; Yan, D.; Wang, Z. *Synth. Met.* **2005,** *148*, 123.

167. Zhang, J. D.; Yu, H. A.; Wu, X. G.; Wang, Z. Y. *Optic. Mater.* **2004,** *27*, 265.

168. Groenendaal, L. B.; Zotti, G.; Aubert, P.-H.; Waybright, S. M.; Reynolds, J. R. *Advanced Materials* **2003,** *15*, 855.

169. Xia, C.; Advincula, R. C. *Macromolecules* **2001,** *34*, 5854.

170. de Leeuw, D. M.; Simenon, M. M. J.; Brown, A. R.; Einerhand, R. E. F. *Synth. Met.* **1997,** *87*, 53.

171. Santos, L. F.; Faria, R. C.; Gaffo, L.; Carvalho, L. M.; Faria, R. M.; Gonc¸alves, D. *Electrochim. Acta* **2007,** *52*, 4299.

172. Zhong, Z. Y.; Jiang, Y. D. *European Physical Journal: Applied Physics* **2006,** *34*, 173.

173. Wu, C. C.; Wu, C. I.; Sturm, J. C.; Kahn, A. *Appl. Phys. Lett.* **1997,** *70*, 1348.

174. Quintens, D.; Muys, B.; Van Thillo, E.; Samijn, R. Antistatic coating on hydrophobic resin or paper support. U. S. Patent 5,354,613, 1994.

175. Kawamoto, H. *Proceedings of the IEEE* **2002,** *90*, 460.

176. *IMOD Technology Overview*; QUALCOMM Inc.: 2007.

177. Reader from Sony. http://www.learningcenter.sony.us/assets/itpd/reader/ (November 3, 2007),

178. Motorola MOTOFONE. http://www.motorola.com/motoinfo/product/details.jsp?globalObjectId=164 (November 3, 2007),

179. Cecchi, M.; Smith, H.; Braun, D. *Synth. Met.* **2001,** *121*, 1715.

180. McCluney, R., *Introduction to Radiometry and Photometry*. ed.; Artech House, Inc: Norwood, MA, 1994.

181. Kaufman, J. E., ed., *IES Lighting Handbook-Reference Volume*. ed.; Illuminating Engineering Society of North America: New York, NY, 1984.

182. Edman, L.; Moses, D.; Heeger, A. J. *Synth. Met.* **2003,** *138*, 441.

183. Ratner, M. A.; Shriver, D. F. *Chemical Reviews* **1988,** *88*, 109.

184. Trotzig, C.; Abrahmsén-Alami, S.; Maurer, F. H. J. *Polymer* **2007,** *48*, 3294.

185. Shin, J.-H.; Edman, L. *Journal of the American Chemical Society* **2006,** *128*, 15568.

186. Argun, A. A.; Cirpan, A.; Reynolds, J. R. *Advanced Materials (Weinheim, Germany)* **2003,** *15*, 1338.

187. Brookins, R. N., Synthesis and Characterization of Carbazole-Based Conjugated Polymers for Electrochromic/Electroluminescent Applications. In University of Florida: 2005.

188. Ananthakrishnan, N. Morphology effects on the light emitting properties of conjugated polymer blends. Dissertation, University of Florida, Gainesville, 2005.

189. Schwendeman, I. Optical and transport properties of conjugated polymers and their application to electrochromic devices. Dissertation, University of Florida, Gainesville, 2002.

190. Thomas, C. A. Donor-acceptor methods for band gap reduction in conjugated polymers: the role of electron rich donor heterocycles. Dissertation, University of Florida, Gainesville, 2002.

BIOGRAPHICAL SKETCH

Aubrey Lynn Dedrickson was born July 13, 1978 in Bataan, Philippines to Sheila and Randy Dedrickson. Her father was in the U.S. Navy, and therefore her family moved around quite a bit. They lived in Homestead, FL, Hawaii, Pensacola, FL, and Altamonte Springs, FL. She has one younger brother, Shaun Dedrickson, and one younger sister, Stephanie Dedrickson. She graduated high school in Pensacola, FL after which she attended the University of West Florida for her first year of college while working full-time. She and Nathan Dyer married in 1999 in Pensacola, Florida and they both moved to Shippensburg, PA where Aubrey attended Shippensburg University of Pennsylvania full-time. She received her B.S. in Chemistry in the Summer of 2002 and began her graduate studies at the University of Florida that August. In the Fall of 2002, she joined the Reynolds research group.